Aus dem Max von Pettenkofer-Institut für Hygiene und Medizinische Mikrobiologie der
Ludwig-Maximilians-Universität München
Vorstand (Lehrstuhl Virologie): Prof. Dr. Dr. h.c. Ulrich Koszinowski

Assembly and Budding of Rabies Virus: The Phosphoprotein as Critical Determinant of Particle Production

Dissertation zum Erwerb des Doktorgrades der Naturwissenschaften
an der Medizinischen Fakultät
der Ludwig-Maximilians-Universität München

vorgelegt von
Anika Kern

aus
Lemgo

2011

Gedruckt mit Genehmigung der Medizinischen Fakultät
der Ludwig-Maximilians-Universität München

Betreuer:	Prof. Dr. Karl-Klaus Conzelmann
Zweitgutachter:	Prof. Dr. Andres G. Ladurner
Dekan:	Prof. Dr. med. Dr. h.c. Maximilian Reiser, FACR, FRCR
Tag der mündlichen Prüfung:	15.05.2012

Ich will Euch mein Erfolgsgeheimnis verraten:

Meine ganze Kraft ist nichts anderes als Ausdauer.

Louis Pasteur (1822 – 1895)

Table of content

List of figures

List of abbreviations

α	anti
A	ampere
aa	amino acid(s)
BDV	Borna disease virus
BF	bright field
BSA	bovine serum albumin
°C	degree Celsius
Co-IP	Co-immunoprecipitation
CPE	cytopathic effect
C-terminus	carboxy-terminus
d	day
DEPC	diethylpyrocarbonate
DLC	dynein light chain
DNA	deoxyribonucleic acid
dNTP	deoxyribonucleotide
Dyn	dynamin
EBOV	Ebola virus
EIAV	equine infectious anemia virus
EM	electron microscopy
ER	endoplasmic reticulum
ESCRT	endosomal sorting complex required for transport
EV	empty vector
FBS	fetal bovine serum
ffu	focus forming unit
fig.	figure
G	glycoprotein
g	gram
h	hour
HIV	human immunodeficiency virus
HRP	horse raddish peroxidase
IFA	immunofluorescence analysis
IFN	interferon
IGR	intergenic region
IRF	interferon regulatory factor
J	joule
L	large protein (polymerase)
l	liter
iVLP	infectious virus-like particle
L domain	Late domain

LB	lysogeny broth
LBV	Lagos bat virus
µ	micro (10^{-6})
M	matrix protein
M	molar
m	milli (10^{-3})
MBP	maltose-binding protein
min	minute
MOI	multiplicity of infection
MOKV	Mokola virus
mRNA	messenger ribonucleic acid
MVA	modified vaccinia virus Ankara
MVB	multivesicular body
N	nucleoprotein
n	nano (10^{-9})
NCS	newborn calf serum
N-terminus	amino-terminus
o/n	over night
P	phosphoprotein
p.i.	post infection
p.t.	post transfection
PAGE	polyacrylamide gelelectrophoresis
PCR	polymerase chain reaction
PEI	polyethyleneimine
PEP	post-exposure prophylaxis
PFA	paraformaldehyde
pH	pondus hydrogenii
PLB	passive lysis buffer
r.t.	room temperature
RIG-I	retinoic acid inducible gene-I
RNA	ribonucleic acid
RNP	ribonucleoprotein
rpm	revolutions per minute
RSV	Rous sarcoma virus
RT	reverse transcription
RV	rabies virus
s	second
SAD	Street Alabama Dufferin
SeV	Sendai virus
siRNA	small interfering RNA
STAT	Signal Transducer and Activator of Transcription
U	unit

UV	ultraviolet
V	volt
v/v	volume per volume
VAMP	vesicle-associated membrane protein
VLP	virus-like particle
Vps4	Vacuolar protein sorting-associated protein 4
VSV	vesicular stomatits virus
w/v	weight per volume
WB	Western blot
WHO	World Health Organization
wt	wild type

Summary

Rabies virus (RV) is an enveloped virus with a negative-sense, single-strand RNA genome (*Rhabdoviridae*, *Mononegavirales*). Following replication in the cytoplasm of infected cells, budding of virions occurs mostly at the plasma membrane. As a prerequisite for the generation of new particles, all structural components of the virus have to assemble at the site of budding. In addition, the cellular environment required for virus release has to be established, i.e. lipids for the viral envelope have to be supplied and proteins for the vesiculation need to be recruited. The RV matrix protein (M) has been proven to be the essential driving force of virus budding (Mebatsion et al., 1996) and disruption of the PPEY Late domain in M which confers interaction with components of the MVB pathway reduces viral titers by one order of magnitude (Harty et al., 2001).

In order to identify new motifs in M which are critical for assembly, an M mutant bank was subjected to a functionality screen (NPgrL assay). Amino acids S20, P21 (M 20AA) and C170 were identified to play a role in release. The recombinant viruses SAD M 20AA, SAD M C170A and SAD M 20AA/C170A showed a decrease in virus titers comparable to L domain mutants. Since the viruses were not severely attenuated, we considered other requirements of RV assembly to exist and found the phosphoprotein (P) to play an essential role in this process. A virus with a mutation at the C-terminus of P, SAD P 288AAA, displayed approx. 10,000-100,000fold reduced cell-free infectious titers but maintained the capacity to spread the infection from cell to cell. The specific defect in budding was verified by demonstrating that the function of P as polymerase cofactor and N binding were not affected by the mutation. A virus which only harbored a single amino acid exchange at the C-terminus (SAD P D290A) had a very similar phenotype with respect to its budding activity and confirmed this intriguing new function of P.

A direct link between P and M could be demonstrated in binding studies. The ten C-terminal amino acids of M were required for binding of M to an internal stretch within the P protein. We hypothesize that the M-P interaction is either directly required for the incorporation of RNP complexes into budding virions or that it plays a role in the regulatory function of M during the transition from transcription to replication. In this work, the C-terminus of P was shown to bind to a component of the SNARE complex VAMP3 and to its neuronal homologs VAMP2 and VAMP1. It is therefore also possible

that P provides adequate host conditions for the assembly and budding of infectious particles. RNAi directed against VAMP3 indicated reduced release of infectious virus. However, it seems likely that VAMP1/2 can functionally compensate for VAMP3 deficiency.

This work shows for the first time that RV P is of significant importance to the viral assembly process in addition to RV M. The association of the P C-terminus with neuronal SNARE complexes (VAMPs) provides a promising basis for the dissection of the so far uncharacterized transsynaptic retrograde spread of RV.

Zusammenfassung

Das Tollwutvirus (*rabies virus*, RV) gehört zu der Familie der umhüllten RNA-Viren, deren einzelsträngiges Genom in negativer Orientierung im Viruspartikel vorliegt (*Rhabdoviridae*, *Mononegavirales*). Die Virusfreisetzung erfolgt durch Knospung an der Plasmamembran infizierter Zellen. Dieser letzte Schritt des viralen Replikationszyklus erfordert ein komplexes Zusammenspiel multipler Faktoren: Einerseits müssen alle Strukturkomponenten des Virions zur rechten Zeit am rechten Ort zusammenkommen, andererseits werden aber auch zelluläre Bestandteile benötigt (Proteine, Lipide etc.), die ggf. dorthin lokalisiert werden müssen. Das RV Matrixprotein (M) ist hierfür essentiell, da es in der Lage ist, das Glykoprotein (G) direkt zu binden (Mebatsion et al., 1999), Ribonukleoprotein- (RNP-)Komplexe zu kondensieren und diese an die Membran zu rekrutieren (Chong and Rose, 1993; Newcomb and Brown, 1981).

Zur Identifizierung von neuen Motiven, die an der Partikelfreisetzung beteiligt sind, wurden M-Mutanten einem transienten Funktionstest unterzogen (*NPgrL assay*). Hierdurch gelang es, die Aminosäuren S20, P21 (M 20AA) und C170 als wichtige Bausteine zu charakterisieren. Die Analyse der drei mithilfe der reversen Genetik hergestellten Viren SAD M 20AA, SAD M C170A und SAD M 20AA/C170A zeigte jedoch, dass lediglich ein geringer Defekt in der Freisetzung infektiöser Partikel vorlag. Demnach bestand die Möglichkeit, dass andere Viruskomponenten ebenfalls zu diesem Prozess beitragen. Der Phänotyp des rekombinanten Virus SAD P 288AAA deutete darauf hin, dass das Phosphoprotein (P) des Tollwutvirus dieser virusimmanente Faktor sein könnte, da die infektiösen Partikel dieses Virus fast ausschließlich intrazellulär zu finden waren. Die extrazellulären infektiösen Titer waren 10.000-100.000fach niedriger als im Wildtypvirus SAD L16. Es konnte bestätigt werden, dass P entscheidend zur Virusbildung beiträgt, da sich die Mutation am C-Terminus in keiner Weise negativ auf andere essentielle Funktionen von P auswirkte. Des Weiteren konnte dies durch ein unabhängig generiertes Virus mit nur einem Aminosäureaustausch (SAD P D290A), das denselben Phänotyp aufwies, verifiziert werden. Die Mitwirkung von RV P bei der Virusknospung ist eine gänzlich neue Funktion dieses Proteins, die in dieser Arbeit zum ersten Mal beschrieben werden konnte.

Daraufhin wurde untersucht, ob und inwiefern RV M, das unbestritten essentiell für die Virusfreisetzung ist, mit P interagiert. Mithilfe von Koimmunpräzipitationen konnte erstmalig eine direkte Bindung zwischen M und P gezeigt werden, welches als essentieller Kofaktor der Polymerase (L) ein Bestandteil des RNP-Komplexes ist. Die letzten zehn Aminosäuren des M-Proteins waren nötig, um an den Anfang der C-terminal gelegenen globulären Domäne von P zu binden.

Weiterhin wurden in dieser Arbeit zelluläre Interaktionspartner des RV P-Proteins untersucht. VAMP3 und seine neuronalen Homologe VAMP1 und VAMP2 kopräzipitierten mit RV P. RNAi gegen VAMP3 reduzierte die Freisetzung von RV um 50 %.

Diese Arbeit zeigt zum ersten Mal, dass neben M auch P des Tollwutvirus eine wichtige Rolle im viralen Assemblierungsprozess spielt. Die hier beschriebene direkte Bindung der beiden Proteine aneinander verknüpft P mit M, der treibenden Kraft für die Virusknospung. Der C-Terminus von P könnte entweder direkt essentielle Faktoren für die Virusfreisetzung rekrutieren oder als Assemblierungsplattform dienen. Eine Assoziation dieser P-Domäne mit neuronalen SNARE-Komplexen (VAMPs) stellt einen ersten Hinweis dar, wie der bislang unbekannte Mechanismus der charakteristischen transsynaptischen Ausbreitung des Tollwutvirus vonstattengehen könnte.

1 Introduction

1.1 Rabies virus

1.1.1 Pathology and treatment

Rabies is a zoonotic disease caused by rabies virus (RV) which can infect a broad host spectrum, in particular mammals. RV infects hosts at the periphery, enters motoneurons and reaches the central nervous system via retrograde axonal transport. Natural infections mostly occur via bites and scratches by rabid animals such as dogs or bats. After a highly variable incubation period (one week to one year), the first clinical presentation of the infection is mostly non-specific and symptoms can include fever and paraesthesia at the wound site. Two forms of disease may follow: (i) furious rabies with signs of hyperactivity and hydrophobia and (ii) paralytic rabies. The latter causes muscle paralysis and coma slowly develops (WHO, 2010). After onset of clinical symptoms, the outcome of the disease is almost invariably fatal. Wilde et al. suggest symptomatic and comfort care as palliative treatment for most patients because so far only an early endogenous immune response (high cerebrospinal fluid antibody titers without detectable virus levels) was attributed to be beneficial for survival (Wilde et al., 2008). Production of neutralizing antibodies against the RV glycoprotein is crucial for the clearance of the infection and depends on B lymphocytes and CD4+ T cells which are stimulated by the ribonucleoprotein (RNP) complex of RV (Dietzschold et al., 2008; Dietzschold et al., 1987; Hooper et al., 2009). The most abundant viral protein, the nucleoprotein, is the stimulative component of the RNP and it has been reported to have superantigen-like properties (Lafon et al., 1992).

Already in 1885, Louis Pasteur treated a boy with desiccated spinal cords derived from rabies-infected rabbits after the boy had been bitten by a rabid dog. This was the first successful use of a post-exposure prophylaxis (PEP). To date, more than 55,000 individuals, mostly children, still succumb to the infection per year although a safe vaccine is available. However, the confirmed numbers of fatal infections are believed to be highly underestimated due to the lack of both surveillance and post mortal detection of RV in rural areas of the world (Bourhy et al., 2010). About 320,000 deaths are thought to be

prevented annually by administration of 15 million PEP treatments which to date comprises RV-specific IgG and five doses of vaccine (WHO, 2010).

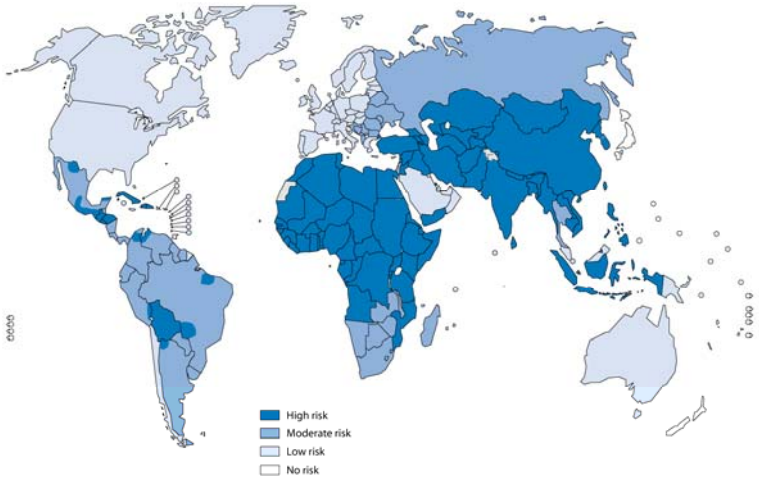

Figure 1: Distribution of risk levels for human to contract rabies.

Data Source: WHO, 2010

1.1.2 Viral taxonomy

The RV belongs to the *Rhabdoviridae* virus family. Together with the *Paramyxoviridae*, *Filoviridae* and *Bornaviridae*, the *Rhabdoviridae* constitute the order of *Mononegavirales*, also known as the nonsegmented negative-strand RNA viruses. The *Rhabdoviridae* are further divided in six genera (*Lyssavirus*, *Vesiculovirus*, *Ephemerovirus*, *Novirhabdovirus*, *Cytorhabdovirus*, *Nucleorhabdovirus*). Members of the seven genotypes of the *Lyssavirus* genus besides RV (genotype I) include Lagos bat virus (LBV, genotype II), Mokola virus (MOKV, genotype III), Duvenhage virus (genotype IV), European bat lyssavirus 1 and 2 (EBLV-1 and -2, genotypes V and VI, respectively) and the Australian bat lyssavirus (ABLV, genotype VII). Vesicular stomatitis virus (VSV) is representative for the *Vesiculovirus* genus.

1.1.3 Virion structure and protein functions

The negative-sense twelve kb single-strand RNA genome of RV comprises only five genes all of which encode viral structural proteins: the nucleoprotein (N), phosphoprotein (P), matrix protein (M), glycoprotein (G) and the viral RNA-dependent RNA polymerase (L).

Figure 2B shows a schematic depiction of the virus particle. The N protein encapsidates the viral RNA to form a helical nucleocapsid (Naeve et al., 1980). Together with its essential cofactor P, L can only use this N-RNA hybrid as functional template for transcription and replication. Altogether, the proteins associated with the RV genome build the RNP complex.

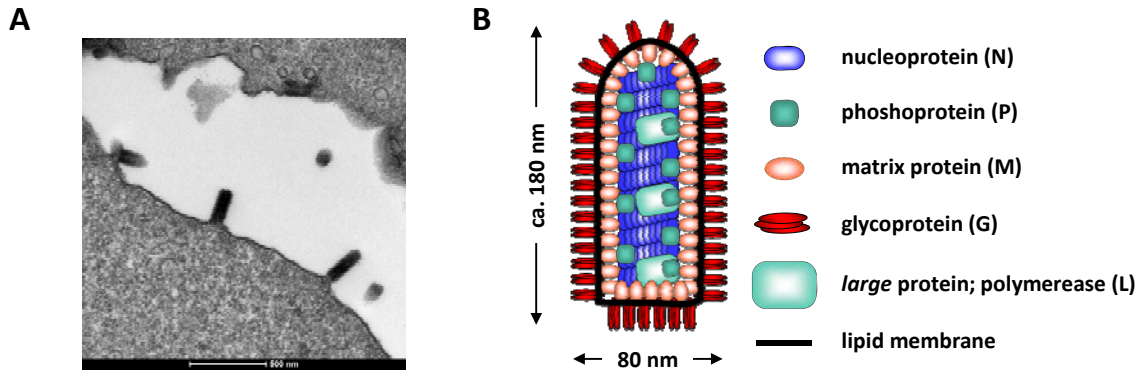

Figure 2: Rabies virus particle.

(A) Electron micrograph of RV particles budding from the plasma membrane of BSR T7/5 cells (courtesy of O. Berninghausen). (B) Schematic representation of a RV virion (adapted from (Doerr and Gerlich, 2009))

M condenses the RNP and forms a lattice underneath the viral envelope, thereby bridging the space between the RNP and the membrane. The only viral protein inserted into the envelope is G, of which the C-terminus interacts with M (Mebatsion et al., 1999). The trimeric spikes of G are required for cell attachment, entry and pH-dependent membrane fusion. So far, three different neuronal receptors have been identified which facilitate RV entry: nicotinic acetylcholine receptor (nAChR), neuronal cell adhesion molecule (NCAM), and p75 neurotrophin receptor (p75NTR). The latter is exclusively expressed in neuronal tissue and is therefore discussed to be involved in the synaptic transmission of RV whereas the former two most likely enable virus entry at the neuromuscular junction (Lafon, 2005). Probably, there will be more RV receptors discovered in the future since phospholipids, glycolipids, sialic acid, and carbohydrates have been proposed to play a role in RV entry into non-neuronal cells such as fibroblasts (Superti et al., 1984; Superti et al., 1986; Wunner et al., 1984). G not only determines the cell tropism but also accounts for the neuroinvasive phenotype of RV (Etessami et al., 2000). The characteristic retrograde axonal transport is mediated by the G protein and it could be shown that

intact enveloped RV particles serve as transport cargo of axonal vesicles (Klingen et al., 2008; Mazarakis et al., 2001).

1.1.4 Viral gene expression

The order of the genes from 3´ to 5´ is conserved within the order *Mononegavirales*. Transcription and replication of the virus occur upon release of the RNP into the cytosol of infected cells. For a schematic overview see Figure 3.

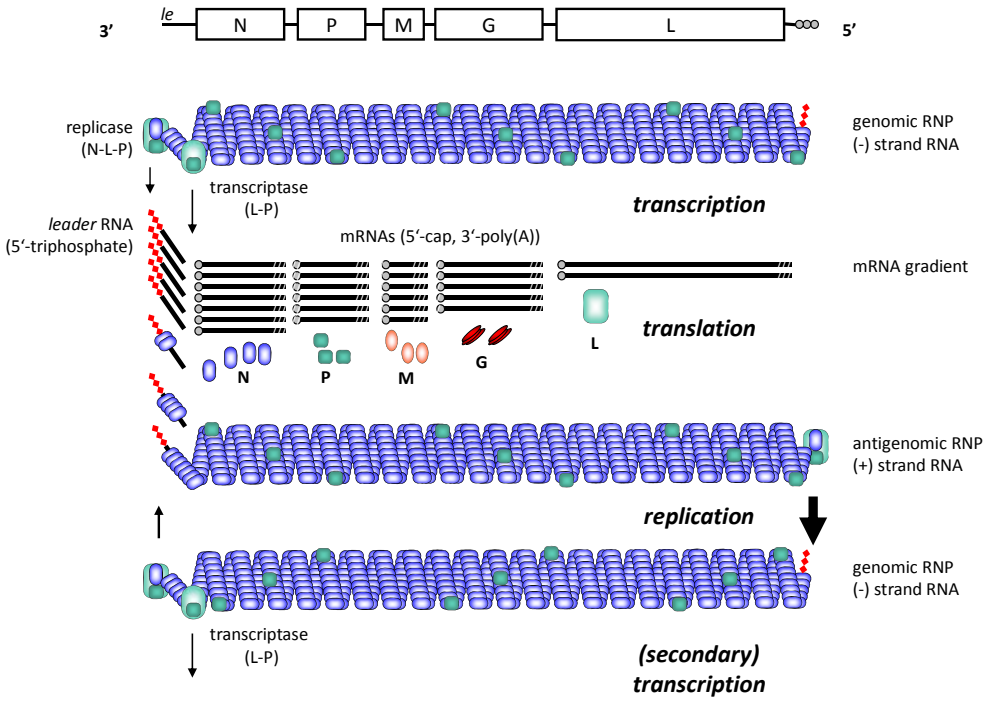

Figure 3: Schematic overview of RV transcription and replication.

The genomic organization is represented schematically at the top. The viral polymerase complex (L and P) transcribes the viral genome to generate six products: leader RNA plus five protein coding mRNAs. Due to eventual dissociation of the polymerase at gene borders, a transcript gradient is formed. For replication, full-length copies of the genome are produced from the genomic and antigenomic promoters when sufficient N protein is present to co-transcriptionally encapsidate the genome and antigenome RNAs.
(adapted from (Doerr and Gerlich, 2009))

The viral polymerase complex starts transcription at the 3´-end of the genome. This region is called leader region or genomic promoter and consists of 58 untranslated nucleotides. The leader transcript carries a 5´-triphosphate group, is not capped and

presumably harbors the N encapsidation signal (Abraham and Banerjee, 1976). The sequential transcription of the viral genes is subsequently started and results in the generation of five monocistronic, 5´-capped and polyadenylated mRNAs. The genes are flanked by intergenic regions (IGRs) which contain the transcription stop and start signals. Due to the chance of dissociation of the polymerase complex from its template and the need to reinitate transcription at the 3´-end, the mRNAs of the genes most proximal to the 3´-leader sequence are the most abundant and the amount of transcribed mRNAs decrease towards the 5´-end (mRNA gradient). In contrast to VSV in which all genes are separated by only two nucleotides, the IGRs of RV vary in length from two to 24 nucleotides. They are considered intrinsic regulators of the transcription gradient since the likelihood of the polymerase to fall off its template correlates with the number of nucleotides (Finke et al., 2000).

Viral replication occurs at later stages of infection when abundant viral proteins have been made. During the reaction, genome-length RNAs are transcribed first from the genomic and second from the antigenomic promoter in order to generate genome copies. Ample N protein is required for replication since the transcripts need to be encapsidated co-transcriptionally over their entire length.

While a high concentration of N and P is a prerequisite for replication, RV M was shown to control the balance between transcription and replication such that high M levels favor replication over transcription. A single amino acid exchange in M (R58G) led to a loss of its regulatory function (Finke and Conzelmann, 2003; Finke et al., 2003).

(For a discussion on transcription/replication initiation of RNA-dependent RNA polymerases in *Mononegavirales* see (Curran and Kolakofsky, 2008) and the two responses (Banerjee, 2008; Whelan, 2008)).

1.2 The phosphoprotein of rabies virus

The expression of the RV P protein occurs from a single mRNA but due to ribosomal leaky scanning and subsequent translation initiation at downstream in-frame AUGs the SAD strain expresses three N-terminally truncated P forms (P2-P4) in addition to full-length P (P1, Figure 4) (Chenik et al., 1995). P1 and P2 are the most abundant forms.

Although no sequence similarity between P proteins even within one virus family exists, *Rhabdoviridae* and *Paramyxoviridae* share a conserved organization of their respective P proteins: concatenated functional domains alternate with intrinsically disordered regions. This is a characteristic property of a modular protein in which the separate domains are able to fold autonomously. The overall fold of these domains however is only conserved among virus family members (between VSV and RV or Sendai virus (SeV) and measles virus) (Gerard et al., 2009). The crystal structure of the C-terminal 112 amino acids of RV P indicates that the globular domain folds into six helices (α1-α6) and a small, antiparallel β-sheet made of two strands (Mavrakis et al., 2004).

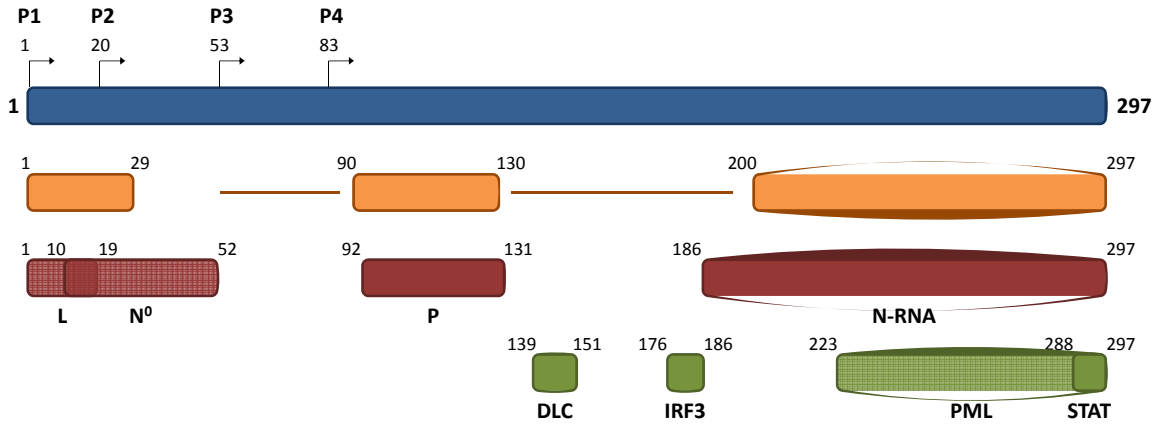

Figure 4: Modular organization and functions of SAD P.

The SAD P protein is depicted in blue. The N-terminally truncated P2, P3 and P4 are translated from downstream AUG codons due to by ribosomal leaky scanning. Gerard et al. predicted structured and disordered regions of RV P (Gerard et al., 2009). Structured regions are indicated as orange boxes, predicted disordered regions as orange lines. For non-filled spaces, the predictions were not conclusive. Regions involved in intraviral functions/interactions are shown in red. Those required for host protein interactions are indicated in green.

RV P forms dimers in solution (Gerard et al., 2007) and the crystal structure of the required dimerization domain (aa 92-131) reveals that in addition to the lack of sequence conservation, even the structure differs from the known P oligomerization domains of related viruses such as VSV and SeV (Ivanov et al., 2010).

P is a multifunctional protein of RV which is essentially required during the virus life cycle. Most importantly, it is the non-catalytic subunit of the viral transcription and replication complexes. The polymerase by itself cannot associate with nucleocapsids. However, P is able to bind to L and to N-RNA via its C-terminus (Chenik et al., 1994; Chenik et al., 1998; Schoehn et al., 2001) and thereby is thought to mediate joining of L and its template, the viral RNA genome. In addition, P acts as a chaperone for newly synthesized N and keeps it in its soluble RNA-unbound form (N^0) until N encounters viral RNA (Chenik et al., 1994; Mavrakis et al., 2003; Mavrakis et al., 2006). This prevents N aggregation and unspecific association of N with cellular RNAs present in the cytoplasm of infected cells.

In addition to its intramolecular and intraviral interactions, P is able to bind to several cellular proteins. An internally located domain of P (aa 139-151) is able to strongly interact with dynein light chain (DLC1, LC8) (Jacob et al., 2000; Raux et al., 2000). Initial assumptions that this interaction confers the retrograde axonal transport were disproven by the finding that DLC-binding is dispensable for spread *in vivo* and that G mediates transport of intact viral particles (Klingen et al., 2008; Mebatsion, 2001). Instead, a supportive effect of DLC-binding on viral transcription in neurons was discovered (Tan et al., 2007).

Another very important function of P *in vivo* is the ability to interfere with the host´s innate immune response upon infection. Type I and type III interferon (IFN) is induced after recognition of RV 5´-triposphate RNA by RIG-I and subsequent recruitment of adapter molecules ultimately leads to signaling to the nucleus via the transcription factor IRF3 (Hornung et al., 2006; Pichlmair et al., 2006). RV P is able to interrupt the signaling cascade by preventing IRF3 phosphorylation and thereby abrogating dimerization of the transcription factor which is essential for its nuclear translocation (Brzózka et al., 2005). The amino acids 176-186 of RV P are crucially required for IRF3 inhibition and a deletion of these residues in the virus is associated with induction of IFN and a lack of pathogenicity in mice (Rieder et al., 2011).

Moreover, P is also able to counteract IFN signaling by direct binding of phosphorylated STAT1 and STAT2 and in that way preventing nuclear accumulation of STATs (Brzózka et al., 2006; Vidy et al., 2005). A deletion of the ten C-terminal amino acids of P (aa 288-297) leads to the loss of JAK-STAT inhibition (Brzózka et al., 2006).

1.3 Completion of the infectious cycle: Virus release

In order to complete the virus life cycle, progeny virions have to exit the infected cell, thereby allowing virus dissemination by either infection of neighboring cells, different organs or a new host. As a prerequisite, all structural components of the infectious particle (including the genetic information) have to assemble correctly. The information for (helper protein-assisted) self-assembly is an intrinsic feature of every virus and is based on recognition of sequences allowing distinct transport of virus components e.g. single proteins, protein complexes or even intact virus particles.

The presence or absence of a lipid envelope is the major discriminant by which mechanism viruses are released. This is irrespective of other viral determinants such as RNA or DNA genome or replication in the nucleus or cytoplasm. Non-enveloped virus particle liberation requires the breakdown of the host´s cellular membrane either induced by apoptosis or cell lysis (cell burst), thus terminating the infection by killing the host cell.

Viruses which are surrounded by a lipid bilayer achieve their envelope through a process called budding. In general, this is the release of membranous vesicles. In the specific case of virus infection, budding requires the deformation of an intact cellular membrane, the incorporation of the viral components required for a new infectious cycle and the final fission event which leads to the creation of distinct cellular and viral membranes. Budding can occur at intracellular membranes or at the plasma membrane. Examples are *Coronaviridae* budding at the ER-Golgi intermediate compartment (ERGIC) (Tooze et al., 1984), *Bunyaviridae* budding at the Golgi compartment (Hung et al., 1985; Pettersson, 1991) and RV being released from the plasma membrane (Jayakar et al., 2004). There is evidence that some RV strains are also able to accumulate particles intracellularly (e.g. SAD) but the ability to be released from the plasma membrane seemed to be common to the lyssaviruses tested in the study by Finke and coworkers (2010).

1.4 The matrix protein of rabies virus

Matrix proteins of *Mononegavirales* are peripheral membrane proteins and fill the space between the RNP and the viral membrane. This has been shown biochemically e.g. for VSV M (Chong and Rose, 1993; Ogden et al., 1986) and also by electron microscopy (EM) for RV M (Mebatsion et al., 1999). Membrane association is conferred by a mixture of hydrophobic and electrostatic interactions with a probable contribution of post-translational palmitoylation of M (Chong and Rose, 1993; Gaudin et al., 1991; Ye et al., 1994). More recently, the results of cryo-EM of VSV particles (together with data from already solved crystal structures of rhabdovirus proteins) allowed a more detailed understanding of the virus particle composition (Ge et al., 2010). It was known that VSV M and RV M condense the RNP (Mebatsion et al., 1999; Newcomb and Brown, 1981; Newcomb et al., 1982) and recruit them to the site of budding (plasma membrane) (Chong and Rose, 1993). The cryo-EM model by Ge et al. now shows that the virion contains two interlaced helices. The inner one is composed of N-RNA and the outer is made of M proteins such that M sits in the cleft between and makes contact to two turns of the N-RNA helix. This architecture leads to stabilization and packing of the RNP. In addition, M homotypically interacts with its neighboring M and M in the above helix. From the cryo-EM structure, the binding of M to the G tail is discussed to be stoichiometric (three M bind to one G trimer).

Matrix proteins are predestined to be the major driving force of viral budding since they fulfill all requirements for correct virus assembly. They are able to associate with lipid membranes, bind to the respective glycoproteins via their cytoplasmic tails and interact with the viral RNPs (reviewed in Jayakar et al., 2004). Experimental evidence for RV was obtained when Mebatsion et al. observed particle formation even in the absence of G. Complete deletion of M reduced released virus titers more than 500,000fold (Mebatsion et al., 1996; Mebatsion et al., 1999).

For many different viruses which require the matrix protein for budding, the glycoproteins have supportive effects. This holds true for RV particle release. Deletion of RV G accounts for a 30fold reduction of RV budding. These data led Mebatsion and colleagues in 1996 to raise the model for RV budding in which a concerted action of an

internal membrane pushing force (provided by M, the main player in release) and a supportive, membrane external pulling force (provided by G) act in synergy.
In addition to its function in budding, the formation of the characteristic bullet-shape of the virion requires the M protein. The few G-containing vesicles released from M-deleted virus resembled rod-like structures and were therefore distinct from RV. Providing the M protein *in trans* restored wild type (wt)-like morphology of the particles (Mebatsion et al., 1999).

As opposed to RV M, VSV M has been shown to have intrinsic budding activity (Justice et al., 1995; Li et al., 1993), meaning that solely expressing M leads to the release of the protein within lipid vesicles whereas N, P or G alone did not (Justice et al., 1995). A study by the Rose laboratory, however, demonstrated that high VSV G expression also results in vesiculation and thus G release (Rolls et al., 1994). Further studies confirmed a supportive effect of VSV G to the budding process. Both, the cytoplasmic domain and the membrane proximal stem located on the extracellular side of VSV G, were shown to contribute to efficient budding (Robison and Whitt, 2000; Schnell et al., 1998).
In vitro studies revealed the ability of VSV M to induce membrane curvature without the requirement of any other viral or cellular protein (Solon et al., 2005). However, in this study, Solon and colleagues never observed the final membrane fission event. Other factors, either of viral or cellular origin, have to come into play to overcome the energy barrier of the final pinching off event.

1.5 The role of ESCRT in RNA virus budding

Cellular pathways, e.g. the endosomal sorting complex(es) required for transport- (ESCRT) 0-III, are known to contribute to the release of many enveloped viruses such as retroviruses or Ebola virus (EBOV). The ESCRTs function in a sequential or concentric manner (Babst et al., 2002; Nickerson et al., 2007). Action of ESCRT-III and the AAA-type ATPase Vps4 leads the final fission of vesicles harboring the respective cargo and disassembly/recycling of ESCRT-III, respectively (reviewed in Hurley and Hanson, 2010).

In the uninfected cell, the ESCRTs are required for the formation of an endosomal compartment, the multivesicular body (MVB). MVBs are for example involved in the targeted lysosomal degradation of membrane proteins (e.g. receptor downregulation) and in antigen presentation. Mono-ubiquitin attached to most cargo proteins is recognized by ESCRT-0, I and II and serves as a sorting signal into MVBs. ESCRT-III then recruits deubiquitinating enzymes (Katzmann et al., 2001; Reggiori and Pelham, 2001; Stuffers et al., 2009a). Topologically, the budding process is identical to exocytosis because membrane curvature is induced away from the cytoplasm (as opposed to vesicle formation in the secretory pathway).

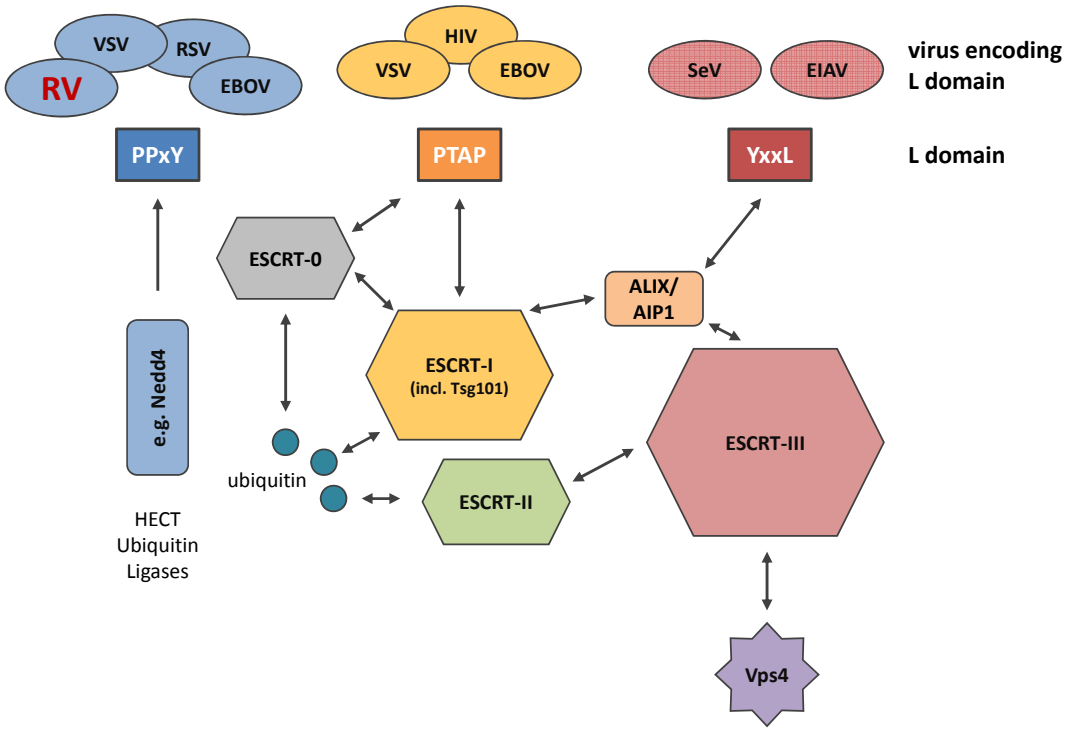

Figure 5: The ESCRT pathway.

Schematic overview of the ESCRT components required for MVB formation which is hijacked by viruses. All multi-protein complexes are shown as hexagons. Examples of viruses encoding the respective Late (L) domains in their matrix/gag proteins are shown at the top. (RV: rabies virus, VSV: vesicular stomatits virus, RSV: Rous sarcoma virus, EBOV: Ebola virus, HIV: human immunodeficiency virus, EIAV: equine infectious anemia virus, SeV: Sendai virus) (modified and adapted from Bieniasz, 2006)

Several virus-ESCRT interactions are known and all of them are mediated by so-called Late (L) domains. This name refers to the phenotype late during an infection, namely the release process, which is observed in electron micrographs after disruption of the motif.

Originally, the three L domains known by now were identified in retroviruses; the PPxY motif in Rous sarcoma virus (RSV) (Xiang et al., 1996), PT/SAP in the human immunodeficiency virus-1 (HIV-1) (Gottlinger et al., 1991; Huang et al., 1995) and the YxxL sequence in equine infectious anemia virus (EIAV; see Figure 5) (Puffer et al., 1997). These motifs are present in the respective Gag polyprotein which harbors the matrix protein equivalent of retroviruses. Gag proteins are able to produce virus-like particles (VLPs) without other viral components. The only exception of this rule is the foamy virus which only needs the gp130Env protein for budding (Shaw et al., 2003). The functionality of the L domains has been shown mostly by mutational analyses in which disruption led to a loss or reduction of budding in the mutant protein but reintegration of a heterologous L domain restored the function. The functional interchangeability has been demonstrated for L domains of several enveloped viruses including exchange of the RSV L domain with that of HIV-1 (Parent et al., 1995) and that of the overlapping EBOV VP40 L domains with the two separate L domains present in VSV M (Irie et al., 2005).

RV contains two overlapping L domains in its M protein: ^{35}PPEYVPL^{41}. The PPxY motif mediates binding to Nedd4 which is an E3 ubiquitin ligase of the HECT family. Indeed, release of infectious particles from RV infected cells is slightly sensitive to depletion of free ubiquitin leading to a 10-20fold decrease in virus titers. For VSV, this effect was demonstrated to be dependent on the PPPY motif, since disruption of the L domain itself decreased titers but rendered the virus resistant to proteasome inhibitors (Harty et al., 2001). Although experimental data is not published for RV, the VSV system is most likely transferable to the closely related RV L domain.

Many RNA viruses which depend on ubiquitin for their release are also influenced by the action of Tsg101, a component of ESCRT-I which mediates cargo binding, and Vps4, the most downstream effector of MVB formation. Using stable cell lines inducibly expressing dominant-negative mutants of Vps4, Taylor and colleagues demonstrated that RV release is 18-28fold reduced upon inhibition of MVB formation (2007). In a study by the Harty laboratory, however, neither dominant-negative Vps4 expressed from a recombinant RV nor siRNA directed against Tsg101 mRNA impaired RV budding (Irie et al., 2004).

In general, the YxxL motif could mediate binding to ALIX/AIP1, a protein associated with ESCRT-III. In spite of the presence of this second L domain in RV M (^{38}YVPL^{41}), no

contribution to efficient budding could be assigned to this amino acid motif (Wirblich et al., 2008).

1.6 Aim of this study

The formation and release of intact viral particles from infected cells which then can initiate a new infectious cycle is a complex process and requires highly coordinated actions of all virion components. The M protein of RV is known to be essential for budding and an L domain conferring interaction with the cellular ESCRT machinery within the protein was shown to contribute to release. This supportive effect is dependent on ubiquitin and the proteasome system. However, recombinant L domain mutant RV showed a reduction in infectious virus titers of only one order of magnitude, still leaving 10^7 ffu/ml released in the cell culture supernatant of infected cells.

This work addresses the question which amino acid sequences, other than the already described L domain, substantially contribute to the formation of RV particles. The overall goal being the identification of cellular interaction partners underlying the molecular mechanism for virus release.

For other RNA viruses, a significant contribution to budding by viral proteins other than the respective matrix proteins was shown. Here, the RV P protein and its role in the assembly and release of new virions were investigated. Reverse genetics allowed the detailed analysis of P mutant viruses which are defective in the budding of virus particles, revealing a so far unappreciated role in the assembly of new virions.

2 Materials and Methods

2.1 Materials

2.1.1 Chemicals

Chemicals were purchased from INC Biochemicals Inc., Invitrogen, Merck, New England Biolabs, Riedel-de-Häen, Roche, Roth, and SIGMA-Aldrich. The radiochemical ^{32}P-αCTP was provided by Amersham Pharmacia and Hartmann Analytic.

2.1.2 Buffers and solutions

Mini Preparation

Flexi I	100	mM	Tris-HCl, pH 7.5
	10	mM	EDTA
	200	µg/ml	RNase
Flexi II	200	mM	NaOH
	1	% (w/v)	SDS
Flexi III	3	M	K-acetate
	2	M	Acetic acid, pH 5.75

Immunoprecipitation

Co-IP buffer	50	mM	Tris-HCl, pH 7.5
	150	mM	NaCl
	2	mM	EDTA
	1	mM	Na_3VO_4
	0.5	% (v/v)	NP-40 substitute
(directly before use:	1	tablet	Complete protease inhibitor cocktail / 50 ml)

Protein gels

10 % APS	10	% (w/v)	Ammoniumpersulfate
Jagow gel buffer	3	M	Tris-HCl, pH 8.45
	0.3	% (w/v)	SDS
Jagow anode buffer	2	M	Tris-HCl, pH 8.9
Jagow kathode buffer	1	M	Tris-HCl, pH 8.25
	1	M	Tricine
	1	% (w/v)	SDS
Protein lysis buffer	62.5	mM	Tris-HCl, pH 6.8
	2	% (v/v)	SDS
	10	% (v/v)	Glycerine
	6	M	Urea
	5	% (v/v)	β-Mercaptoethanol
	0.01	% (w/v)	Bromphenol blue
	0.01	% (w/v)	Phenol red
Staining solution	50	% (v/v)	Methanol
	10	% (v/v)	Acetic acid
	0.1	% (w/v)	Brilliant blue
Wash solution	50	% (v/v)	Methanol
	10	% (v/v)	Acetic acid

Western blotting

10x Semi dry buffer	480	mM	Tris-HCl, pH 8.6
	390	mM	Glycine
	0.05	% (w/v)	SDS

1x Semi dry buffer	100	ml	10x Semi dry buffer
	180	ml	Methanol abs.
	720	ml	H_2O
1x PBS	1.37	M	NaCl
	27	mM	KCl
	12	mM	KH_2PO_4
	65	mM	$Na_2HPO_4x2H_2O$ (pH 7.4)
PBS/Tween	1	X	PBS
	0.05	% (v/v)	Tween-20

Agarose gels

10x TAE	2	M	Tris-HCl, pH 7.8
	250	mM	Na-acetate trihydrate
	250	mM	EDTA
1x TAE + EtBr	300	ml	10x TAE
	2700	ml	H_2O
	150	µl	Ethidium bromide solution 1 % (w/v)
OG loading buffer	50	% (v/v)	10x TAE
	15	% (w/v)	Ficoll 400
	0.125	% (w/v)	Orange G
10x TE	100	mM	Tris-HCl, pH 7.5
	10	mM	EDTA
Blue juice	0.125	% (w/v)	Bromphenol blue
	0.125	% (w/v)	Xylenecyanol
	0.125	% (w/v)	Orange G
	15	% (w/v)	Ficoll 400

	50	% (v/v)	10x TAE
1 kb marker buffer	380	µl	1x TE
	100	µl	Blue juice
	20	µl	1 kb DNA ladder

Northern blot

RNA agarose gel	2	g	Agarose (RNA grade)
	4	ml	50x phosphate buffer
	26.7	ml	Formaldehyde, 37 %
	167.3	ml	H_2O ultra pure
50x phosphate buffer	250	mM	$Na_2HPO_4x2H_2O$ (pH 6.8-7.0)
	250	mM	$NaH_2PO_4xH_2O$
Glyoxal solution	8.8	M	Glyoxal
10x SSC	1.5	M	NaCl
	150	mM	Na-citrate $x2H_2O$ (pH 7.0)
Zeta hybridizing buffer	250	mM	$Na_2HPO_4x2H_2O$ (pH 7.2)
	250	mM	$NaH_2PO_4xH_2O$
	1	mM	EDTA
	7	% (w/v)	SDS
Zeta wash buffer 5 %	8	% (v/v)	50x phosphate buffer
	1	mM	EDTA
	5	% (w/v)	SDS
Zeta wash buffer 1 %	8	% (v/v)	50x phosphate buffer
	1	mM	EDTA
	1	% (w/v)	SDS

Bacteria growth media

LB	85	mM	NaCl
	0.5	% (w/v)	Bacto yeast extract
	1	% (w/v)	Bactotryptone
	1	mM	$MgSO_4$
(LB-Amp	25	mg/ml	Ampicillin)
LB++	1	X	LB
	20	mM	$MgSO_4$
	10	mM	KCl

Immunofluorescence

3 % PFA/PBS	1	X	PBS
	3	% (w/v)	Paraformaldehyde (PFA)
80 % Acetone	800	ml	Acetone p.a.
	200	ml	dH_2O
50 mM NH_4Cl/PBS	1	X	PBS
	50	mM	NH_4Cl
0.5 % Triton X-100/ PBS	1	X	PBS
	0.5	% (v/v)	Triton X-100

Cell culture

5 mM EDTA/PBS	1	X	PBS
	5	mM	EDTA
TEN buffer	50	mM	Tris-HCl, pH 7.4
	150	mM	NaCl

	1	mM	EDTA
Fixing solution	1	X	PBS
	2	%	Formaldehyde
	0.2	%	Glutaraldehyde
Staining solution	1	X	PBS
(light sensitive)	5	mM	$K_3Fe(CN)_6$
	5	mM	$K_4Fe(CN)_6 \times 3H_2O$
	2	mM	$MgCl_2 \times 6H_2O$

2.1.3 Kits

Plasmid purification:	Nucleobond PC 100 (Macherey-Nagel)
	Nucleobond Xtra Midi (Macherey-Nagel)
Cloning:	QIAquick PCR Purification Kit (QIAGEN)
	QIAquick Gel Extraction Kit (QIAGEN)
RNA isolation:	RNeasy Mini Kit (QIAGEN)
Transfection:	Mammalian Transfection Kit (Stratagene)
Luciferase reporter gene assay:	Dual-Luciferase® Reporter Assay System (Promega)
Northern blot:	Nick Translation Kit (Amersham, GE Healthcare)

2.1.4 Enzymes

BioPfu DNA Polymerase (Biomaster)

Phusion High-Fidelity DNA Polymerase (Finnzymes)

Transcriptor Reverse Transcriptase (Roche)

Restriction enzymes (New England Biolabs)

Shrimp Alkaline Phosphatase (New England Biolabs)

T4 DNA Ligase (New England Biolabs)

2.1.5 Antibodies

primary antibodies

	spec.	appl.	dilution	manufacturer
anti-actin	rabbit	WB	1:10,000	Sigma-Aldrich
anti-Dyn2	rabbit	WB	1:20,000	Thermo Scientific (Pierce Antibodies)
anti-flag M2	mouse	IFA	1:200	Sigma-Aldrich
anti-flag M2	rabbit	WB	1:10,000	Sigma-Aldrich
anti-Rab1B	rabbit	WB	1:1,000	santa cruz biotechnology
anti-RV G	mouse	IFA	1:2 (or undiluted)	hybridoma cell line (monoclonal)
anti-RV G (HCA05/1)	rabbit	WB	1:10,000	Metabion
anti-RV M (M2D4)	rabbit	WB/IFA	1:10,000/1:200	J. Cox (BFAV, Tübingen)
anti-RV N (S50)	rabbit	WB	1:20,000	J. Cox (BFAV, Tübingen)
anti-RV N-FITC (Centocor™)	mouse	IFA	1:200	FDI Fujirebio Diagnostics
anti-RV P (FCA05/1)	rabbit	WB	1:10,000	Metabion
anti-RV P (160-5)	rabbit	WB	1:50,000	S. Finke (FLI, Insel Riems)
anti-RV P (25G6)	mouse	IFA	1:200	D. Blondel (CNRS, France) (Raux et al., 1997)
anti-VAMP3	rabbit	WB	1:1,000	Acris Antibodies
anti-MBP HRP	mouse	peptide spot	1:1,000	Abcam

secondary antibodies

anti-rabbit Alexa Fluor® 488	goat	WB/IFA	1:10,000/1:200	Molecular Probes, Invitrogen
anti-mouse Alexa Fluor® 488	goat	IFA	1:200	Molecular Probes, Invitrogen
anti-mouse Alexa Fluor® 633	goat	IFA	1:200	Molecular Probes, Invitrogen
anti-mouse tetramethylrhodamine	goat	IFA	1:200	Molecular Probes, Invitrogen
To-Pro®-3		IFA	1:1,000	Molecular Probes, Invitrogen
anti-rabbit HRP	goat	WB	1:10,000	Dianova
HRP-Protein A		WB	1:10,000	Zymed

2.1.6 Primers

AK5	*M Acc65I fwd*	CGAGGTACCATGAACCTCCTACGTAAG
AK8	*M NheI rev*	CGAGCTAGCTTATTCTAGAAGCAGAGAG
AK21	*fwd Rab1B Acc65I*	CGAGGTACCATGAACCCCGAATATG
AK22	*rev Rab1B NheI*	CGAGCTAGCCTAGCAACAGCCACC
AK23	*fwd VAMP3 Acc65I*	CGAGGTACCATGTCTACAGGTCCAAC
AK24	*rev VAMP3 NheI*	CGAGCTAGCTCATGAAGAGACAAC
AK25	*VAMP3 flag fwd Acc65I*	CGAGGTACCATGGATTACAAGGATGACGACGATAAGTCTACA GGTCCAACTGCTG
AK28	*M flag fwd Acc65I*	CGAGGTACCATGGATTACAAGGATGACGACGATAAGAACCTC CTACGTAAGATAG
AK33	*Dyn2 fwd Acc65I*	CGAGGTACCATGGGCAACCGCGGGATG
AK34	*Dyn2 rev SphI*	CGAGCATCGTTAGTCGAGCAGGGAC
AK35	*Dyn2 fwd EcoRI*	CGAGAATTCATGGGCAACCGCGGGATG
AK36	*Dyn2 rev Acc65I*	CGAGGTACCTTAGTCGAGCAGGGAC
AK38	*flagVamp1A/B fwd Acc65I*	CGAGGTACCATGGATTACAAGGATGACGACGATAAGTCTGCT CCAGCTCAACCGC
AK40	*Vamp1B rev NheI*	CGAGCTAGCTCAGCGATACTTAC
AK42	*flagVamp2 fwd Acc65I*	CGAGGTACCATGGATTACAAGGATGACGACGATAAGTCGGC T ACCGCTGCCACC
AK43	*Vamp2 rev NheI*	CGAGCTAGCTTAAGTGCTGAAGTAAAC
AK46	*M ΔC10 rev Nhe*	CGTGCTAGCTTATTCGGACCTTTGTGTCTG
AK51	*Pd185-209 rev#1*	AAGGGCTGGAGGGCCAGAAGC
AK52	*Pd185-297 fwd#2*	TCCAAAAAATATAAGTTTCCC
AK62	*P fwd HpaI*	CGAGTTAACATGAGCAAGATCTTTGTC
AK70	*P rev NarI n*	TCGGGCGCCTTAGCAAGATGTATAGCG
AK76	*Pd191-219 rev#1*	ATTGGTAGCCGACCATTC
AK77	*Pd191-219 fwd#2*	GGGATACTCTTGTAT
AK86	*P Muta Q288A fwd*	CTGAGTAAAATCATG GCAGATGACTTGAATCGCTATACATC
AK87	*P Muta D289A fwd*	CTGAGTAAAATCATGCAAGCTGACTTGAATCGCTATACATC
AK88	*P Muta D290A fwd*	CTGAGTAAAATCATGCAAGATGCCTTGAATCGCTATACATC
KB21	*pCR3-P1 3´EcoRI*	ATGAATTCTTAGCAAGATGTATAGCGATTCAA
KB147	*P ΔQDD rev*	CATGATTTTACTCAGCTTGTCGGAT
M20AA	*C. Schnellhammer*	GACACTCAAAAATCCGCTGCAGCGTCAGCCCCTC
20rev	*C. Schnellhammer*	GGATTTTTGAGTGTCCTCGTCCCTGC

2.1.7 siRNA sequences

CO3	GCGCAUUCCAGCUUACGUAtt	(Besch et al., 2007)
Rab1B#1	AGAAGGUGGUGGACAACACtt	
Rab1B#2	GAAUGCACCAAUGUCGAGtt	
Dyn2	GACAUGAUCCUGCAGUUCAUUtt	(Pizzato et al., 2007)
Vamp3#1	GAAGCUCUCUGAGUUAGACtt	
Vamp3#2	GAGACCAGAAGCUCUCUGAtt	

2.1.8 Plasmids

The following plasmids are commercially available:

pCR3	Invitrogen	eucaryote expression vector (CMV promoter)
pEGFP-N3	Clontech	eGFP vector (CMV promoter)
pRL-CMV	Promega	*Renilla* luciferase vector (CMV promoter)
pDNR-LIB VAMP3	imaGenes	vector with VAMP3 cDNA
pCMV-SPORT6 Rab1B	imaGenes	vector with Rab1B cDNA

The following plasmids were kindly provided:

pCAGGS	M. Schwemmle, Freiburg
p125Luc	T. Fujita, Kyoto, Japan (Yoneyama et al., 1996)

The following plasmids were generated in the laboratory of K.-K. Conzelmann:

pTIT	S. Finke (Finke and Conzelmann, 1999)
pTIT N	S. Finke
pTIT P	S. Finke
pTIT L	S. Finke
pTIT G	S. Finke
pTIT M	S. Finke
pTIT M 20AA	S. Finke
pTIT M 2AAA	S. Finke
pTIT M C170A	S. Finke
pTIT M I164A	S. Finke
pTIT M L99R	S. Finke
pTIT M R167G	S. Finke
pTIT M 20AA/C170A	A. Kern (primer: M20AA + 20rev)
pTIT M Mokola	S. Finke
pTIT P 288AAA	A. Kern (primer: AK44 + KB21)
pTIT PΔQDD	A. Kern (primer: AK44 + KB21)
pTIT P Q288A	A. Kern (primer: AK86 + KB147)
pTIT P D289A	A. Kern (primer: AK87 + KB147)

pTIT P D290A	A. Kern (primer: AK88 + KB147)
pCAGGS N	A. Ghanem
pCAGGS P	A. Ghanem
pCR3 flag P	K. Brzózka
pCR3 flag PΔQDD	K. Brzózka
pCR3 P	K. Brzózka
pCR3 P288AAA	K. Brzózka
pCR3 PΔ139-161	K. Brzózka
pCR3 PΔ191-297	K. Brzózka
pCR3 PΔ220-297	K. Brzózka
pCR3 PΔ245-297	K. Brzózka
pCR3 PΔQDD	K. Brzózka
pCR3 PΔ185-209	A. Kern
pCR3 PΔ191-219	A. Kern
pSDI flash_SC	M. Schnell (Schnell and Conzelmann, 1995) + A. Ghanem (Ghanem et al., 2011)
pCAGGS Dyn2	A. Kern
pCAGGS Dyn2 K44A	A. Kern
pCAGGS flag M	A. Kern (primer: AK28 + AK8)
pCAGGS flag MΔC10	A. Kern (primer: AK28 + AK46)
pCAGGS flag VAMP1B	A. Kern (primer: AK38 + AK40)
pCAGGS flag VAMP2	A. Kern (primer: AK42 + AK43)
pCAGGS flag VAMP3	A. Kern (primer: AK25 + AK24)
pCAGGS Rab1B	A. Kern (primer: AK21 + AK22)
pCAGGS VAMP3	A. Kern (primer: AK23 + AK24)

full-length constructs

pSAD L16_SC	A. Ghanem (Ghanem et al., 2011)
pSAD M20AA/C170A	A. Kern
pSAD P288AAA	K. Brzózka
pSAD PΔQDD	K. Brzózka
pSAD P D289A	A. Kern (primer AK62 + AK70)
pSAD P D290A	A. Kern (primer AK62 + AK70)
pSAD P Q288A	A. Kern (primer AK62 + AK70)
pSAD PΔ185-209	A. Kern (primer AK62 + AK70)
pSAD PΔ191-219	A. Kern (primer AK62 + AK70)
pSAD ΔP_eGFP	A. Ghanem

2.1.9 Viruses

SAD L16
SAD M 20AA

SAD M C170A
SAD M 20AA/C170A
SAD ΔPLP
SAD PΔ185-209
SAD PΔ191-219
SAD P 288AAA
SAD PΔQDD
SAD P Q288A
SAD P D289A
SAD P D290A
SAD ΔP_eGFP
SAD Ambi
NPgrL
MVA-T7pol

2.2 Methods: Working with nucleic acids

2.2.1 Polymerase chain reaction (PCR)

PCR for cloning

With the help of the PCR it is possible to amplify DNA fragments. Therefore, template specific primers were used which flank the DNA of interest. Primers were also used in order to add nucleotides to the desired 3´- or 5´-ends of the DNA (e.g. restriction sites, tags).

The standard PCR was set up as follows:

10-100	ng	template DNA
10	µl	10x polymerase reaction buffer incl. $MgSO_4$
10	µl	DMSO
250	nM	Primer forward
250	nM	Primer reverse
1	µl	dNTPs (25 µmol each)
2.5	U	DNA polymerase
ad 100	µl	dH_2O

The reaction was carried out in a thermocycler with heated lid.

	time	temperature	step	
1.	30 s	95 °C	(enzyme activation)	
2.	30 s	95 °C	(denaturing)	
3.	30 s	43 °C	(primer annealing)	30-35 cycles
4.	60 s / 500 bp	72 °C	(elongation)	
5.	10 min	72 °C	(final elongation)	
6.	∞	4 °C	(end)	

The QIAquick PCR Purification Kit (QIAGEN) was used to purify the DNA following the supplier´s instructions. The DNA was eluted from the column using 40 µl dH_2O.

Mutagenesis PCR

In order to introduce mutations in a given plasmid, mutagenesis PCR was used. The reaction was set up without DMSO. The temperature for primer annealing depended on the melting temperature of the primer pair used in the reaction.

	time	temperature	step	
1.	30 s	95 °C	(enzyme activation)	
2.	30 s	95 °C	(denaturing)	
3.	30 s	50-60 °C	(primer annealing)	18-20 cycles
4.	60 s / 500 bp	72 °C	(elongation)	
5.	10 min	72 °C	(final elongation)	
6.	∞	4 °C	(end)	

The mutagenesis PCR reaction was digested with 20 U *Dpn*I at 37 °C for 1 hour (h). *Dpn*I cleaves methylated DNA, therefore cutting only the DNA template of bacterial origin. Without further purification, 3.5 µl of the PCR reaction were transformed into XL1-Blue chemically-competent bacteria.

2.2.2 Agarose gel electrophoresis of DNA

Gels containing 1 % agarose in 1x TAE were used to analyze the length of PCR products and the outcome of restriction digests.

For the analysis of DNA fragments >10,000 bp and <500 bp, gels containing 0.7 % and 2 % agarose, respectively, were used.

DNA samples were mixed with 20 % (v/v) Orange G loading buffer, loaded onto the gels and subjected to electrophoresis at 120 V for 45 min or longer, depending on the length of the fragments and agarose concentration. The electrophoresis buffer was 1x TAE + EtBr. Gels were analyzed on a Biorad GelDoc System using UV light.

2.2.3 Purification of DNA from agarose gel

After preparative digest of DNA fragments the samples were subjected to agarose gel electrophoresis and bands of the expected sizes were cut out of the gel. Long wavelength UV light was used to limit DNA damage and exposure time was kept as short as possible. The DNA was purified from the gel slice using the QIAquick Gel Extraction Kit (QIAGEN) and DNA was eluted from the column using 40 µl dH_2O.

2.2.4 Restriction digest

Restriction endonucleases cut DNA and thereby create sticky or blunt ends on double-strand DNA molecules. They were used for molecular manipulation of plasmids (preparative digest) and for the subsequent analysis of generated constructs (analytical digest). The reaction was performed according to the manufacturer´s protocol.

Preparative digest:

3-5	µg	DNA
5	µl	10x buffer
(5	µl	10x BSA if required)
10-20	U	restriction enzyme(s)
ad 50	µl	dH_2O

Analytical digest:

0.1-0.5	µg	DNA
1	µl	10x buffer

(1	µl	10x BSA; if required)
1-5	U	restriction enzyme(s)
ad 10	µl	dH_2O

Residual buffer, enzyme and DNA fragments had to be removed if the DNA was used in subsequent reactions. The DNA was purified either with the QIAquick PCR Purification Kit (QIAGEN) according to the manufacturer´s protocol (elution in 40 µl dH_2O) or with a preparative agarose gel and subsequent gel extraction.

2.2.5 Dephosphorylation of DNA

Directly after the restriction digest, vector DNA was dephosphorylated at its 5´-end by the shrimp alkaline phosphatase according to the manufacturer's instructions. Open ends of the vector could therefore not religate in the following ligation reaction and thus prevented growth of bacterial colonies which did not contain insert DNA.

2.2.6 Ligation

The cut insert and vector DNA fragments were ligated using T4 DNA Ligase. The standard reaction mix contained:

0.5	µl	purified vector backbone
5	µl	purified DNA fragment (insert)
1	X	T4 DNA Ligase reaction buffer
200	U	T4 DNA Ligase
ad 20	µl	dH_2O

For three-fragment-ligations the same amount of both insert DNA fragments was used. Reactions were incubated either at room temperature (r.t.) for 1-2 h or at 16 °C o/n. The ligation mix was transformed into XL1-Blue chemically-competent cells.

2.2.7 Transformation of plasmid DNA into competent bacteria

50 µl of chemically-competent XL1-Blue bacteria were thawed on ice and either 100 ng of plasmid DNA or the ligation mix were added. The mixture was incubated for 20 min on ice, followed by a heat shock at 42 °C for 2 min and further incubation on ice for another

2 min. Afterwards, 200 µl of LB++ medium were added and the bacteria were shaken at 37 °C for 45 min.

Transformed bacteria were plated on LB-agar plates including 25 mg/ml of ampicillin, the resistance gene of the transformed plasmid. The plates were incubated at 37 °C o/n or until single colonies were visible.

2.2.8 Isolation of plasmid DNA from bacteria

Small scale (mini preparation)

For small scale plasmid preparation, 1 ml of LB-Amp was inoculated with single bacteria colonies picked from a LB-agar plate and grown at 37 °C o/n while shaking (liquid culture). The bacteria suspension was pelleted (14,000 rpm, 30 s, r.t.) and the supernatant was discarded. The pellet was resuspended in 200 µl of Flexi I. Then, 200 µl of Flexi II were added, mixed gently and incubated at r.t. for 5 min. After complete lysis of the bacteria had occurred, 200 µl of Flexi III were added, again mixed gently and incubated on ice for another 5 min. The emerging debris was pelleted by centrifugation (14,000 rpm, 7 min, r.t.) and the cleared lysate was mixed with 360 µl of pure isopropanol in order to precipitate the DNA. Plasmid DNA was pelleted by centrifugation (14,000 rpm, 7 min, r.t.) and the supernatant was discarded. The air-dried pellets were resolved in 50 µl dH_2O by shaking for several minutes.

Medium scale (midi preparation)

For medium scale plasmid preparation, 100 µl of the suspension of transformed bacteria were directly added to 50 ml of LB-Amp and shaken at 37 °C o/n. The plasmid DNA was extracted using the NucleoBond® AX-100 or the NucleoBond® Xtra Midi/Maxi Kit (Machery & Nagel) according to the manufacturer's instructions. The DNA concentration was determined using the Nanodrop 1000 (peqlab) and plasmid DNA was stored at -20 °C until further use.

2.2.9 Sequencing of DNA

Sequencing reactions were performed by *MWG Eurofins* (Martinsried, Germany) using the *Value Read Tube protocol*. 1 – 2 µg of template DNA were mixed with 15 pmol of a sequencing oligo and the total volume was adjusted to 15 µl with dH_2O.

The results were analyzed with the two softwares DNAMAN (Version 5.0 or higher) and Chromas (Version 1.45).

2.2.10 Isolation of RNA from eukaryotic cells

Total cellular RNA was isolated using the RNeasy Mini Kit (QIAGEN). $1x10^6$ cells were lysed in 350 µl RLT buffer containing 0.1 % β-mercaptoethanol. The lysates were mixed thoroughly with 1 equivalent of DEPC treated 70 % ethanol. Then, the lysates were loaded onto the columns and centrifuged (10,000 rpm, 15 s, r.t.). The flow-through was discarded and the columns were washed once with 700 µl of RW1 buffer and once with 500 µl of RPE buffer via centrifugation (10,000 rpm, 15 s, r.t.). Afterwards, the columns were centrifuged (10,000 rpm, 1 min, r.t.) without the addition of liquid in order to remove residual buffer. The RNA was eluted with 30 µl of DEPC-treated dH_2O and centrifugation (10,000 rpm, 1 min, r.t.). Then, the eluate was reloaded on the same column and centrifuged again. The RNA concentration was determined using the Nanodrop 1000 (peqlab) and the extracted RNAs were stored at -20 °C or -80 °C.

2.2.11 Reverse transcription

Reverse transcription (RT) PCR was performed using the Roche Transcriptor RT (Roche). Therefore, 1 µg RNA was mixed with 3 µl specific reverse primer (0.3 M) in a final volume of 13 µl. After incubation at 65 °C for 10 min, 4 µl RT buffer, 0.5 µl RNase inhibitor, 2 µl dNTPs and 0.5 µl Transcriptor RT were added and incubated at 55 °C for 30 min. The reaction was heated to 85 °C for 5 min in order to inactivate the enzyme.

2.2.12 Northern blot

The RNA for Northern blot was extracted as described above. 1.8 µl glyoxal solution and 3 µl 5x phosphate buffer were added to 2.7 µg RNA in a total volume of 7.2 µl of RNase free H_2O. The mix was incubated at 56 °C for 45 min. The preparation of RNAs for Northern Blot was completed by adding 3 µl Blue juice.

The samples were loaded on a denaturing agarose gel. The gel consisted of 2 g agarose heated and thereby dissolved in 167.3 ml ddH_2O (ultrapure) and 4 ml 50x phosphate buffer. 26.7 ml 37 % formaldehyde were added to the lukewarm solution and the gel was subsequently poured.

Electrophoresis was performed in 1x phosphate buffer at 25 V o/n. The RNA was stained in acridine orange solution and as a control rRNA was visualized under UV light.

The Vacu-Blot system (Biometra) was used for the transfer of the RNAs onto nylon membranes. The transfer was carried out at -100 mbar for 2 h. Afterwards, the membrane was air-dried and the RNA was UV-crosslinked using 0.125 J.

In order to generate probes labeled with ^{32}P the Nick Translation Kit (Amersham) was used. Therefore, 100 ng of DNA were mixed with 4.2 µl dNTPs without cytosin, 2 µl ^{32}P-dCTP and 3 µl of the polymerase to a final volume of 20 µl. After incubating the reaction for 90 min at r.t., the probe was purified using the QIAquick Nucleotide Removal Kit (QIAGEN) and thereafter denatured at 95 °C for 5 min.

The nylon membranes were preincubated with Zeta hybridizing buffer at 68 °C for 10 min and then incubated o/n in 8 ml fresh buffer supplemented with the probes. The next morning, the membranes were washed once with Zeta wash buffer 5 % and twice with Zeta wash buffer 1 %. All washing steps were carried out at 68 °C for 20 min. The membranes were air-dried and the radioactively labeled RNAs were detected by exposing the membrane to a photosensitive screen or a ^{32}P-sensitive film (GE Healthcare) at -80 °C for 2 h or longer. The screen was analyzed using the Storm scanner (GE Healthcare) and the software ImageQuant (GE Healthcare).

2.3 Methods: Working with cells

2.3.1 Cell culture

Cell lines were grown and maintained at 37 °C and 5 % CO_2 gas mixture. The growth medium required for each cell line is depicted below. All cell culture reagents were purchased from Invitrogen.

cell line	origin	details	medium
BSR T7/5	hamster	kidney cells expressing the T7 polymerase	G-MEM 4+
P cells	hamster	derivative of BSR T7/5 cells expressing RV P	G-MEM 4+
$MG_{on}136$	hamster	derivative of BSR cells inducibly expressing RV	G-MEM 4+

		M and G	
HEK 293T	human	kidney cells expressing the SV40 large T antigen	D-MEM 3+
Huh7	human	hepatoblastoma cell line	D-MEM 3+
NA	mouse	neuroblastoma cell line	D-MEM 3+

medium	**composition**
G-MEM 4+	G-MEM
	10 % (v/v) NCS
	30 mg/ml tryptose phosphate
	2 % (v/v) amino acids
	penicillin/streptomycin
D-MEM 3+	D-MEM
	10 % (v/v) FBS
	1 % 100x L-glutamine
	penicillin/streptomycin

All cell lines used are adherently growing cells. They were split 1:6 to 1:10 2-3 time per week depending on the growth rate. For splitting, they were detached from the cell culture flask using trypsin/EDTA.

BSR T7/5 cells´ medium was supplemented with 1 mg/ml G418 every other passage. P cells and $MG_{on}136$ received 1 mg/ml G418 and 0.5 mg/ml hygromycin every passage as selection medium.

2.3.2 Transfection

Cells were transfected with plasmid DNA using either $CaPO_4$ (*Stratagene Mammalian Transfection Kit*), Lipofectamine™ 2000 (Invitrogen) or FuGENE® (Roche) according to the manufacturers´ protocols. For co-immunoprecipitation (Co-IP) experiments, per µg DNA

2.5 µl PEI (1 mg PEI per ml in H_2O) were used according to the protocol for FuGENE®. siRNAs were transfected with Lipofectamine™ RNAiMAX (Invitrogen).

2.3.3 Fixation of cells

Acetone

The cell supernatants were discarded and cells were washed once with PBS and once with 80 % ice-cold acetone. Cells were overlayed with fresh 80 % acetone and fixed at 4 °C for 20 min. The acetone was discarded and fixed cells were air-dried before being further processed.

Paraformaldehyde

All steps below-mentioned were carried out at r.t.. The cells were washed once with PBS and once with 3 % PFA/PBS in PBS and thereafter fixed in fresh PFA/PBS buffer. After 20 min, the cells were washed three times with PBS and incubated in 50 mM NH_4Cl/PBS for 10 min. Subsequently, the cells were treated with 0.5 % Triton-X100/PBS for 10 min in order to permeabilize the membrane and then washed again with PBS.

2.3.4 Immunofluorescence

For confocal imaging, the fixed cells on cover slips were blocked in 0.5 % skim milk in PBS at r.t. in order to minimize unspecific binding of the primary antibody. The blocking solution was discarded and the incubation with primary antibody was carried out for 2 h at 37 °C (for dilutions see chapter 2.1.5). Following the staining, the cells were washed 3x in PBS and thereafter incubated with the secondary antibody solution as required. After 30 min at 37 °C the cover slips were washed 3x with PBS, once with dH_2O and then fixed on a microscope slide either using VECTASHIELD® HardSet™ Mounting Medium or VECTASHIELD® Mounting Medium (Vector Labs); the latter required sealing of the cover slip with nail polish.

Confocal imaging was performed with a *Laser Scanning Microscope* (Axiovert 200M, Zeiss) and data analyses carried out using the corresponding software (*LSM Meta* software).

2.4 Methods: Working with virus

2.4.1 Virus stock production

Rabies virus

In this work the RV strain SAD L16 was used which is a recombinant derivative of the attenuated SAD B19 strain. For virus stock production, $1x10^6$ BSR T7/5 cells were seeded in a T25 flask and the cell suspension was infected (MOI=0.01-0.1). The cells were grown under standard conditions and 72 h post infection (p.i.) supernatants were collected. Cell debris was removed by low speed centrifugation (1,800 rpm, 4 °C, 5 min) and aliquots of the cleared supernatant were stored at -80 °C. The infected cells were provided with fresh media in order to allow a second harvest of virus after another 48 h.

NPgrL virus

The NPgrL virus is a recombinant RV derivative in which the M and the G genes are replaced by an eGFP- and a dsRed-coding cassette, respectively (Finke et al., 2003). In order to produce virus stocks, the cell line $MG_{on}136$ was used which, upon induction by doxycycline, expresses the M and G proteins of RV.

$1x10^6$ $MG_{on}136$ cells were seeded in a T25 flask and the cell suspension was infected with NPgrL virus (MOI=0.1). The cells were grown to confluency and thereafter split in a T175 flask. M and G expression was induced by addition of doxycycline (1 µg/ml) at approx. 90 % confluency of the cell layer. After 3 days, the supernatants were collected and processed as for RV stocks. Fresh medium was again supplemented with doxycycline and 3 days later supernatants were harvested a second time.

Vaccinia virus (MVA-T7pol)

The modified vaccinia virus Ankara (MVA) is a highly attenuated vaccinia virus strain which is unable to replicate in most mammalian cell lines. The MVA-T7pol is a recombinant derivative and expresses the bacteriophage T7 RNA polymerase (Sutter et al., 1995).

In order to generate MVA-T7pol stocks, $1x10^6$ BSR T7/5 cells were seeded in a T25 flask and infected (MOI=1). Fresh BSR T7/5 cells in T175 flasks grown to 90 % confluency were infected with 50 % of the cell-supernatant mix from the initial infection at the time of

cytopathic effect (CPE) occurrence. Again, the cells were monitored for CPE induction (approx. 2 days after transfer) and the virus was harvested as follows: Cells and supernatant were collected and centrifuged (3,500 rpm, 4 °C, 20 min). The supernatant was discarded and cells were resuspended in 1 ml G-MEM 4+. The cells were lysed by repeated freeze-thaw cycles (3x) in liquid nitrogen and 3 shots of ultrasonic sound. Lysates were stored in aliquots at -80 °C.

2.4.2 Virus titration

Rabies virus

The determination of infectious titers was carried out in 96well dishes with 1.2 x 10^4 BSR T7/5 cells per well. 2 h after seeding, a serial 10x dilution of the virus containing solution (e.g. virus stock, cell culture supernatant) was prepared (10^0 -10^{-7}) in G-MEM. 100 µl of each dilution was added to one well in duplicates and cells were incubated at 37 °C for 48 h. The cells were fixed with acetone and stained with an antibody coupled to FITC against the RV N protein (Centocor) for 2 h at 37 °C.

Foci were counted from each well using non-confocal UV microscopy (Olympus IX71) and foci forming units per ml (ffu/ml) were calculated from these results.

Vaccinia virus (MVA-T7pol)

In order to determine the titers of virus stocks, the lacZ gene in the MVA-T7pol genome was used as a reporter.

The titration was carried out in 24well dishes with 5 x 10^4 BSR T7/5 cells per well. 2 h after seeding, a serial 10x dilution of the virus stock was prepared (10^0 -10^{-9}) in G-MEM. 100 µl of each dilution was added to one well in duplicates and cells were incubated at 37 °C for 24-48 h. The supernatant was removed, the cells were fixed for 10min at r.t. in fixing solution and afterwards washed once with PBS. 250 µl of X-Gal solution (1 mg/ml in DMSO) were freshly added to 10 ml of staining solution and the cells were incubated in staining solution for 30-60 min at 37 °C. Afterwards the cells were again washed in PBS once, foci were counted under the microscope and titers were calculated.

2.4.3 Generation of recombinant rabies virus (virus rescue)

In order to reconstitute infectious virus from cloned cDNA, BSR T7/5 cells seeded in 6well dishes were used. 1 h before transfection the medium was taken off the cells and replaced by 1 ml of D-MEM. 10 µg of the plasmid coding for the RV antigenome (pSAD) together with the helper plasmids pTIT N (5 µg), pTIT L (2.5 µg) and pTIT P (2.5 µg) were transfected using the $CaPO_4$ method. After incubation for 3.5 h under standard conditions the transfected cells were washed once with G-MEM 4+ and then grown in 2 ml G-MEM 4+. The supernatant was collected 72 h post transfection (p.t.), cell debris was removed (2800 rpm, 4 °C, 5 min) and passaged onto fresh BSR T7/5 cells seeded in 6well dishes (passage 1A). The cells were grown for 48-96 h. 2 ml of fresh G-MEM 4+ were added to the transfected cells at the time of passage 1A and let grown for another 72 h. The supernatants of the transfected cells were then passaged as described before (passage 1B). In order to verify that recombinant virus was rescued, the supernatants of passage 1A and B were collected at the indicated time points and stored for further analyses. The cells were fixed with acetone and stained against RV N using Centocor as proof of positive rescue. Supernatants of positive rescues were titrated and used for stock production.

If there were no foci present in either passage 1A or 1B, the transfected cells were trypsinized and ¼ was seeded in a new 6well dish and ¾ into a T25 flask (splitting). After another 72 h incubation at standard conditions the cells in the 6well plate were fixed and stained as described above. In case foci were detected, the supernatant of the T25 flask was harvested, titrated and used for stock generation.

2.4.4 Density gradient centrifugation of rabies virus particles

In order to analyze the protein composition of virus particles, analytical ultracentrifugation was performed. 12 ml of a continuous 6 to 21 % iodixanol gradient were prepared using 6 ml each of 10 % and 35 % OptiPrep™ solutions (Axis-Shield). The gradient was overlaid with the virus containing medium and centrifuged to equilibrium (18 h, 27,000 rpm, 4 °C, SW32.1 Ti (Beckman Coulter)). Twelve 1 ml fractions were collected from top to bottom of the gradient (no. 1-12) and stored at -80 °C until further analyses. For Western blot analysis, equal amounts of protein lysis buffer and the respective fractions were mixed and subjected to SDS-PAGE.

2.4.5 Minigenome assay

Minigenome assays are used in order to study transcription and replication of RV. In this work specifically, the ability of P mutants to act as polymerase cofactor were analyzed. The assay was carried out essentially as previously described (Ghanem et al., 2011). Briefly, BSR T7/5 cells in 6well dishes were transfected with pSDI flash_SC (4 µg) and pRL-CMV (5 ng), pTIT N (5 µg), pTIT L (2.5 µg) and pCR3 P (2.5 µg) using CaPO4 (Stratagene). In a negative control pCR3 P was omitted. 48 h p.t. the cells were harvested in passive lysis buffer (Promega) and lysates were subjected to reporter gene assays using the Dual-Luciferase® Reporter Assay System (Promega). Luciferase activity was measured with a luminometer (Berthold Lumat LB 960) according to the manufacturer's instruction.

2.4.6 Infectious virus-like particle assay

In order to study the ability of different P proteins to support the budding of infectious virus particles, we made use of the infectious virus-like particle (iVLP) assay (Finke and Conzelmann, 1999). The plasmids for a minigenome assay were transfected in BSR T7/5 cells: pSDI flash_SC (4 µg) and pRL-CMV (5 ng), pTIT N (5 µg), pTIT L (2.5 µg) and - as opposed to the assay described above - pTIT P (2.5 µg). In addition, pTIT M (2 µg) and pTIT G (2 µg) were included in the transfection mix to allow the formation of iVLPs. 3 d p.t. the supernatants were collected and 100 µl of the cell-free supernatants (2,800 rpm, 4 °C, 5 min), which were expected to contain iVLPs, were passaged onto freshly seeded BSR T7/5 cells. 1 h after the passage, the cells were infected with SAD Ambi (MOI=1). This helper virus supports transcription of the minigenome best (Finke and Conzelmann, 1999) and allows for reporter assays which were carried out 48 h after the passage. The cells of the initial transfection were also harvested in passive lysis buffer (Promega) at the time of passage and lysates were subjected to reporter gene assays using the Dual-Luciferase® Reporter Assay System (Promega). Luciferase activity was measured with a luminometer (Berthold Lumat LB 960) according to the manufacturer's instruction.

2.4.7 Interferon reporter gene assay

The Dual-Luciferase® Reporter Assay System (Promega) was used for analysis of IFN induction. $1x10^5$ HEK 293 T cells were transfected with 100 ng firefly reporter construct (p125Luc), 2-5 ng *Renilla* firefly expression construct for normalization (pRL-CMV) and

6 h p.t. the cells were infected with the indicated viruses (MOI=3). 24 h p.t. the cells were lysed in 200 µl 1x Passive Lysis Buffer (PLB) according to the manufacturer´s protocol (Promega) and 1/10 of the lysate was used for measuring the respective luciferase activities. Read-out was performed in a luminometer (Berthold Lumat LB 960) with 5 s/well counting time. The results were analyzed with the MikroWin2000 (Mikrotek) software and Excel (Microsoft).

2.5 Methods: Working with proteins

2.5.1 SDS-PAGE

Denaturing gels for polyacrylamide gelelectrophoresis (PAGE) were poured as follows:

	separating gel			*stacking gel*
	8 %	10 %	12 %	4 %
dH_2O	21.9 ml	19.4 ml	16.7 ml	18 ml
Jagow gel buffer	18 ml	18 ml	18 ml	7 ml
Glycerol	3 ml	3 ml	3 ml	---
Acrylamide	11.3 ml	13.5 ml	16.2 ml	2,8 ml
10 % APS	262.5 µl	262.5 µl	262.5 µl	232 µl
TEMED	25.5 µl	25.5 µl	25.5 µl	36 µl

The separating gel was prepared first and overlaid with isopropanol to allow complete polymerization of the acrylamide by exclusion of oxygen. Next, the isopropanol was discarded, the stacking gel was poured onto the polymerized separating gel and the comb was inserted.

Protein lysates were incubated at 95 °C for 5 min prior to loading. In addition, Co-IP samples were centrifuged (14,000 rpm, r.t., 2 min) to pellet the beads before loading.

The gels were placed in an electrophoresis chamber (peqlab) and Jagow anode and cathode buffers were added. 30-100 µl of protein lysates and 5 µl of Precision Plus Protein™ Standards (*BIO-RAD*) were loaded. Gels were run at 30-75 V o/n.

2.5.2 Western blot

After SDS-PAGE the proteins were transferred onto either nictrocellulose or PVDF membranes (Millipore) using the semi-dry Western blot method. Therefore, the separating gel was washed in cold 1x semi-dry buffer for 5 min. In the meantime Whatman papers and the membrane were soaked in cold 1x semi-dry buffer. The PVDF membranes had to be activated in methanol prior to use.

The blot was assembled as followed (from bottom to top):

1. Whatman paper
2. membrane (nitrocellulose or PVDF)
3. gel
4. Whatman paper

It was made sure that no air bubbles were between the different layers. Blotting was carried out in a blotting chamber (peqlab) with 400 mA/gel for 2 h. Afterwards, the membrane was blocked in 5 % skim milk in PBS for a minimum of 30 min.

2.5.3 Immunodetection

For antibody staining of blotted proteins, the blocking solution was removed from the membrane by extensive washing steps with PBS/Tween. Thereafter, the membrane was incubated with the respective required primary antibodies (for dilutions see 0) either on a shaker at r.t. for 2 h or on a rolling incubator o/n at 4 °C. Again, the membrane was washed 3x in PBS/Tween to remove unbound primary antibody. The HRP-coupled secondary antibody (species according to primary antibody) was used in a 1/10,000 dilution in PBS/Tween and binding to the primary antibody was allowed for 2 h at r.t. on a shaker. For most Co-IP Western blots, HRP-conjugated Protein A was used instead of antibodies. With the help of three washing steps in PBS/Tween the excessive secondary antibody was removed.

1-3 ml of Western Lightning® *Plus*-ECL substrate (PerkinElmer) were prepared per blot. Blots were incubated with the solution and chemiluminescence was detected immediately using *Hyperfilm-ECL* (GE Healthcare Amersham) as long as required or blots were directly scanned and light emission detected with the Fusion FX7 (Vilber Lourmat).

For protein quantification using fluorescence imaging, a special PVDF membrane (Immobilon-FL) was used for blotting and further dealt with as described above with one exception: Instead of HRP-conjugated secondary antibodies, Alexa Fluor® dye-conjugates (Molecular Probes, Invitrogen) were applied. After the final washing step, the membrane was directly scanned in a Typhoon Scanner (GE Healthcare) and data were analyzed with the ImageQuant software (GE Healthcare).

2.5.4 Co-immunoprecipitation

In order to study protein-protein interactions, Co-IP experiments were performed in HEK 293T cells grown in 6 cm dishes. 2-6 µg of each plasmid were transfected per dish using PEI or Lipofectamine™ 2000. The medium was removed 24 h p.t. and 1 ml PBS/EDTA was added in order to detach the cells for harvest. All following steps were carried out on ice or at 4 °C. The cells were transferred into a reaction tube and subsequently pelleted (2,800 rpm, 4 °C, 5 min). The supernatant was discarded and cells were resuspended in 400 µl Co-IP buffer and then lysed on a rolling shaker for a minimum of 45 min. After complete cell lysis had occurred, cell debris was removed by centrifugation (14,000 rpm, 4 °C, 10 min). 40 µl of the cleared lysate were mixed with protein lysis buffer. This sample was used as expression control (INPUT). The remaining 90 % of the lysate were supplemented with 80 – 200 µl of ANTI-FLAG® M2 Affinity Gel (Sigma; in the following referred to as anti-flag beads) and incubated on a rolling shaker for at least 3 h to allow binding of protein complexes to the antibody-coated beads. In a next step, the beads were pelleted by centrifugation (14,000 rpm, 4 °C, 2 min), the supernatant was discarded, 500 µl fresh Co-IP buffer were added to the beads and incubated on a rolling incubator (≥ 20 min). Complete removal of the unbound proteins was achieved by three consecutive washing steps. After the last spin and supernatant removal, 100 µl protein lysis buffer were added to the beads (Co-IP). The samples (INPUT and Co-IP) were subjected to SDS-PAGE and Western blotting.

2.5.5 Peptide spot assay

In this work, CelluSpots™ peptide arrays from Intavis Bioanalytical Instruments were used. These customized peptide arrays displayed the complete RV P protein sequence spotted as peptide-cellulose-conjugates on a planar glass surface. The peptides were 15

amino acids in length of which twelve overlapped with the peptide sequence of the following spot. Incubation of the array with purified proteins of interest allows the identification of linear binding epitopes.

In order to carry out the assay, the array was put in a chamber and appropriate liquid volumes were used to fully cover the glass surface of the array in all incubation steps.

Unspecific binding of proteins was blocked by incubation of the array in 2.5 % skim milk in PBS/Tween for 2 h at r.t.. The array was washed twice with PBS/Tween and then incubated with 2 µg/ml purified maltose-binding protein-tagged RV M protein (MBP-M) in PBS/Tween to allow specific protein binding (3.5 h, r.t., shaking followed by 4 °C incubation o/n). As control, MBP alone was incubated with a separate RV P peptide array under equal conditions. The arrays were washed three times with PBS/Tween and then incubated with a HRP-conjugated MBP antibody for immunodetection (1:1,000 in 2.5 % skim milk in PBS/Tween, r.t., 3 h). ECL substrate was prepared and detection was carried out with a Fusion FX7 (Vilber Lourmat).

3 Results

3.1 M protein sequences involved in RV assembly and budding

The RV M protein is known to be essential in the viral budding process. It is also required for the formation of the characteristic bullet-shape of the viral particle. As it is unknown which amino acids or domains of M are specifically involved in the assembly and budding process besides its well characterized PPxY L domain, we wanted to address this question in an M mutant screen (complementation assay). The M mutant bank which was used for the complementation assays was previously generated in the laboratory. The M sequence of the SAD L16 strain which is a recombinant clone of the vaccine strain SAD B19 served as template for mutagenesis. Almost thirty M mutants were tested in total and the results of selected, representative mutants will be described and discussed here.

3.1.1 Identification of budding-defective M mutants

For the identification of budding-defective M mutants, we made use of a recombinant RV lacking the M and G genes but instead harboring eGFP and dsRed coding cassettes (NPgrL). BSR T7/5 cells were infected with NPgrL virus (MOI=2) and the deficiencies of the virus were complemented *in trans* by transfection of RV G and varying M expression plasmids. RNPs were allowed to accumulate within the cells before expression of M and G was induced by transfection of the respective plasmids 3-4 d p.i.. The expression of M and G proteins was confirmed by Western blot analysis (data not shown). Complementing the two structural proteins leads to the release of viral particles. The supernatants of the transfected cells were collected 18 h p.t. and the amount of infectious virus released from the cells was quantified via endpoint titration of which results obtained with selected M mutants are depicted in Figure 6. Most mutants completely lost their ability to support virus release (e.g. M 2AAA, M I164A). This might be due to incorrect folding, altered transport behavior or different interaction profiles of the protein. Other mutants, such as M L99R, showed little changes compared to M wt behavior, indicating that the mutation does not affect amino acids relevant for virus assembly. A third phenotype observed displayed residual competence to perform M wt protein function (M 20AA, M C170A).

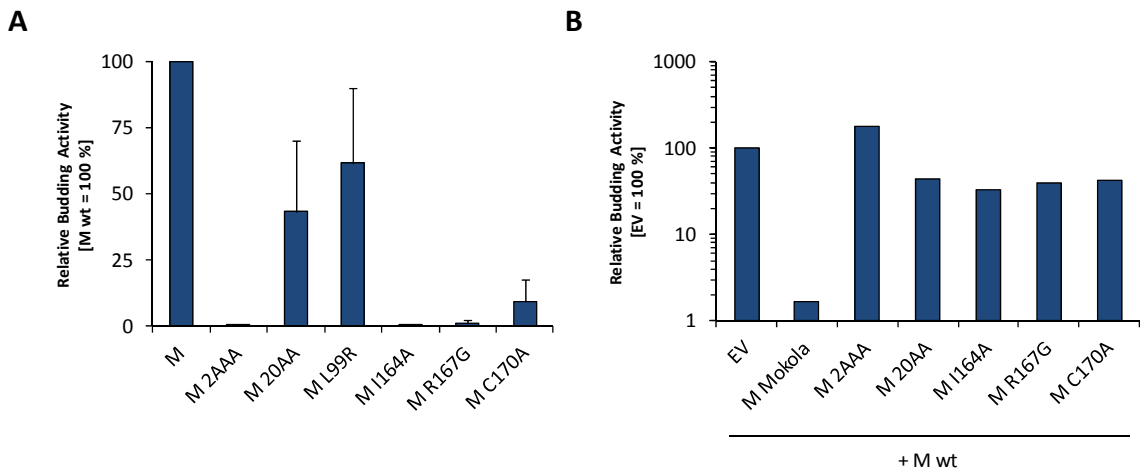

Figure 6: Identification of budding-defective RV M mutants.

(A) BSR T7/5 cells were infected with NPgrL virus (MOI=2). Four d p.i. the cells were transfected with 5 µg each of pTIT G and pTIT M expression plasmids and infected with MVA-T7pol 3. 5 h p.t. (MOI=3). 18 h p.i. the supernatants were harvested, cleared of cell debris and titrated. Three days later, the eGFP positive cells were counted. The results are shown relative to M wt (=100 %). (B) Dominant-negative effects of M mutants. For complementation, M wt expression plasmid was co-transfected with M mutants (2.5 µg each) in addition to G. Mokola virus M displayed a dominant-negative effect on RV budding whereas none of the RV M mutants seem to be inhibitory. EV: empty vector.

The mutants showing reduced infectivity in the afore-mentioned assay were checked whether they can inhibit particle release even in the presence of M wt. Notably, the M protein of MOKV (*lyssavirus* genotype III, distantly related to SAD) interferes with RV M function and was therefore used as a control for dominant-negative effects. The complementation assay was carried out as described above with the exception that two M coding plasmids were transfected (equal amounts of expression constructs for M wt and M mutant). None of the tested SAD L16 M mutants show inhibitory effects in this assembly assay (Figure 6B).

3.1.2 Analysis of G and M mutant co-localization at the plasma membrane

As a prerequisite to induce vesiculation, the M protein has to localize to the plasma membrane. There, M wt co-localizes with G in infected or co-transfected cells even without being an integral membrane protein. We used confocal immunofluorescence microscopy to study the intracellular localization of the mutants which were unable or less able to support virus release in the budding assay. We chose not to include the M 2AAA mutant in our following studies because it is known that N-terminal mutations in

VSV M affect its membrane and RNP association and thereby interfere with its function (Black et al., 1993; Chong and Rose, 1994).

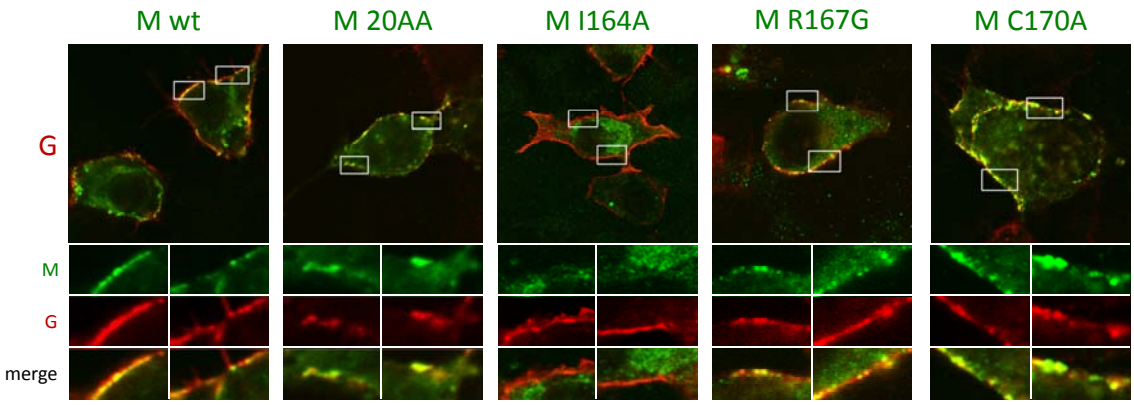

Figure 7: Localization of RV M mutants in the presence of RV G.

BSR T7/5 cells were transfected with 5 µg pTIT M and G expression plasmids as indicated. The cells were fixed with acetone 24 h p.t.. RV M and G were detected with M2D4 and the hybridoma antibody E559, respectively. As secondary antibodies anti-rabbit Alexa Fluor® 488 and anti-mouse Alexa Fluor® 633 were used. M20AA, M R167G and M C170A co-localized with RV G at the plasma membrane (indicated in yellow). M I164A was exclusively distributed within the cytoplasm. Red: G, green: M.

BSR T7/5 cells were transfected with expression plasmids using $CaPO_4$ as indicated in Figure 7. 24 h p.t. the cells were fixed with acetone, stained with specific antibodies and analyzed with a laser scanning microscope. Green color in the micrograph indicates M, red G and yellow co-localization of the respective proteins. The I164A mutation in M completely abolished particle formation as seen in our previous assay. From the microscopic data it became clear that this mutant had lost its ability to be transported to the plasma membrane, showing intracellular accumulation. Its distribution was completely distinct from that of G locating to microdomains at the plasma membrane. Interestingly, three mutants with an obvious defect in the complementation assay did not show aberrant localization compared to M wt: M 20AA, M R167G and M C170A. As shown in the blow-ups, these M mutant proteins were still able to co-localize with G at the cell surface. Notably, we observed increased intracellular localization with some of the mutants compared to wt M which might be the reason for reduced amounts of particles in the supernatant.

3.1.3 RNP recruitment of M mutants

Another function of M during the formation of infectious particles is the recruitment of RNPs to the site of budding and their subsequent incorporation into budding particles (Newcomb and Brown, 1981; Newcomb et al., 1982). Since the overall goal was to identify distinct amino acids required for budding, we wanted to exclude a defect of the M mutants in RNP recruitment and/or RNP condensation. In order to address this question, we made use of the VSV G protein which is known to be sufficient for the formation of vesicles from the plasma membrane (Rolls et al., 1994). Based on the assumption that our candidate M mutant is able to recruit RNPs to its cell surface localization but unable to pinch off, VSV G would mobilize the complexes and incorporate them into the newly formed vesicles in a non-specific manner. VSV G is unable to recruit and condense RV RNPs without RV M.

We set up complementation assays with M mutants as described for Figure 6 but used either RV G or VSV G to supplement NPgrL virus. The results for the M mutants are displayed relative to the respective M wt complementation (RV G or VSV G) (Figure 8)

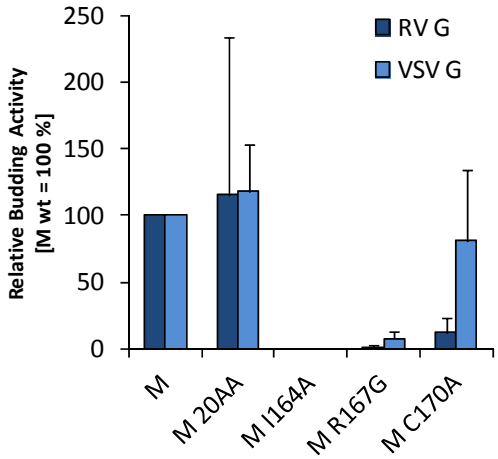

Figure 8: Rescue of M budding defects by the intrinsic budding activity of VSV G.

BSR T7/5 cells were infected with NPgrL virus and transfected with M and G expression plasmids as described for Fig. 6. In addition to complementation with RV G, the VSV G protein was expressed in a separate approach. Results are displayed relative to M wt complementation with either RV G or VSV G (=100 %). The budding defect of M 20AA and M C170A were compensated by expression of VSV G. The mean of at least three independent experiments is shown.

As expected, the mislocalized M I164A failed to produce infectious NPgrL particles even in the presence of VSV G. Moreover, although partially located at the plasma membrane, M R167G gave rise to only very few infectious particles in the supernatant in either of the two settings. This might be due to a failure in RNP recruitment or condensation. Most interestingly, the M C170A mutant´s defect described before could be almost entirely overcome with the help of the VSV G protein; meaning that RNP incorporation into budding particles had occurred. Noteworthy, M 20AA did not exhibit consistent results. On the one hand, the complementation with VSV G led to release of wt-like amounts of infectious particles (77 % to 142 %). On the other hand, the wide range of the data obtained for the mutant M 20AA together with RV G was striking and ranged from 6 % to 240 % relative to the wt control.

Taken together, it could be shown that M C170A is able to co-localize with G at the cell surface, that it can recruit RNPs to the plasma membrane and that it supports genome incorporation into budding virions. However, it fails to fulfill M function in the NPgrL virus complementation assay. We therefore conclude that the M C170A protein has a specific defect in the budding process.

3.1.4 Characterization of M mutant viruses

We intended to gain deeper insight into the release of RV with the help of reverse genetics and selected the M C170A mutant for analysis in the authentic viral context. A RV cDNA harboring the M mutant gene instead of M wt was constructed and the virus was rescued. In addition, we decided to further investigate the phenotype of M 20AA and included this mutant in our viral studies.

The recombinant viruses were characterized with respect to their growth kinetics and transcription and replication rates in comparison to the parental strain SAD L16. Growth kinetics were analyzed in BSR T7/5 cells using multi-step (MOI=0.01) and single-step (MOI=1) growth curves (Figure 9A). The given titers represent the infectious virus particles released in the cell culture supernatant at the indicated time points. The titer differences observed for the multi-step setting were minor and therefore not considered to be significant. No differences could be observed in the case of the single-step growth curve when comparing the three recombinant viruses.

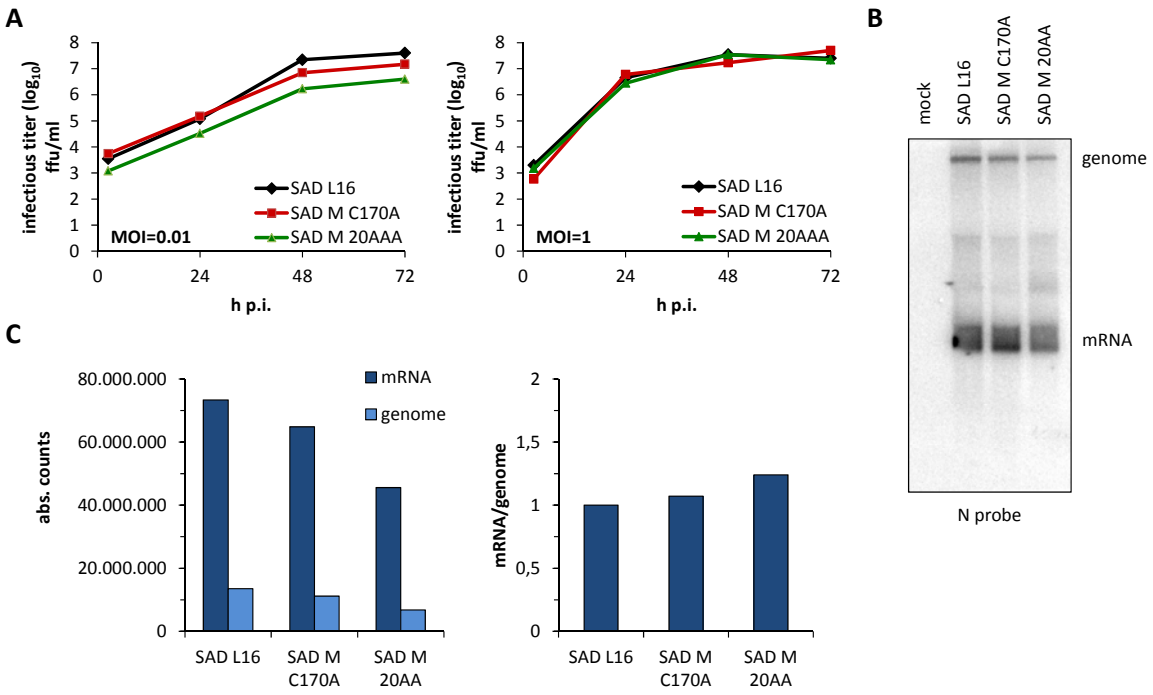

Figure 9: Wt-like growth characteristics of recombinant viruses SAD M C170A and SAD M20AA.

(A) BSR T7/5 cells were infected (MOI=0.01 or MOI=1) and aliquots of culture supernatants were collected at the indicated time points. Infectious titers were determined by titration. (B) BSR T7/5 cells were infected with the indicated viruses (MOI=1). 48 h p.i., total RNA was extracted and Northern blot analysis was carried out. N mRNA and viral genome/antigenome were detected via autoradiography after ^{32}P-αCTP labeling. (C) Quantification of the Northern blot data. The ratio of SAD L16 mRNA/genome was set to 1 (right graph).

Assuming that the M mutant viruses had a defect in particle release, the results could only be explained if the viruses had a higher transcription and replication rate than SAD L16 which would lead to more intracellular accumulation of RNPs. We used Northern blot analysis to evaluate mRNA and genome/antigenome levels in infected cells (Figure 9B). Detected band intensities were quantified with the help of the ImageQuant software (Figure 9C). When comparing the absolute counts (left graph), it could be observed that the overall amount of viral RNA present in cells infected with either SAD M C170A or SAD M 20AA was slightly reduced compared to SAD L16. This finding correlated with their growth kinetics seen in the multi-step growth curve but not with a defect in budding.

Since it is known that the M protein is involved in the switch between transcription and replication (Finke et al., 2003), it was important to compare the ratio of mRNA to

genomic/antigenomic RNA (right graph). No obvious differences could be seen between the two recombinant M mutant viruses and SAD L16 (wt ratio set to 1).

3.1.5 Analyses of M 20AA/C170A *in trans* and in the viral context

The data obtained with the recombinant M mutant viruses neither explained the phenotype of M 20AA observed in the complementation assays nor led to a deeper understanding of the RV budding process. As a next step, we opted for combining both mutations because this double mutant M protein might show a more severe defect as a result of additive effects.

First, pTIT M 20AA/C170A was constructed and subsequently tested in the NPgrL virus complementation assay (Figure 10A). The double mutant M protein behaved like the M C170A protein mutation analyzed before and showed a 75 % reduction in virus release compared to M wt. This defect could be rescued with the help of VSV G.

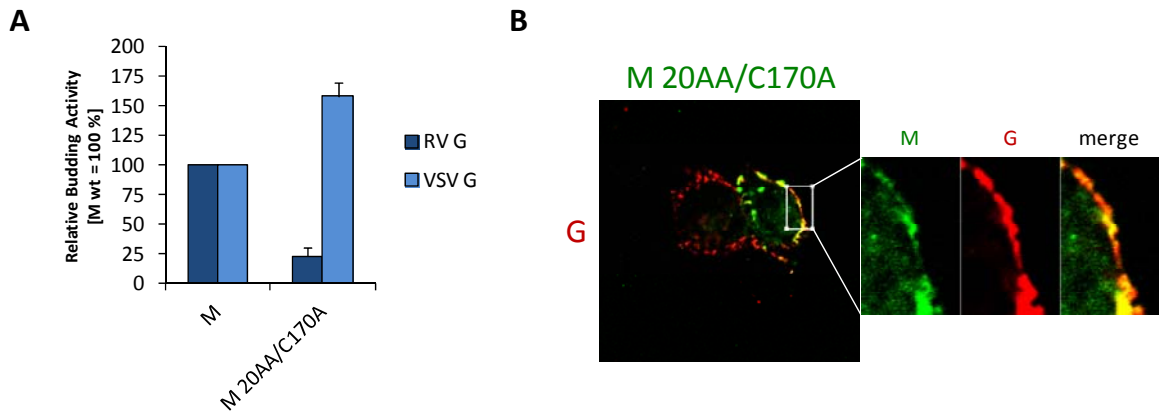

Figure 10: Budding defect of M 20AA/C170A is rescued by VSV G and M mutant protein co-localizes with RV G.

(A) NPgrL complementation assay was carried out as described for Fig. 8. The double mutant M 20AA/C170A has a defect in budding which was overcome by expression of VSV G. (B) Immunofluorescence staining of transfected BSR T7/5 cells was performed as for Fig. 7. Co-localization of M 20AA/C170A and RV G is observed in cells expressing both proteins (indicated in yellow). Red: G, green: M.

We also checked the intracellular localization of the protein upon co-expression with RV G. We could not detect major differences compared to M wt localization except for a more abundant appearance of M 20AA/C170A in the cytoplasm (Figure 10B). In some

cases the M protein seemed to form aggregates within the cell which led to a speckled picture after M staining.

Again, we made use of the reverse genetics system for further analyses and generated recombinant RV carrying the M 20AA/C170A mutation. The growth kinetics of the viruses described before (SAD M 20AA, SAD M C170A) and the newly generated SAD M 20AA/C170A were compared to those of SAD L16 (Figure 11A). The results of multi-step and single-step growth curves were almost indistinguishable from each other.

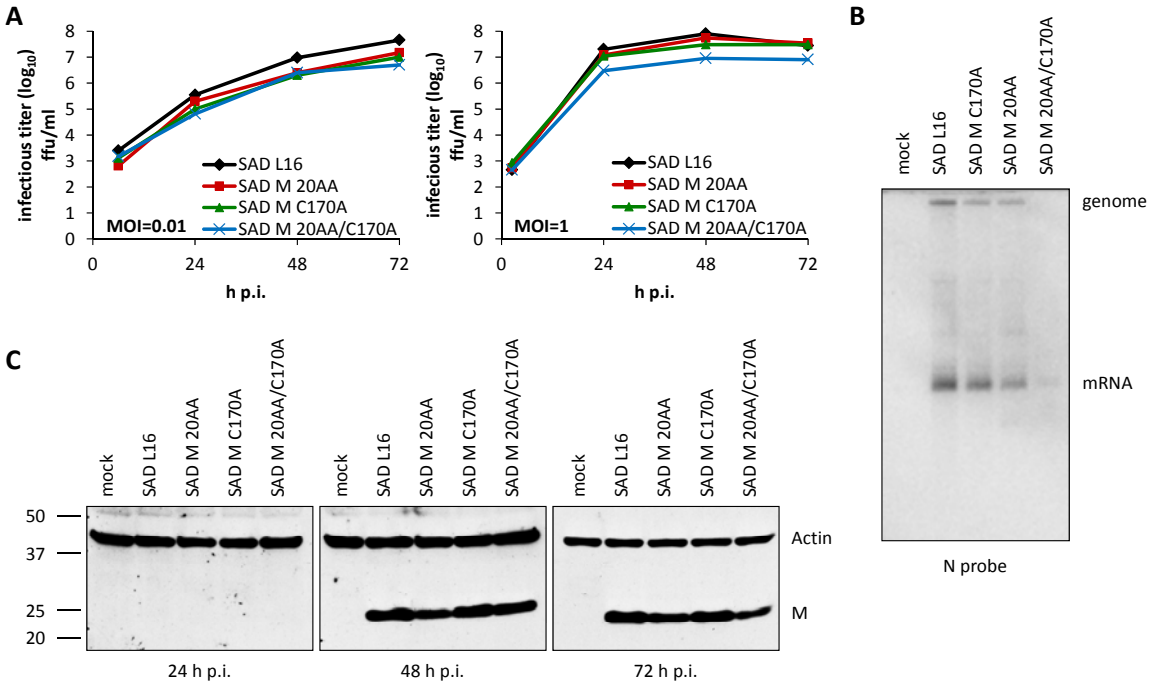

Figure 11: Minor growth defects of the recombinant virus SAD M 20AA/C170A.

(A) BSR T7/5 cells were infected (MOI=0.01 or MOI=1) and aliquots of the supernatants were collected at the indicated time points. Infectious titers were determined via titration. (B) BSR T7/5 cells were infected for 48 h (MOI=1), total RNA was purified and assayed with Northern blot analysis. N mRNA and viral genome/antigenome were detected via autoradiography after ^{32}P-αCTP labeling. (C) BSR T7/5 cells were infected (MOI=0.01) and lysed at the indicated time points. Western blot analysis was carried out and RV M and actin were detected using M2D4 and anti-actin antibodies, respectively. The viruses showed similar protein expression levels. Note that for the 72 h p.i. time point, less cell lysate was used than for the 24 and 48 h time points.

Northern blot analysis, however, indicated a severe reduction of mRNA and genome/antigenome levels for the SAD M 20AA/C170A mutant (Figure 11B). This was not in agreement with the growth kinetics. Therefore, we decided to have a look at the

protein expression levels in infected cells (Figure 11C). BSR T7/5 cells were infected with an MOI of 0.01 and whole cell lysates were taken. As early as one day after infection, no M protein was detectable. 48 h p.i. viral antigen was readily detectable in all cell lysates analyzed. The slightly reduced protein levels seen for SAD M 20AA and SAD M 200/C170A were in accordance with the respective viral titers of the growth curve. No significant variation in the protein content could be seen between the four different viruses even after this time point.

3.1.6 IFN inhibitory function of M mutant viruses is not affected

Since RV is known to inhibit the IFN induction in infected cells (Brzózka et al., 2005; Rieder et al., 2011), we wanted to address the question if the M mutant viruses were still able block this pathway. Therefore, we made use of a reporter gene assay in which a plasmid-encoded luciferase gene under control of the IFN-β promoter (p125Luc) was transfected into HEK 293T cells 6 h before infection with the respective viruses. SAD ΔPLP is known to be unable to interfere with the IFN induction in infected cells and served as a positive control (Brzózka et al., 2005).

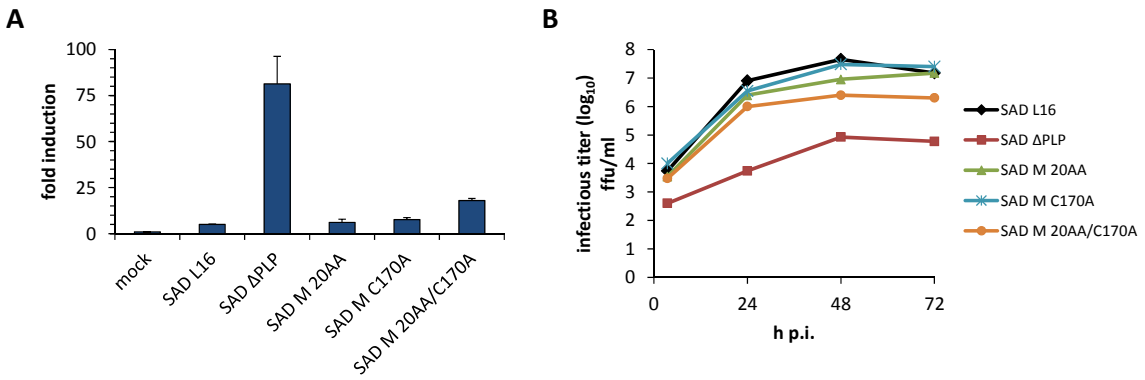

Figure 12: Recombinant M mutant viruses have normal IFN inhibiting capacity.

(A) HEK 293T cells grown in 24 well dishes were transfected with 100 ng INF-β promoter reporter construct (p125Luc) and 2 ng pRL-CMV. 6 h p.t. the cells were infected with the indicated viruses (MOI=3). SAD ΔPLP is not able to interfere with IFN induction and served as control virus. 24 h p.t. the cells were lysed in 200 µl PLB and subjected to the Dual-Luciferase® Reporter Assay. Firefly luciferase counts were normalized to CMV-*Renilla* counts (ratio in mock infected cells was set to 1). (B) Huh7 cells were infected with the indicated viruses (MOI=3), 2.5 h p.i. cells were washed to remove input virus and aliquots of the culture supernatants were collected. Virus titers were determined by titration on BSR T7/5 cells. SAD L16 and M mutant viruses grow to similar titers in IFN-competent cells. Only SAD ΔPLP has a major growth defect.

As expected, SAD L16 infection did not lead to the expression of luciferase which would have been a sign for IFN-β promoter activation (Figure 12A). SAD M 20AA and SAD M C170A showed a wt-like phenotype. Except for the positive control, only SAD M 20AA/C170A displayed a slight increase of IFN induction. However, this was still comparable to wt RV and most likely only due to delayed onset of gene expression and a later availability of the IFN antagonist P.

The growth curve analyses shown so far for the M mutant viruses were performed in BSR T7/5 cells. These cells are incompetent in IFN induction (Habjan et al., 2008). In order to test viral behavior in IFN competent cells, we chose to repeat the assay with Huh7 cells. As a control for an IFN-sensitive virus, SAD ΔPLP was used (Figure 12B). The growth kinetics of the analyzed M mutant viruses were comparable on BSR T7/5 and on Huh7 cells. As expected, SAD ΔPLP was unable to grow to the same titers as the other viruses.

The results confirmed our previous finding that the M mutant viruses had no major defect in their growth kinetics compared to SAD L16.

3.2 A new intraviral interaction partner of RV M

With the M mutant screen, it was intended to genetically dissect individual M protein functions and to identify amino acids required for the RV budding process. Since it proved to be difficult to identify M mutants specifically defective in their budding function, a different approach was persued in order to study the generation of infectious RV particles.

It is known that RV M is able to interact with the G protein and that M condenses and recruits RNPs to the site of budding (Mebatsion et al., 1999; Newcomb and Brown, 1981; Newcomb et al., 1982). So far, the molecular basis of the latter remains elusive. Therefore, the intraviral interactions of the M protein were examined. Notably, an interaction between the RV M protein and the P protein could be newly discovered.

3.2.1 M interacts with P

In order to study protein-protein interactions, we co-expressed flag-tagged M protein and RV P in HEK 293T cells. 24 h p.t. the cells were lysed in Co-IP buffer under physiological

conditions and protein complexes were pulled down with anti-flag beads. Western blot analysis showed a co-precipitation of P with flag-tagged M (Figure 13). Deletion of the ten C-terminal aa of M abolished the association of the two proteins.

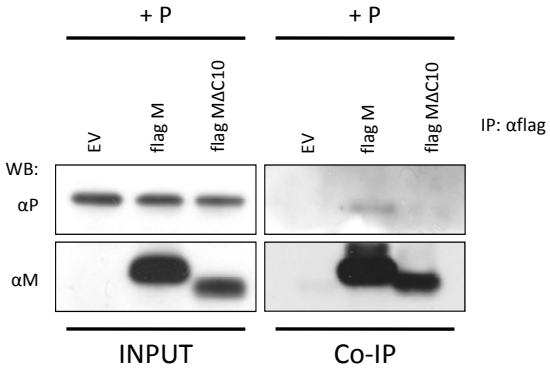

Figure 13: The C-terminus of RV M is required for binding to P.

HEK 293T cells were co-transfected with 3 µg of pCR3 P and 3 µg pCAGGS flag M constructs as indicated. Anti-flag beads were used to pull-down protein complexes. Western blots were stained with specific antibodies directed against RV P (FCA05/1) and RV M (M2D4). Flag-tagged M was able to co-precipitate RV P. The ten C-terminal aa of M were required for P pull-down.

Next, we wanted to map the M-interaction domain within the P protein. Therefore, it was made use of several P deletion mutant constructs which were already used in a different study carried out in the laboratory and co-expressed the P mutants together with flag-tagged M protein in HEK 293T cells (Figure 14A). Using C-terminal truncations of P it could be shown that the M interaction was preserved for deletions up to aa 220 (PΔ220-297). Larger deletions led to the loss of M association (PΔ191-297). We therefore concluded that a region in P required for M binding is located between aa 191 and 219. In addition, we were able to demonstrate that deletion of the region required for DLC-binding (PΔ139-161) did not interfere with M co-precipitation. The schematic drawing in Figure 14B summarizes the data of the interaction studies.

In further studies, we wanted to confirm the found interaction domain by Co-IP studies with a P protein harboring the internal deletion only (PΔ191-219). Unfortunately, we were unable to express this P mutant to high enough levels to draw conclusions from the obtained results. This was most likely due to instability of the protein.

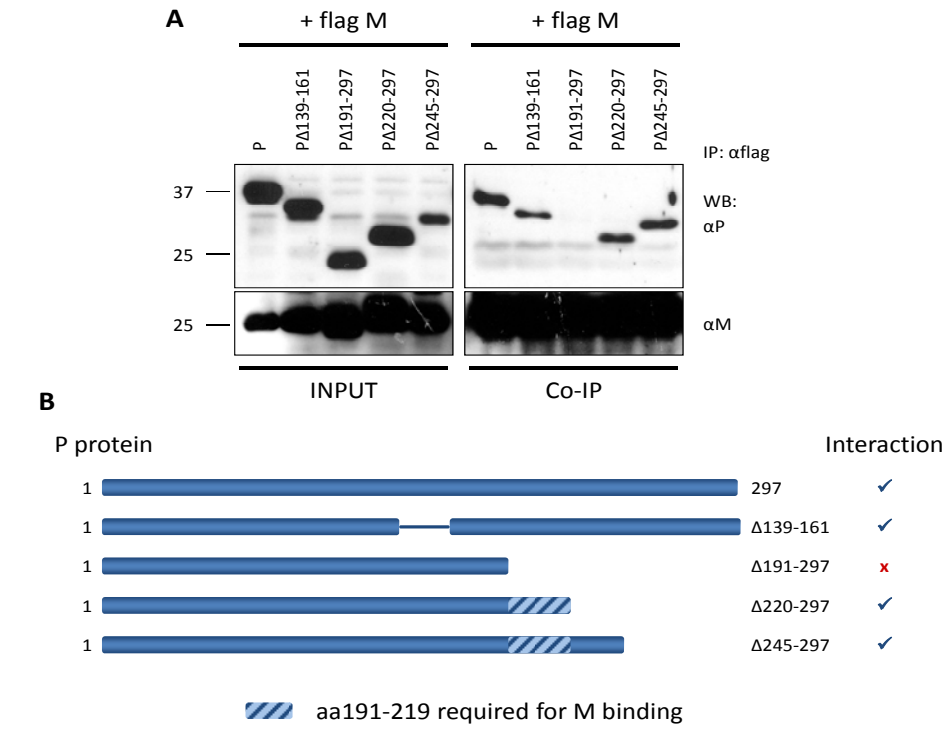

Figure 14: Amino acids 191-219 are required for M binding.

(A) HEK 293T cells were co-transfected with 3 µg pCAGGS flag M and 3 µg of pCR3 P constructs as indicated. Protein complexes were pulled down with anti-flag matrix. Co-IP samples were analyzed with Western blot and stained against P (FCA05/1) and M (M2D4). (B) Schematic overview of the Co-IP results. The region critically involved in M binding is highlighted (striated box).

We decided to take another approach; namely, we made use of a RV P peptide spot array. This consists of cellulose-bound peptides spotted on a glass slide (continuous from N- to C-terminus of P). In case the P epitope needed for M binding was linear, this assay would allow the identification amino acids involved in the binding. Stefan Finke (FLI, Insel Riems) kindly provided M protein expressed in *E. coli* which was purified via an MBP-tag and the control MBP alone. The respective proteins were incubated with the peptide array (2 µg/ml). After the incubation, the read-out was performed as for Western blots including extensive washing steps, immunostaining with an anti-MBP antibody covalently linked to HRP and subsequent chemiluminescence detection (Figure 15). The arrays indicated a major importance for the C-terminus of P to bind to M since weak positive signals were detected throughout the last one hundred amino acids of P. In addition, the Co-IP results could be confirmed in that the most N-terminal peptides binding MBP-M spanned the region from aa199-213 to aa217-231 (underlined in blue) which nicely

corresponds to the domain identified with the C-terminal truncation mutants and Co-IP experiments (aa191-219). The second motif identified matches the dimerization domain of P (underlined in grey). The bound peptides comprised aa 97 to 123 which is almost identical to its homooligomerization domain (92-131) (Gerard et al., 2009; Ivanov et al., 2010). This motif is most likely not accessible when full-length P is expressed and should therefore not contribute to M binding. Another possibility would be that M could also interact with monomeric P or even compete with P dimerization.

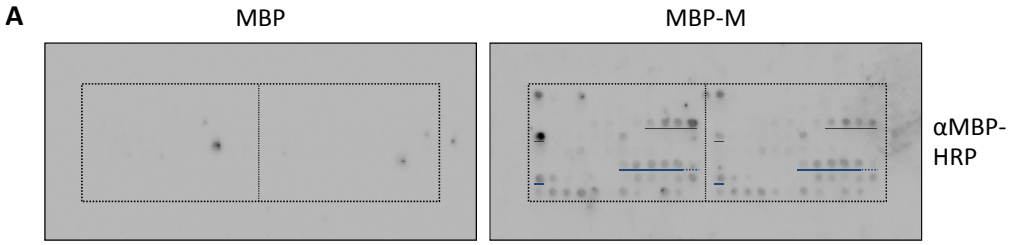

B

C19	A-E-I-A-H-Q-I-A-E-S-F-S-K-K-Y	aa199-213
C20	A-H-Q-I-A-E-S-F-S-K-K-Y-K-F-P	aa202-216
C21	I-A-E-S-F-S-K-K-Y-K-F-P-S-R-S	aa205-219
C22	S-F-S-K-K-Y-K-F-P-S-R-S-S-G-I	aa208-222
C23	K-K-Y-K-F-P-S-R-S-S-G-I-L-L-Y	aa211-225
C24	K-F-P-S-R-S-S-G-I-L-L-Y-N-F-E	aa214-228
D1	S-R-S-S-G-I-L-L-Y-N-F-E-Q-L-K	aa217-231

Figure 15: Peptide spot assay confirms binding of RV M to P.

(A) RV P peptide spot arrays were incubated with 2 µg/ml MBP or MBP-tagged M protein purified from bacteria and stained with anti-MBP HRP-coupled antibody. Chemiluminescence was measured by scanning of the arrays. For better visibility, the edges of the arrays are indicated with dashed lines. The positive spot signals corresponding to the results of the Co-IP assays are underlined in blue. Grey lines represent spots belonging to amino acids 97 to 123 (dimerization domain of P). (B) Sequences of the P peptides bound by M (underlined in blue in Figure 15A).

3.2.2 Transcription efficiency of P mutants unable to bind M

The next goal was to analyze the M-P interaction in more detail, in particular in the viral context. Since several functional and structural studies were carried out on the RV P protein already, it is known that the C-terminus is required for the binding to N-RNA complexes (aa185-297) (Chenik et al., 1994; Chenik et al., 1998). Manipulation of the protein in this region was expected to hinder viral gene expression. Anyway, two P expression plasmids were constructed harboring internal deletions, pCR3 PΔ185-209 and

pCR3 PΔ191-219. Prior to the generation of recombinant viruses the P mutants were first analyzed with respect to their ability to function as polymerase cofactor.

Therefore, a minigenome reporter assay was used in which the expression of firefly luciferase is dependent on the formation of active viral transcription/replication complexes consisting of N, P and L proteins. The minigenome construct (pSDI flash_SC) was transfected in BSR T7/5 cells together with N, L and the respective P coding plasmids. As a negative control P was omitted from the transfection mix.

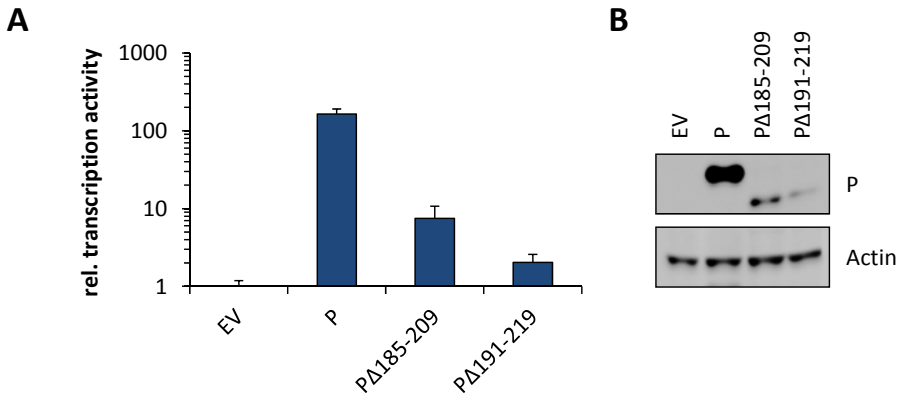

Figure 16: Analysis of transcription activity of P deletion mutants.

(A) 4 µg of a minigenome encoding firefly luciferase (pSDI flash_SC) were transfected in BSR T7/5 cells together with 5 µg pTIT N, 2.5 µg pTIT L, 2.5 µg pCR3 P helper plasmids as indicated and 5 ng pRL-CMV for normalization. 2 d p.t. the cells were lysed in PLB and 1/10 of the lysate was subjected to Dual-Luciferase® Reporter Assay. (B) Protein expression control of the lysates generated in (A). Western blots were stained with FCA05/1 and anti-actin.

The two mutant P proteins show a clear reduction in firefly expression by more than one order of magnitude (Figure 16A). When comparing the protein amounts from the experiment in Figure 16A, reduced expression of the mutants relative to P wt levels was consistently observed which is most probably due to instability of the protein (Figure 16B).

Nevertheless, we assumed that the transcription activity of PΔ185-209 was sufficient to support viral gene expression and replication. Therefore, a viral full-length cDNA was generated (pSAD PΔ185-209) and rescue of the respective recombinant virus was set up. Unfortunately, it was not possible to generate the P mutant virus with the established standard rescue protocol (data no shown).

3.2.3 Generation of cell lines stably expressing RV P

We reckoned that the rescue of SAD PΔ185-209 failed because the P mutant was unable to support viral transcription and replication to sufficient extents and decided to generate a cell line stably expressing the wt RV P protein in order to complement the defect. To this end, BSR T7/5 cells were co-transfected with a plasmid expressing RV P under the chicken β-actin promoter (pCAGGS P) and a plasmid coding for hygromycin resistance. The cells were grown under antibiotic pressure to ensure selection of transfected cells. From the surviving cells, single clones were isolated and checked for P expression in Western blot analysis. As a P expression control, a lysate of BSR T7/5 cells infected with SAD L16 was used.

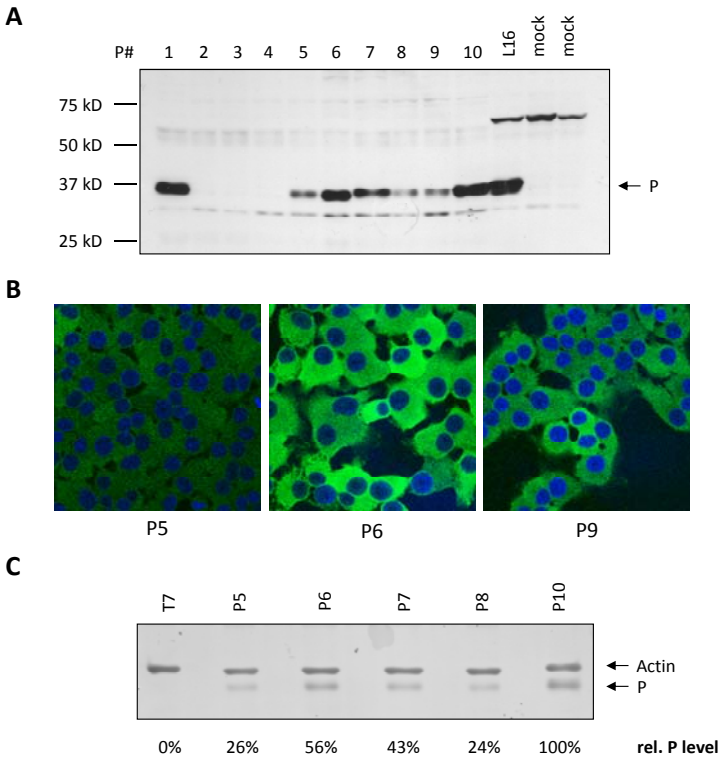

Figure 17: Generation and characterization of cell lines stably expressing RV P.

(A) Cell lysates of P expressing cell clones were subjected to SDS-PAGE and Western blot analysis. Protein expression was detected with P-specific antibody (FCA05/1). (B) P cell clones were grown on cover slips, fixed with acetone and stained with a monoclonal antibody against P (25G6) and anti-mouse Alexa Fluor® 488 (indicated in green). To-Pro®-3 was used to dye DNA (indicated in blue). Confocal images were taken with a Laser Scanning Microscope (Zeiss). (C) Lysates of the selected cell clones were subjected to SDS-PAGE and subsequent Western blot analysis. Specific primary antibody staining, fluorescence-labeled secondary antibodies (anti-rabbit Alexa Fluor® 488) and direct scanning of the membrane with a Typhoon scanner were used for quantification. Relative P protein expression levels normalized to actin levels are given underneath the image. The strongest P expression (P10) was set to 100 %.

Clearly, most cell clones expressed the RV P protein but the level of expression was highly variable (Figure 17A). This could be verified in immunofluorescence assays in which the P protein was stained specifically with the primary monoclonal antibody 25G6 and anti-mouse Alexa Fluor® 488. Fluorescence intensities represent a measure of the P quantity within the cells (Figure 17B).

After the initial check, we quantified the amounts of expressed P protein from selected cell clones with the help of fluorescence imaging after Western blotting (Figure 17C). The P10 cell clone showed the highest levels of P expression, whereas P5 and P8 were lowest. Since we intended to use the stable cell line for complementation of P mutant virus, we selected P10 for future experiments.

3.2.4 Generation and analyses of recombinant SAD PΔ185-209

Using the newly generated cell line P10 stably expressing RV P, we succeeded in generating SAD PΔ185-209 as follows: Rescue transfections were carried out following the standard protocol, meaning transfection of BSR T7/5 cells with the required plasmids. Supernatant passages carried out at 3 and 6 d.p.t. did not lead to infection of freshly seeded BSR T7/5 cells. Therefore, when the transfected cells were split, P10 cells were added and mixed with the transfected BSR T7/5 cells. The cells were grown in 6well dishes until confluent (approx. two days) and then split in T25 cell culture flasks. At this time point, G418 and hygromycin were added to the culture medium in order to select for P cells. From here, the samples were treated as if virus stocks were produced, including first and second harvest of supernatants. This protocol proved to be successful.

Growth curve analyses (MOI=1) on BSR T7/5 cells and on P10 cells were performed to compare SAD L16 and SAD PΔ185-209 and the supernatants and cell lysates were collected at the time points indicated in Figure 18.

In BSR T7/5 cells, the infectious titers of SAD PΔ185-209 were massively reduced compared to SAD L16 suggesting severe defects of the P mutant virus to support viral RNA synthesis in non-complementing cells (Figure 18A). This was reflected in the Western blot analysis of cell lysates from the growth curve experiment (Figure 18B). Staining against M and P after infection with SAD PΔ185-209 did not show any detectable viral gene expression in BSR T7/5 cells although infectious virus was apparently produced (10^3 ffu/ml). Complementation with wt P supported transcription and replication of the P

mutant virus as demonstrated by the growth kinetics and the expression of virus-encoded M in infected P10 cells.

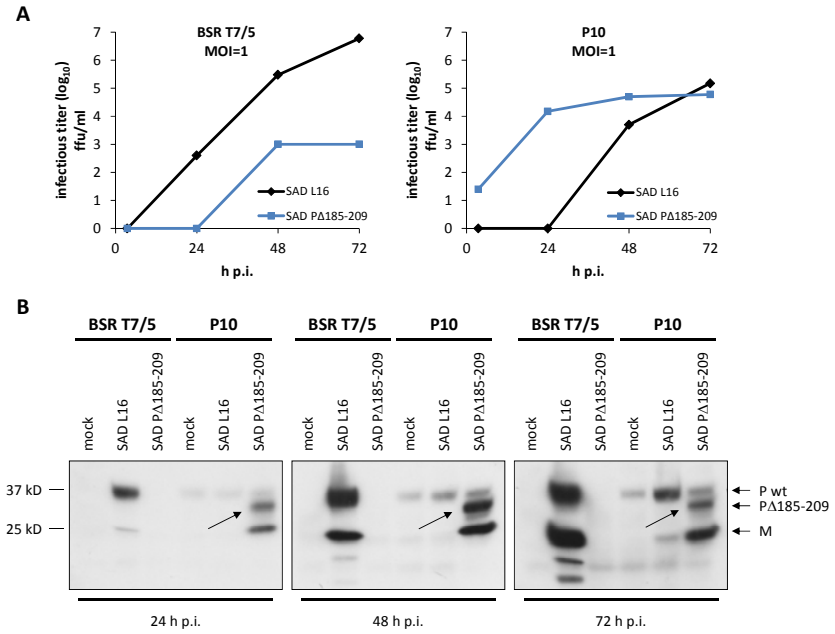

Figure 18: Efficient growth of SAD PΔ185-209 requires P wt complementation.

(A) BSR T7/5 cells and cells stably expressing RV P (P10) in 24well dishes were infected with SAD L16 and SAD PΔ185-209 (MOI=1). Input virus was removed and the supernatants were collected at the indicated time points. At the same time, cells were lysed for further use in Western blot analysis. Infectious titers were determined. (B) Western blot analysis of cell lysates from (A) were stained against RV M and P proteins with M2D4 and FCA05/1, respectively. No protein expression from SAD PΔ185-209 was detectable in BSR T7/5 cells. Arrows indicate virus derived gene expression in P10 cells. Note that for the 72 h p.i. time point less cell lysate was used for SDS-PAGE.

Notably, the PΔ185-209 protein seemed to be stabilized in the presence of other viral proteins (see arrows in Figure 18B). Since the dimerization domain of P is not directly affected by the mutation we presume that the more stable expression of the mutant is due to formation of heterodimers with wt P. Preliminary experimental data confirm intact P wt-P mutant binding (data not shown).

3.2.5 Functional differences between P cell line clones

For the experiments shown in the previous figure, SAD L16 served as control virus. The growth characteristics of the wt virus on P cell clones attracted our attention since the infectious titers and in accordance the intracellular protein levels were markedly reduced

compared to its replication on BSR T7/5 cells. We sought to further analyze this phenomenon by growth curve analyses of SAD L16 on five different P cell clones, namely P5, P6, P7, P8 and P10. In parallel to the P cells clones, BSR T7/5 cells were infected with SAD L16 (MOI=0.01) in 24well dishes. The results shown in Figure 19 confirmed a defect of SAD L16 growth in cells expressing RV P. The defect correlated with the measured expression level of P with P10 (best P expression) showing the most severe attenuation (1,000fold reduction of infectious titers compared to BSR T7/5 cells).

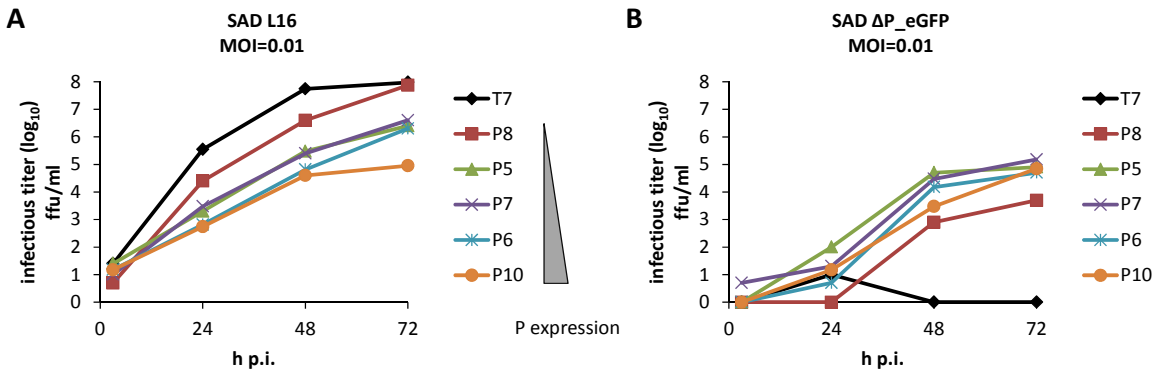

Figure 19: Attenuated growth of SAD L16 in RV P expressing cells.

(A) BSR T7/5 cells and five different P cell clones were infected with SAD L16 (MOI=0.01). Aliquots of the supernatant were collected at the indicated time points and infectious titers were determined. (B) Growth curve analysis a P gene deleted virus (SAD ΔP_eGFP) was carried out as described for (A). Infectious titers were determined via titration on P5 cells. No correlation of titers with P expression levels of the respective P cell clones apply to SAD ΔP_eGFP.

In order to address the question if P-deleted virus was affected accordingly, the same cell lines as in Figure 19A were used and growth curve analyses with SAD ΔP_eGFP was performed. This virus does not code for the P gene but instead harbors an eGFP coding cassette. Transcription and replication of the recombinant virus completely depend on supplementation of P *in trans*. As expected, replication of SAD ΔP_eGFP was precluded in BSR T7/5 cells whereas all P cell lines supported viral growth although the titers never exceeded 10^5 ffu/ml (Figure 19B). Again, the individual P cell clones showed varying capacities to complement ΔP virus replication. In this case, however, no correlation with P expression levels was obvious (compare P10 and P8).

We decided to further study the recombinant P mutant viruses in P5 and P8 cells because they both expressed low levels of P, supported SAD L16 growth best and in addition showed opposing effects for SAD ΔP_eGFP virus (P5: high titers, P8: low titers).

3.2.6 Generation and analyses of recombinant SAD PΔ191-219

In the previous rescue experiments, P10 was used to complement P mutant virus. With this cell line, SAD PΔ185-209 could be rescued but we were unable to generate recombinant SAD PΔ191-219 (data not shown). Knowing about the distinctive behavior of the P cell clones, the P5 cell line was now used. The rescue procedure was identical to that described for SAD PΔ185-209 except for the P cell line (P5 instead of P10). This time, the P mutant virus was successfully rescued and virus stocks could be produced.

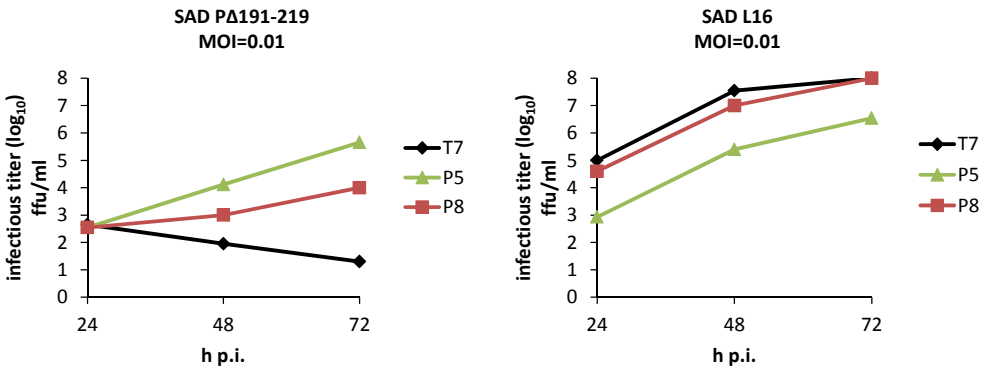

Figure 20: Replication of SAD PΔ191-219 completely depends on P wt complementation.

BSR T7/5, P5 and P8 cells were used to compare SAD L16 and SAD PΔ191-219 growth. The cell lines were infected (MOI=0.01) and aliquots of the supernatants were collected at the indicated time points. Infectious titers of SAD PΔ191-219 were determined via titration on P5 cells. In the case of SAD L16, BSR T7/5 cells were used for titration.

For characterization of the recombinant virus, growth curve analyses were performed on BSR T7/5, P5 and P8 cells. Clearly, SAD PΔ191-219 was unable to replicate in BSR T7/5 cells. On the other hand, P5 and P8 supported virus growth but to different extents. P5 complemented the mutant´s growth defect better than P8. Moreover, like SAD PΔ185-209, the growth of SAD PΔ191-219 was strongly attenuated reaching a maximum titer of about 10^5 ffu/ml compared to SAD L16 (10^8 ffu/ml). This is similar to the virus with a full deletion of the P protein (SAD ΔP_eGFP).

Taken together, we could demonstrate that RV P and M proteins interact. The ten C-terminal aa of M are required to bind to an internal stretch within the P protein (aa191-219), as shown with truncated P proteins. Analysis of the binding region using peptide spot arrays identified the C-terminus of P to also contribute to M binding. The strongest interaction in that assay was observed between aa 199 and 231.

So far, we were unable to confirm the loss of M binding for the internal P deletion mutant due to scarce protein expression. The recombinant P mutant viruses, SAD PΔ185-209 and SAD PΔ191-219, were unable to replicate without supplementation of P wt.

3.3 P and its cellular interaction partners

A previous study in the laboratory focused on the cellular interaction partners of RV P using mass spectrometry (MS). Strep-tagged P protein was purified from HEK 293T cells under physiological conditions. The obtained MS data revealed a total of 64 potential interaction partners with an ion score > 95 % which was considered to be a specific hit (Brzózka, unpublished data). We reexamined the dataset and screened for proteins which might play a role in membrane association and vesiculation of RV.

We decided to further analyze the following proteins which were pulled down with Strep-tagged P: Dynamin2 (Dyn2), Rab1B and vesicle-associated membrane protein 3 (VAMP3). Dyn2 is the ubiquitously expressed isoform of the GTPase Dyn1 and is crucially required for endocytosis (Kasai et al., 1999). It could also be related to other membrane fission and fusion events within cells such as vesicular transport from the Golgi complex to the plasma membrane (Jones et al., 1998). Rab1B was shown to be involved in the regulation of ER to Golgi transport via COPII vesicles (Plutner et al., 1991; Slavin et al., 2011) whereas VAMP3 is the non-neuronal isoform of the VAMP/synaptobrevin protein family which functions as R-SNARE (McMahon et al., 1993). Synonyms for VAMP3 are synaptobrevin3 and Cellubrevin due to its ubiquitous expression. Members of the protein family are crucial for docking and fusion of e.g. synaptic vesicles with the presynaptic membrane. VAMP3 could be localized to an endosomal membrane pool mainly consisting of recycling endosomes (McMahon et al., 1993).

3.3.1 P interacts with VAMP3 but not with Rab1B and Dyn2

For further analyses, the open reading frames of Dyn2, Rab1B and VAMP3 were cloned under control of the chicken β-actin promoter (pCAGGS) for gene expression in mammalian cells. Using Co-IP assays, we sought to confirm an association of P with the three proteins. Flag-tagged P was expressed together with the proteins in HEK 293T cells as indicated in Figure 21. Pull-down via anti-flag beads confirmed the interaction of RV P to VAMP3. In the blot shown here for Rab1B precipitation, the protein co-purified unspecifically with the beads as revealed by detection of the protein in the empty vector (EV) control. Increased protein band intensity in the Co-IP with flag P suggested only moderate (if any) association with P. In repeated experiments, Rab1B could not be confirmed to be a specific binding partner of P since it either bound to the matrix or did not bind at all. Dyn2 on the other hand, never produced any positive signal after pull-down with RV flag P.

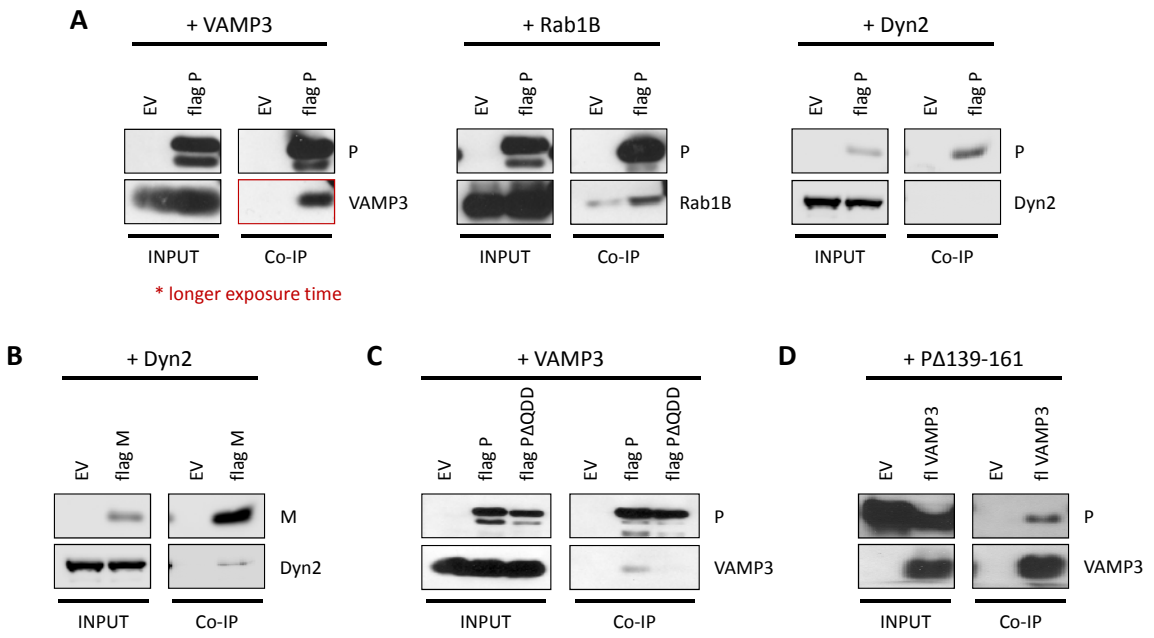

Figure 21: Co-IP experiments demonstrate interaction of RV P with VAMP3 but not with Rab1B and Dyn2. (A) HEK 293T cells were co-transfected with 4 µg each of pCR3 flag P and the indicated pCAGGS expression plasmids. Anti-flag beads were used for pull-down of protein complexes 24 h p.t.. (B) Co-IP as indicated for (A) was carried out using pCAGGS flag M co-transfected with pCAGGS Dyn2. Specific pull-down of Dyn2 by flag M can be observed. (C) pCAGGS VAMP3 was co-transfected with pCR3 flag P and pCR3 flag PΔQDD. Note that 6 µg of the deletion mutant construct were transfected in order to adjust for reduced protein expression of the P mutant. Deletion of the QDD motif prevents the interaction of P with VAMP3. (D) Flag-tagged VAMP3 is able to pull-down a P mutant (PΔ139-161) which is unable to bind to DLC.

Notably, VSV M interacts directly with Dyn2 for efficient virus release (Raux et al., 2010). We therefore addressed the question whether RV M possesses the same function. As shown in Figure 21, we were able to demonstrate that RV M interacted with Dyn2.
In contrast to Dyn2 and Rab1B which may represent false positive hits in the MS dataset obtained after Strep-P pull-down, VAMP3 seems to be a true interaction partner of RV P.

Our next goal was to identify the interaction domain in P required for VAMP binding. Using Co-IP experiments, we were able to demonstrate that deletion of aa288-290 (ΔQDD) led to a loss of interaction between VAMP3 and flag P (Figure 21C).
Since in this experiment the interaction between P wt and VAMP3 seemed to be relatively weak, we needed to exclude the possibility that VAMP3 was only pulled down due to indirect interaction via another cellular protein. A candidate bridge protein would have been DLC which is known to be a protein hub in the cell strongly interacting with RV P (Barbar, 2008; Jacob et al., 2000; Raux et al., 2000) and which was highly enriched in the Strep-P co-purification samples used for MS. A DLC-binding mutant of P (PΔ139-161) still co-precipitated with flag VAMP3 (Figure 21D). We therefore exclude indirect binding via DLC. In addition, this experiment showed pull-down of RV P when tagging VAMP3 instead of using flag-tagged P.

3.3.2 Analyses of functional requirement for P-VAMP3 interaction

The data described in the previous chapter identified VAMP3 as novel cellular interaction partner of P. However, the functional relevance remained unclear. Since we already showed direct binding of P to M, the major player in RV assembly and budding, we speculated that the P-VAMP3 interaction contributed to particle formation. We first used an RNAi approach to address this question. siRNAs directed against the mRNAs of VAMP3 and Rab1B were designed using siMAX^{TM} Design Tool (Eurofins, MWG Operon). The two sequences predicted to work best were tested for their ability to knockdown protein expression. In addition, a Dyn2 siRNA was analyzed of which the sequence was proven to knock down protein amounts (Pizzato et al., 2007). The sequence of the siRNA CO3 did not contain any known target sites and served as control siRNA (Besch et al., 2007). All of the tested sequence-specific siRNAs efficiently knocked down the protein expression in HEK 293T cells at 33 nM concentration (Figure 22A). The Rab1B#1 and VAMP3#1 siRNAs

were more effective than the respective #2 when comparing protein levels 48 h after siRNA transfection.

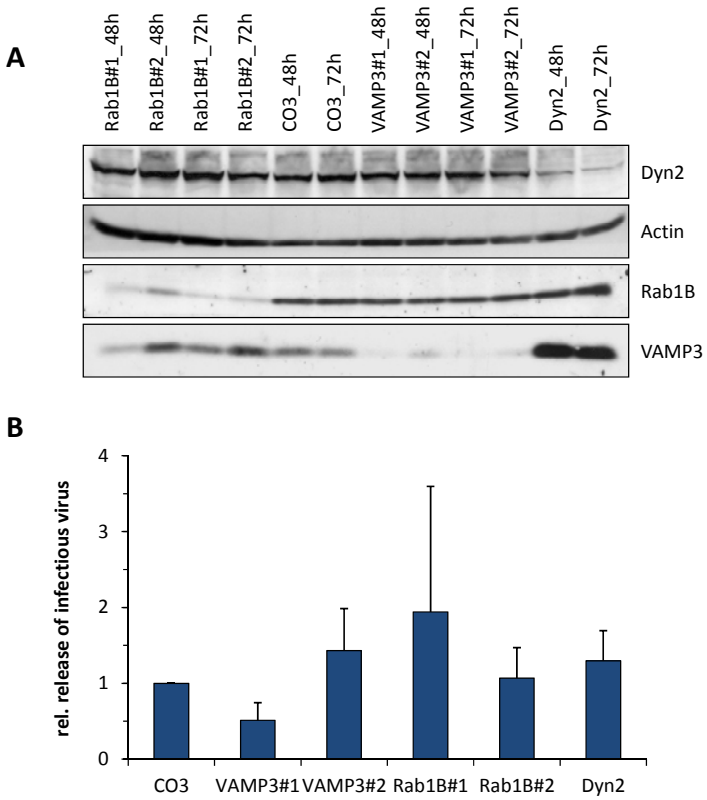

Figure 22: Knockdown of cellular proteins has little effect on RV budding.

(A) Two siRNAs directed against Rab1B, VAMP3 and one against Dyn2 mRNA were transfected into HEK 293T cells using Lipofectamine™ RNAiMAX. CO3 siRNA was used as control. The cells were treated with 33 nM siRNA and cell lysates were taken at 48 and 72 h p.t.. SDS-PAGE and subsequent Western blot analysis was used to check for efficient knockdown of protein levels. (B) HEK 293T cells were treated with siRNAs as in (A). 30 h p.t. the cells were infected with SAD L16 (MOI=1) and supernatants were collected 24 h p.i.. The results (n=3) are shown relative to the infectious titers of control siRNA-treated cells (CO3=1).

To study the importance of the respective proteins on virus release, siRNA-transfected HEK 293T cells were infected with SAD L16 (MOI=3) at 30 h p.t. and infectious viral titers were determined 24 h p.i.. Compared to the control siRNA, only the VAMP3 knockdown with siRNA#1 reduced the release of RV. This effect was reproducible (n=3) albeit being only moderate (approx. 50 %) (Figure 22B).

As opposed to protein knockdown we wondered if protein overexpression would also affect RV budding, particularly if VAMP3 overexpression would stimulate RV particle production. VAMP3 and Rab1B expression plasmids were transfected into HEK 293T cells and infected with SAD L16 6 h p.t. (MOI=0.1). Aliquots of the supernatants were collected

at the indicated time points and titers were determined. The results do not reveal an impact of VAMP3 and Rab1B overexpression on RV release (Figure 23A) maybe due to already saturated budding under physiological amounts of protein. Protein overexpression was confirmed using Western blot analysis. As a control, lysates of uninfected mock transfected cells were loaded on the gel (Figure 23B, right lane).

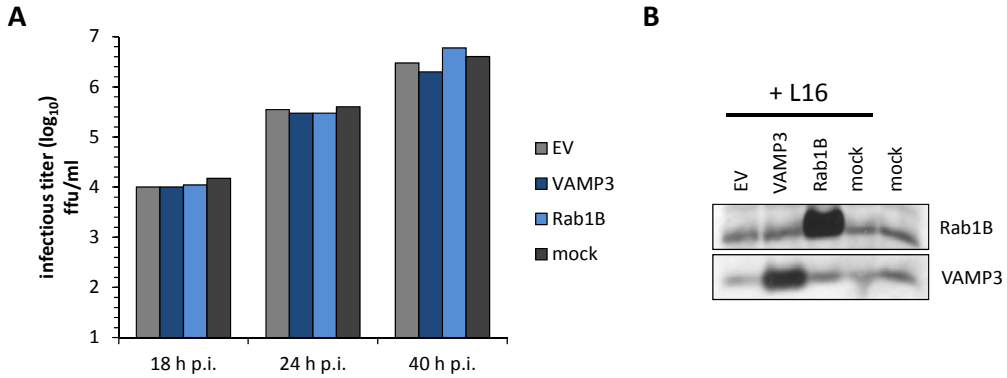

Figure 23: VAMP3 and Rab1B overexpression do not affect RV release.

(A) HEK 293T cells were transfected with 1 µg pCAGGS expression plasmid as indicated or not transfected (mock). The cells were infected 6 h p.t. with SAD L16 (MOI=0.1) and aliquots of the supernatants were collected at the indicated time points. (B) Control of protein expression of cell lysates from (A) taken 40 h p.i..

3.3.3 Interaction of P with VAMP1 and VAMP2

RV is a neurotropic virus which retrogradely spreads via synaptic connections *in vivo*. Since we could demonstrate co-precipitation of RV P and VAMP3, we presumed that the interaction to its neuronal homologs VAMP1 and VAMP2 is conserved. We decided to generate plasmids coding for flag-tagged versions of the respective proteins. Therefore, total RNA extracts of cells from the neuroblastoma cell line NA were prepared, cDNA was generated and the coding sequences of VAMP1B and VAMP2 were amplified with specific primers. After cloning, the resulting constructs, pCAGGS flag VAMP1B and pCAGGS flag VAMP2, were used for Co-IP experiments in order to confirm or disprove our hypothesis. As shown in Figure 24A, all three VAMPs co-purified P although the P band after flag VAMP1B pull-down was poorly detectable, indicating only very weak interactions between the two proteins.

Proteins forming a functional complex should be present in the same compartment or microdomain. We therefore wanted to see whether P co-localized with any one of the

three VAMPs in cells overexpressing the respective proteins and used confocal imaging to address this question. Plasmids coding for P and flag-tagged VAMP proteins were transfected into BSR T7/5 cells. The cells were fixed 24 h p.t. and immunostained. Analysis of the slides, however, do not reveal specific co-localization of P with any of the flag-tagged VAMPs (Figure 24B).

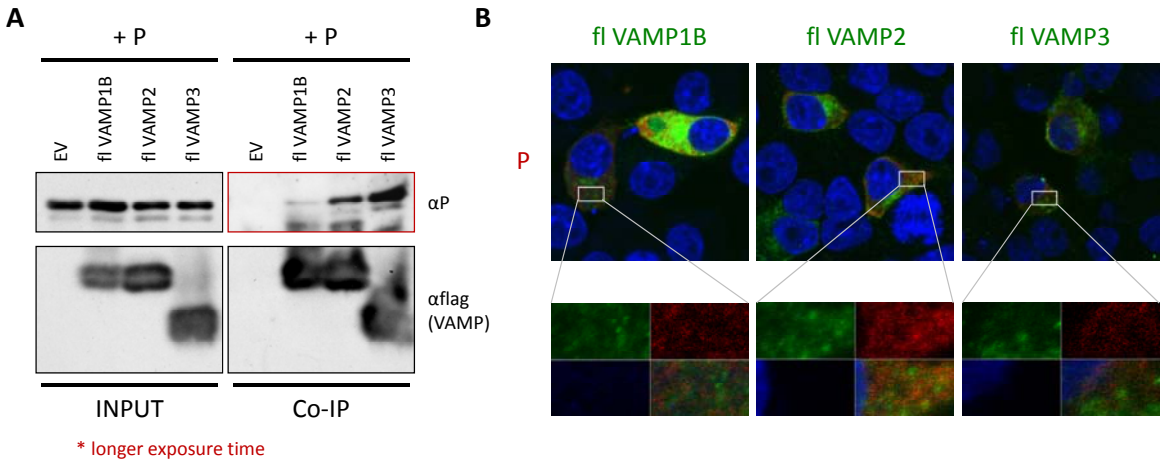

Figure 24: RV P interacts with VAMP family members.

(A) HEK 293T cells were transfected with 3 µg of pCR3 P and 2 µg of the indicated flag VAMP expression plasmids using PEI. Protein complexes were pulled down with 100 µl anti-flag beads. Samples were analyzed with Western blot and stained against RV P (FCA 05/1) and anti-flag for VAMP detection. (B) BSR T7/5 cells were transfected with 0.5 µg of pCR3 P and pCAGGS flag VAMP1B, 2 or 3 using FuGENE®. 24 h p.t. the cells were fixed with PFA and treated according to the immunofluorescence staining protocol. Red: P, green: flag VAMP, blue: DNA (nucleus), yellow: co-localization. Confocal images do not indicate co-localization of RV P and neither VAMP1B, VAMP2 nor VAMP3.

3.4 P is involved in the assembly of infectious viral particles

3.4.1 Severely reduced production of infectious particles by SAD P288AAA

The information we gained on the P interaction partners led us to presume that P is involved in the assembly and budding process of RV probably via its interaction with M or via VAMPs. RV full-length cDNAs harboring a mutation in the P gene (either deletion or substitution) which was previously found to abolish the association with VAMP3 were constructed (pSAD PΔQDD and pSAD P288AAA). We set up rescue experiments for these two viruses and transfected the cDNAs together with the helper plasmids coding for N, P

and L into BSR T7/5 cells. Interestingly, we noticed for the pSAD P288AAA rescue that almost all cells in the transfection well were positive for viral antigen after staining with FITC-conjugated anti-N antibody (Figure 25A).

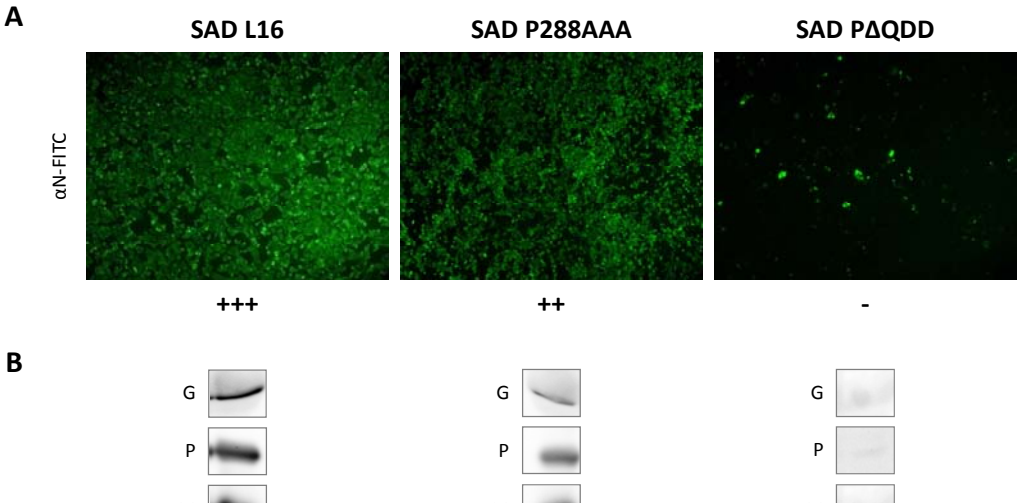

C

Supernatant of:	split cells	1. passage
SAD L16	1 x 10^8	6 x 10^7
SAD P288AAA	2 x 10^3	Not detectable

Figure 25: SAD P288AAA is defective in virus release.

(A) Virus rescue experiments were set up on BSR T7/5 cells. Cells were subsequently split and grown to confluency. Transfected cells were fixed and stained with Centocor. + and – indicate positive and negative rescue of virus, respectively. (B) Western blots of cell lysates from the rescue experiments in (A) and subsequent virus protein-specific staining is shown. Virus-derived expression of G, P and M is clearly observed for SAD L16 and SAD P288AAA samples. The rescue of SAD PΔQDD was negative and therefore no protein expression is detectable. (C) The table displays virus titers (ffu/ml) determined from the indicated cell culture supernatants. One representative result is shown out of at least three independent experiments. In spite of viral protein expression, virus release in SAD P288AAA is severely diminished.

When comparing the N staining pattern in cells transfected for SAD L16, SAD P288AAA and SAD PΔQDD rescue, the latter was clearly different from the other two, showing the typical pattern of a negative rescue attempt in which only helper plasmid-derived N is stained (Figure 25A). The SAD P288AAA microscopic appearance resembled wt SAD L16. This was an unambiguous sign of a positive rescue which had taken place after

transfection. Subsequent transcription and replication of the newly generated virus in the culture ultimately led to a monolayer in which almost every cell was positive for viral antigen due to cell-to-cell spread of the virus. However, many attempts to produce infectious cell-free virus from either of the two cDNA constructs intriguingly failed and recombinant virus could never be passaged to fresh cells.

In order to confirm protein expression derived from viral transcription of the RV genome, we harvested the transfected rescue cells and subjected the lysates to SDS-PAGE and Western blot analysis (Figure 25B). Specific staining of G and M proteins served as a clear mark of virus-specific transcription because only N, P and L expression plasmids were transfected together with the full-length cDNA of RV; and M and G proteins are not expressed until rescue has occurred. Most likely, the majority of P visible in the Western blot is virus-derived wt (SAD L16) and mutant P (SAD P288AAA). Residual wt P might still be present from helper plasmid expression. As seen in the Western blot for the SAD PΔQDD rescue, however, the protein amount was almost undetectable which was in accordance to the negative rescue.

We went on and determined the infectious titers in the supernatants of cells transfected for rescue which were subsequently split ("split cells") and those of fresh cells after infection with supernatant of the rescue experiment ("1. passage") (Figure 25C). In the wt situation, $1x10^8$ infectious particles were detected in the supernatant of "split cells" and $6x10^7$ ffu/ml in the "1. passage". SAD P288AAA was almost completely incompetent to release infectious particles ($2x10^3$ ffu/ml in the supernatant of "split cells"), although the transfected cells contained viral antigen (data not shown). In the supernatant of the first passage no infectious virus was found at all.

This massive reduction in released infectivity was striking and led us to investigate the phenotype of this recombinant P mutant virus in more detail.

3.4.2 P288AAA mutation does not affect known P functions

In order to validate the specificity of the defect, we performed several control experiments addressing P protein functionality. Most importantly, P is the essential cofactor of the viral polymerase. We checked whether P288AAA and also PΔQDD were still able to support viral transcription with the help of minigenome assays as described for Figure 16. As seen in Figure 26A, no alteration of reporter expression compared to P

wt was observed in case P288AAA was expressed. For PΔQDD, however, a reduction was noted.

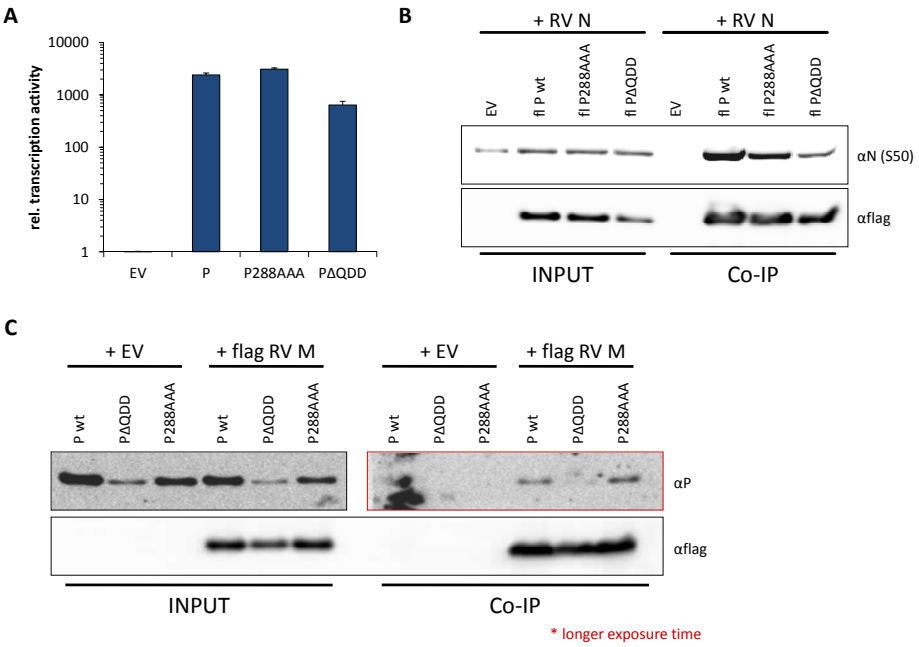

Figure 26: P288AAA is competent to support viral RNA synthesis and is able to bind N and M.

(A) 4 µg of a minigenome encoding firefly luciferase (pSDI flash_SC) were transfected in BSR T7/5 cells together with 5 µg pTIT N, 2.5 µg pTIT L, 2.5 µg pTIT P helper plasmids as indicated and in addition 5 ng pRL-CMV for normalization. 2 d p.t. the cells were lysed in PLB and 1/10 of the lysate was subjected to Dual-Luciferase® Reporter Assay. Normalized luciferase expression is depicted relative to the empty vector control (EV=1). (B) and (C) HEK 293T cells were transfected with 3 µg of each of the expression plasmids as indicated using PEI. Co-IP experiments showed intact N (B) and M (C) binding of all P proteins tested.

P directly binds to soluble N (N^0) and N-RNA complexes. We therefore checked whether the binding of the P mutants to N was impaired. Co-IP experiments confirm intact N-P association for all three flag-tagged P proteins (Pwt, P288AAA and PΔQDD) (Figure 26B).

As demonstrated in previous experiments, P is also an interaction partner of M. If this interaction was essential for the recruitment of RNPs into budding particles, its disruption would abolish particle formation or lead to the formation of non-infectious particles. Although we could already map the P region required for M co-precipitation (aa191-219), we still wanted to make sure that mutation of aa288-290 did not affect M interaction because the peptide spot data indicated a contribution of the whole C-terminus of P. The blot shown here does not contradict our previous results and an intact M-P288AAA interaction is evident (Figure 26C). Notably, in many cases, the PΔQDD mutant was less

well expressed compared to both P wt and P288AAA and gave the false impression that it was unable to bind to M.

3.4.3 Budding defect of SAD P288AAA

The described data strengthened our hypothesis that P is involved in the assembly and budding process of RV since we could exclude a defect in transcription, as well as in N and M binding. The only other possible explanation for the observed phenotype of SAD P288AAA could have been that the virus mutant released non-infectious particles (e.g. due to a defect in G incorporation). To analyze this question we used density gradient ultracentrifugation. Supernatants taken from the rescue experiment shown in Figure 25A were loaded on a continuous OptiPrep™ gradient. Twelve fractions were collected from top to bottom after centrifugation to equilibrium. Results of Western blot analysis of the fractions are shown in Figure 27A.

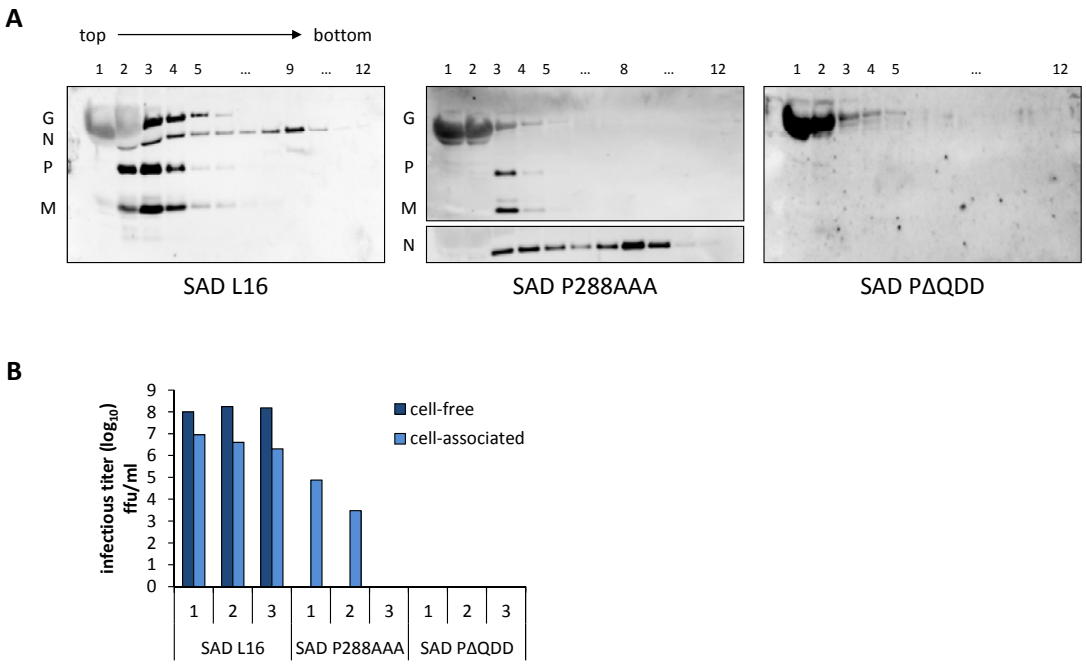

Figure 27: Comparison of physical and infectious particles of SAD P288AAA.

(A) BSR T7/5 cells were transfected for virus rescue, the supernatants were collected 2 d after splitting and subjected to density gradient ultracentrifugation. Aliquots of the twelve fractions were subjected to Western blot analysis and stained against the RV proteins G, N, P and M. Composition of SAD P288AAA virions resembles wt SAD L16. (B) Cells from (A) were frozen (-20 °C) and thawed on ice in 1 ml fresh media. Cell debris was removed. Titers of rescue supernatants compared to cell-associated virus (freeze-thaw

samples) are shown in the graph for one representative experiment carried out in triplicates for each virus rescue. SAD P288AAA is able to generate infectious particles but has a major defect virus release.

SAD L16 displayed abundant virus protein in fractions 2-4. G, N, P and M were present in the same fractions indicating whole and intact viral particles. Similarly, fraction 3 of SAD P288AAA contained the bulk of viral protein, demonstrating that the overall density and protein composition of the mutant virus particles were equivalent to wt. However, the peak of viral protein in the gradient was much narrowed indicating that not the quality but the quantity of released viral particles differed from wt. On the contrary, the SAD PΔQDD rescue transfected cells did not release any detectable viral proteins in the culture supernatant.

In addition to the gradient data, we were able to demonstrate that SAD P288AAA was not incompetent in spreading the infection. By comparing cell-free to cell-associated infectivity (cell-associated virus was obtained by freeze-thawing of the rescue cells), it was obvious that the bulk of wt SAD L16 virus (> 90 % of total) was released into the supernatant (Figure 27). The data are shown for one representative experiment out of two, each carried out in triplicates. In case of SAD P288AAA, the cell-associated virus titers mostly exceeded the cell-free titers by at least 1-2 orders of magnitude which was opposed to wt. In this particular experiment, no infectious particles were detected in the supernatant at all. For the deletion mutant SAD PΔQDD there was neither extracellular nor cell-associated infectivity detectable which confirmed our previous results.

3.4.4 Identification of amino acid D290 in RV P as a critical residue for assembly

The question arose whether amino acids 288 to 290 of P were all contributing to particle assembly to the same extent or whether there was a certain hierarchy. Therefore, three recombinant viruses were generated which harbored a single amino acid exchange within the respective P proteins: SAD P Q288A, SAD P D289A and SAD P D290A. The first two were easily rescuable, i.e. the first supernatant passage gave rise to normal sized foci. This already indicated that Q288 and D289 alone cannot be critically involved in the formation of infectious particles. On the contrary, SAD P D290A did not behave like wt. Most cells died before the time of the second passage. Very few, if any, foci were detected in the first supernatant passage. In order to improve the rescue, the cells were split into T25 flasks as early as three days after transfection and supernatant particles

were harvested another three days later. In that way, we succeeded in generating stocks with a titer of $1x10^5$ ffu/ml. In comparison to SAD P288AA, this is an unexpectedly high titer which might be explained by cell damage having occurred and thereby release of cell-associated infectivity in the culture supernatant.

For reasons of better comparability, we set up the characterization of the recombinant virus SAD P D190A as we did for the triple mutant SAD P288AAA for which no virus stocks were available. Rescue experiments of SAD L16, SAD P288AAA and SAD P D290A were transfected in duplicates. 3 d p.t., the cells were split and another 2 d later the cells were fixed for Centocor staining (Figure 28A). The cells transfected for SAD P D290A rescue were clearly antigen positive. Notably, the CPE of this virus was much stronger than that of SAD P288AAA whereas SAD L16 infection did not seem to affect the cell viability.

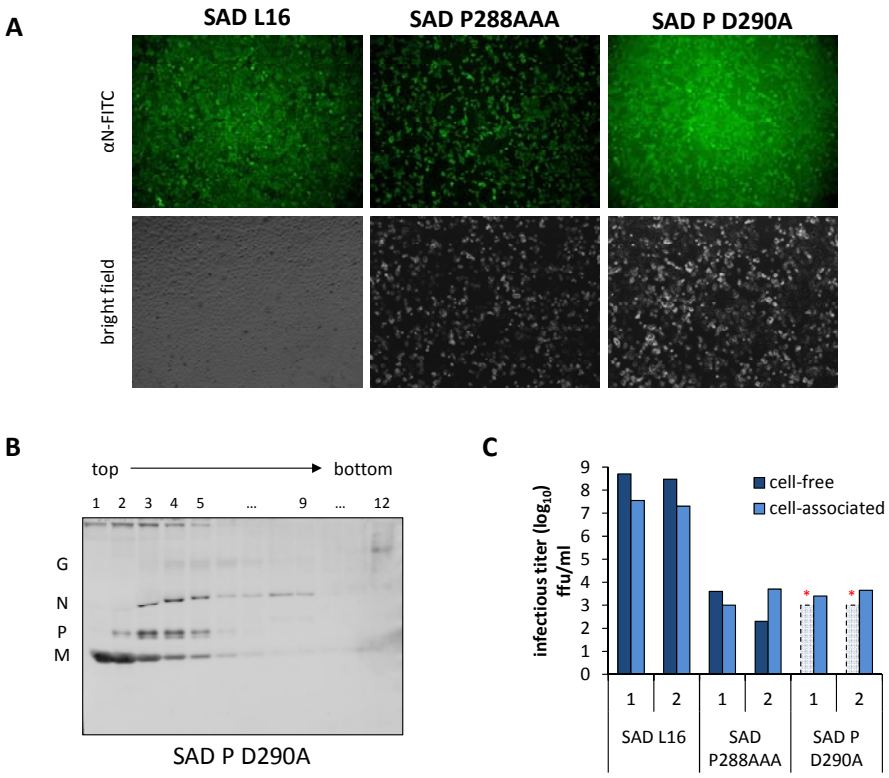

Figure 28: SAD P D290A and SAD P288AAA have similar phenotypes.

(A) Duplicates of the indicated virus rescues were set up on BSR T7/5 cells. 3 d p.t., the cells were split ¼ and another 2 d later fixed and stained with Centocor. The CPE induction of the P mutant viruses is visible in the bright field picture. One representative picture of the duplicates is shown. (B) The supernatants of SAD P D290A rescues were collected and subjected to density gradient ultracentrifugation. Aliquots of the twelve fractions were subjected to Western blot analysis and stained against the RV proteins G, N, P and M. (C) Rescue cells from (A) were frozen (-20 °C) and thawed on ice in 1 ml fresh media. Cell debris was

removed. Titers of rescue supernatants compared to cell-associated virus (freeze-thaw samples) are shown in the graph for the duplicates described in (A). The asterisks mark estimated results since the titers could not be unequivocally determined (see text for details).

Density gradient ultracentrifugation of supernatants after transfection revealed similar virus particle composition as wt virus or SAD P288AAA in fraction 3 and 4 although only weak G staining could be observed (Figure 28B). We still conclude that the composition of typical supernatant virions is not altered compared to wt virus because the protein amount peaks in the same fractions and this requires similar density characteristics (compare Figure 27).

One well of each rescue duplicate was taken for the comparison of cell-associated versus cell-free infectious titers. As expected from the rescue attempts, the cell-free infectivity never exceeded the cell-associated virus titers in case of SAD P D290A (Figure 28C). Notably, however, the determination of the cell-free infectivity proved to be somewhat difficult for this virus. Repeatedly, one dilution of the titration was almost full of viral antigen and at a tenfold higher dilution positive cells were undetectable. This phenomenon cannot be explained by the budding-defective phenotype of the virus. The titers marked with an asterisk in the graph (Figure 28C) represent the most probable but estimated titers from the experiments.

Here, in contrast to the previous characterization of SAD P288AAA in which no released infectious particles were detected, the triple mutant did release detectable amounts of infectious particles. Still, the cell-associated titers leveled or topped the extracellular virus and again, the overall titers were dramatically reduced compared to SAD L16 (10,000-100,000fold). This is consistent with our conclusion that SAD P288AAA has a defect in assembly and budding.

The analyses of the single amino acid exchange mutants demonstrated that SAD P D290A displays a phenotype very much resembling the triple mutant described above. We therefore conclude that amino acid D290 is of major importance to RV P for fulfillment of its role in the assembly and budding of RV whereas Q288 and D289 do not seem to contribute.

3.4.5 Growth curve analysis of recombinant viruses with single amino acid exchanges

In order to directly compare the three recombinant viruses with single amino acid exchanges, growth curve analysis in BSR T7/5 cells was performed with the following P

mutant viruses: SAD P Q288A, SAD P D289A, SAD P D290A and wt SAD L16. The cells were infected with an MOI of 0.01 and aliquots of the supernatants were subsequently collected at the indicated time points. The infectious titers were determined by titration.

The exchange of amino acids Q288A and D289A in the P protein reduced viral titers only slightly (Figure 29). The most severe drop of infectivity was obtained with the D290A mutant virus of which titers were approx. 100fold reduced compared to SAD L16. This is consistent with our previous data showing that SAD P D290A has a defect in particle release although the final titers obtained in the growth curve are remarkably high.

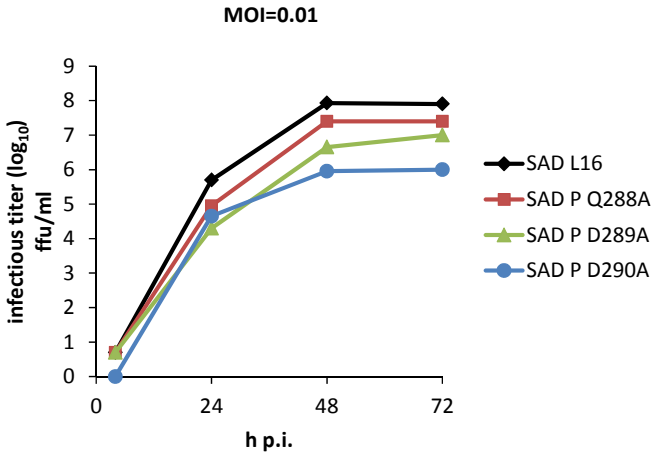

Figure 29: Amino acid D290 significantly contributes to budding defect in P single mutant viruses.

BSR T7/5 cells were infected with SAD L16 and the single aa exchange mutants SAD P Q288A, SAD P D289A and SAD P D290A (MOI=0.01) and aliquots of the supernatant were collected at the indicated time points starting at 4 h p.i.. Infectious titers were determined via titration. Most pronounced defects were seen in the recombinant virus with the D290A substitution mutation.

3.4.6 Infectious virus-like particle assay using P mutants

A function of RV P in the release of viral particles from infected cells was not recognized before. We intended to gain deeper knowledge of the motifs in P which contribute to the assembly process. A plasmid-based assay would be beneficial. As standard method in the field of assembly and budding of RNA viruses the iVLP assay is used in which particles that resemble the authentic virus are generated from plasmids. These particles are unable to replicate because the viral genome sequence is exchanged for a reporter construct, e.g. a minigenome encoding luciferase.

Here, pSDI flash_SC was used and transfected into BSR T7/5 cells together with plasmids coding for all viral proteins: pTIT N, P, L, M and G. Unless stated otherwise in the figure, all

transfection mixes contained wt P protein expression plasmids. Yet, in order to analyze the function of P mutants, different P expression plasmids were tested in this assay. pRL-CMV was transfected for normalization purposes. 3 d p.t. the supernatants of the transfected cells containing iVLPs were taken and used to infect fresh BSR T7/5 cells. The transfected cells were harvested for reporter gene assay. Transcription and replication of the minigenome in the fresh cells could not occur unless RV N, P and L were provided *in trans*. This was accomplished by superinfection of the passage cells with the helper virus SAD Ambi (MOI=1). 48 h p.i. the cells of the passage were harvested for luciferase reporter gene assay.

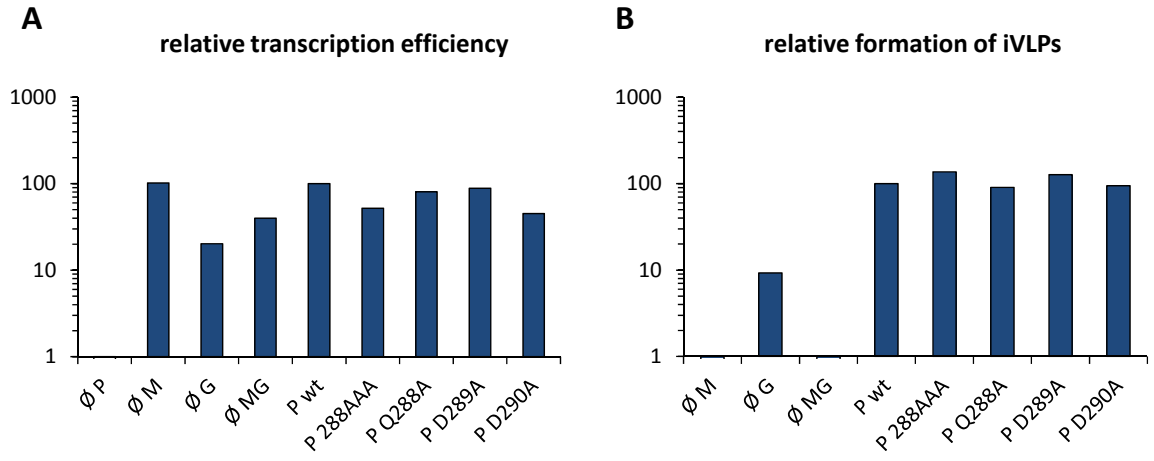

Figure 30: P mutants support the generation of iVLPs to similar extents as P wt.

BSR T7/5 cells were transfected with pTIT expression plasmids coding for N, P, M, G and L. In addition, the minigenome 4 µg pSDI-flash_SC and 5 ng pRL-CMV for normalization were included. As control, either P, M, G or M and G were omitted from the transfection mix as indicated. (A) 3 d p.t., iVLP-containing supernatants were collected and the cells were harvested for Dual-Luciferase® Reporter Assay. The firefly counts were normalized to the *Renilla* transfection control to calculate the transcription efficiency of the respective P mutants. (B) Supernatants from (A) were passaged on fresh BSR T7/5 cells which were superinfected with the recombinant helper virus SAD Ambi 1 h thereafter (MOI=1). Dual-Luciferase® Reporter Assay was carried out 48 h after the passage. The firefly counts are displayed relative to firefly values measured in the respective transfected cells.

For data analysis, it had to be clarified that the different P mutants supported gene expression to comparable levels. The transcription efficiency was calculated from the results of the luciferase assay: firefly counts divided by *Renilla* counts from transfected cells. The ratio obtained for P wt was set to 100 %. From previous experiments we

expected no major defects of the P mutants to act as polymerase cofactor (see Figure 26). Figure 30A clearly showed that the amounts of reporter made in the transfections with varying P mutants were very similar. The absolute firefly counts were used for the calculation of the relative amount of released iVLPs (firefly counts of passage divided by firefly counts of transfected cells; P wt set to 100 %). Either M or G or both plasmids were omitted from the transfection mix to allow the discrimination between specific and non-specific transfer of luciferase to the passage cells. It was not possible to carry over reporter activity unless RV M was present (Figure 30B). Interestingly, the analysis of the different P mutants is not conclusive insofar as neither the single amino acid exchange mutant P D290A nor the completely budding defective P288AAA show detectable differences in the passage of minigenomes to fresh cells compared to P wt. It seems as if minigenome-based iVLP assays do not fully reflect authentic live virus conditions in which e.g. a much larger genome has to be packaged.

Summarizing the data, it was possible to newly discover a critical contribution of RV P to viral assembly and budding. Two independent recombinant viruses harboring a mutation at the C-terminus of P (SAD P288AAA and SAD P D290A) were shown to be unable / severely defective in the release of infectious particles from cells. However, the ability to spread the infection directly from cell to cell was maintained in both P mutant viruses.

4 Discussion

Viral infections ultimately lead to the generation of new infectious particles. As a prerequisite, the virus has to multiply its components (protein and genome) and subsequently assemble. This requires highly coordinated actions of all viral structural elements. Also cellular machineries are abundantly utilized for the virus´ purposes due to the limiting coding capacity of viral genomes.

Mebatsion and colleagues (1996) were the first to show that the glycoprotein was not needed for the formation of RV particles but instead the matrix protein was essential. Until then, the equipment with a viral envelope was assigned to G which is the only membrane-spanning protein in *Rhabdoviridae*. To date, most enveloped RNA viruses which express a matrix protein are considered to depend on this multifunctional protein as major driving force of budding. This is due to experimental evidence that M alone has the ability to bind the three components essential for virus assembly which are (i) the RNP, (ii) the glycoprotein and (iii) lipid membranes (Jayakar et al., 2004). However until to date, it has not been experimentally shown that RV M is as well sufficient to direct particle release.

This work addressed assembly and budding of RV by a mutational screen of the M protein and amino acids S20, P21 and C170 were newly identified to contribute to efficient budding. Most interestingly, in search of other requirements for virus particle assembly, RV P was found to be needed for this process in addition to M. Recombinant P mutant viruses which displayed a specific defect in budding were identified and characterized in detail. Revealing a new intraviral interaction, M and P were shown to directly bind each other, thereby providing the molecular link of how P could be supportive to the assembly of infectious particles.

4.1 M mutant screen for dissection of budding function

The ability to dissect individual functions of the multipurpose RV M protein is fundamental to the identification of mutants with specific defects in either particle

formation, RNA synthesis regulation, or RNP condensation. In fact, this was possible in a former study carried out in the laboratory, in which the transcription and replication regulatory function of M could be attributed to one single amino acid, R58, without affecting the protein´s role in assembly (Finke and Conzelmann, 2003).

Here, a similar system was employed, now specifically addressing the assembly and budding function of M. The approach sought to use mutational analysis of the M protein in order to identify motifs required for the release process different from the already described L domain (^{35}PPEY^{38}). NPgrL virus was used as replicon in these transient assays. Due to the lack of M and G genes, the completion of a single infectious cycle absolutely depends on the functional substitution of the two proteins *in trans*. M mutant proteins which were unable to substitute for M wt in this assay together with the authentic RV G, but which were rescued by virtue of the intrinsic budding capacity of VSV G, were considered to have a defect specifically during viral release. Indeed, two mutants could be identified displaying this phenotype: M 20AA and M C170A. Like wt M, the mutant M proteins were able to colocalize with RV G at the plasma membrane. Interestingly, the infectivity released in the supernatant was clearly reduced and only VSV G expression rescued the defect. The deficiency to compensate for M wt function in the NPgrL system strongly suggested severe virus release defects in a system in which multiple rounds of replication add up to the total infectivity. Therefore, recombinant viruses were generated harboring mutant M proteins (SAD M 20AA, SAD M C170A and SAD M 20AA/C170A). The phenotype of these viruses resembled SAD L16 with respect to RNA synthesis, protein expression and unexpectedly showed only slightly reduced growth kinetics in multi-step growth curves (10fold).

The disruption of the L domain in RV M, which is considered to significantly contribute to efficient viral spread, reduces viral titers to similar extents (Wirblich et al., 2008). However, the specific contribution of the MVB pathway on RV budding is on debate. On the one hand, disruption of the L domain in RV M and depletion of ubiquitin which, among many other roles, serves as a sorting signal for the ESCRTs, led to a reduction of infectious titers by one order of magnitude (Harty et al., 2001). On the other hand, the two crucial ESCRT (-associated) proteins, Tsg101 and Vps4, did not seem to play a role in the budding process of RV and VSV (Chen et al., 2007; Irie et al., 2004) whereas Taylor

and colleagues (2007) demonstrated that VSV release needs Vps4, the most downstream component of the MVB pathway.

In this work, although we did not analyze the ESCRT pathway in detail, we could confirm published data that the disruption of the L domain in M (^{35}PPEY^{38} → ^{35}AAEY^{38}) reduced viral titers to the same extent as did the mutants discussed here (10fold; data not shown). We consider the above mentioned motifs and consequently also the ESCRT-dependent budding to be not essential for the RV release process and suggest that the observed effect might be due to either inefficient or unspecific use of the MVB formation pathway. This hypothesis is supported by two facts: (i) intraluminal vesicles are able to form even in the absence of ESCRT proteins (Babst, 2011; Stuffers et al., 2009b), which would explain the apparently contradictory results on RV release, and (ii) MVBs were observed to be able to fuse with the plasma membrane (Heijnen et al., 1999) which is in principle equivalent to release of virus from the plasma membrane.

Another explanation for the observed titer reductions described here could be the fold of the lyssavirus M protein. As revealed by Graham at al. for LBV (2008), amino acids ^{33}MPPP^{36} of one M molecule form a short polyproline-II helix which is able to bind to a hydrophobic pocket within adjacent M molecules, thereby leading to self-association. This illustrated a novel protein oligomerization mode. Interestingly (and as discussed by Graham et al.), the amino acids forming the short helix partially overlap with the L domain identified in lyssavirus M protein (^{35}PPEY^{38}). The intriguing question now arose if mutations in the L domain might have modulated self-association (and thereby protein function) rather than interaction with the host cell budding machinery. This would imply that the minor reduction in titers seen after disruption of the L domain were due to secondary effects upon changes in the oligomeric state of M.

We cannot exclude that the M protein mutants studied in this work had minor alterations in the protein structure. However, the subcellular distribution exhibited a wt-like phenotype as demonstrated by confocal imaging. Thus, we presume that the observed reductions in infectivity in the transient assays were not due to misfolding and secondary effects.

The results that the mutated amino acids in RV M contributed to viral budding in the transient assays but showed only moderate effects in the viral context are in line with results of studies on recombinant EBOV which show that both L domains of VP40 are

dispensable for viral replication in cell culture despite being essential for the formation of VP40-induced VLPs (Neumann et al., 2005).

As is typical for a multipurpose protein, most mutations in M resulted in a complete loss of at least one of its essential functions. This feature of M is still the major obstacle in separating and subsequently analyzing individual protein functions. Not only could mutations directly affect protein-protein interactions (either intraviral or with host proteins) but amino acid exchanges might also affect the overall protein fold which is of considerable functional importance to M (Graham et al., 2008).

Taken together, the data on the M protein mutants described in this work identified two novel motifs whose mutation led to a titer reduction comparable to L domain mutants. New essentially required amino acids specifically for assembly and budding were however not yet identified. Due to the multifunctional nature of M, the bottleneck of future analyses will be the correct attribution of a mutant´s phenotype to one or the other function of M. It seems likely that all functions carried out by M during the entire assembly pathway contribute to a certain extent to the efficiency of this process. Disruption at any point will at least strongly attenuate the virus or even fully abolish the generation of infectious particles. Minor changes in the M protein sequence as described here will be tolerated or rather compensated for by the virus.

It would be of interest to further investigate the many M mutants which were stably expressed but altogether defective in the complementation assays. Presumably, the proteins have lost the ability to either directly or indirectly (maybe by interaction with another viral protein) bind to cellular partners which are required for correct transport to the site of action. By means of identifying the cellular transport pathway, it might be possible to draw conclusions about the final budding step and its environmental requirements.

4.2 RV M interacts with the RNP component P

Most matrix proteins of RNA viruses were shown to be essential for the release of VLPs and interestingly many of these were also sufficient (reviewed in Chen and Lamb, 2008 and Harrison et al., 2010). For RV, there is only data on the requirement of M (Mebatsion

et al., 1996). In spite of this, evidence for the sufficiency of M in forming and releasing extracellular particles is lacking.

In a collaborative study with T. Strecker and W. Garten at the University of Marburg the generation of VLPs from plasmid-expressed RV M was investigated. So far, this could not be observed (data not shown) although in the same approach Lassa virus Z protein used as a positive control was readily detectable in the supernatant of cultured cells (Strecker et al., 2003).

The poor (if any) intrinsic budding activity of RV M emphasizes that there is a need for other virus proteins in order to achieve efficient budding. The fact that RV G stimulates particle release supports this hypothesis (Mebatsion et al., 1996). In addition, in this work, the phenotype of a recombinant virus carrying a mutation in the C-terminal domain of P was analyzed and directed us to investigate a new, formerly unknown supportive function of P in release of virus from infected cells.

Since M is required for budding, we suggested that either M and P directly interacted or that P was required for other, so far unidentified, steps in the assembly process. M and P, however, do not clearly co-localize in infected cells since the majority of P is found in inclusion bodies which are considered to be the place of viral transcription and replication (Lahaye et al., 2009) whereas M mainly associates with cellular membranes and is located at the plasma membrane together with G. However, a minor fraction of M seems to reside in close proximity to viral inclusions (S. Finke, personal communication).

We decided to study protein-protein interactions using Co-IP assays and were able to demonstrate that M directly binds to P upon transient expression in 293T cells. The ten C-terminal amino acids of M were required for P binding. With the help of C-terminal truncation mutants of the RV P protein, amino acids 191-219 were demonstrated to be critical for the interaction with M. So far, we were prevented from demonstrating a loss of binding for PΔ191-219 directly due to low expression levels of this mutant. RV P peptide spot arrays incubated with purified RV M, however, confirmed binding of M in this region. The whole C-terminal globular domain of P seemed to contribute to binding to some extent. In addition, amino acids 97-123 were identified as a potential binding site for M. Whether these residues are involved in binding remains to be clarified because they are required for dimerization of RV P (Gerard et al., 2007; Ivanov et al., 2010). It

would be interesting to analyze if monomeric P is still able to bind to M, if oligomerization is needed for protein function or if M even prevents P dimerization.

In the approach to generate recombinant P mutant RV harboring the deletion of aa 191-209 which supposedly prevents M binding, we needed to supplement the virus with P wt. The P mutant´s function as polymerase cofactor was severely restricted and therefore gene expression could not be detected.

The P protein of RV is known to be critically involved in a multitude of viral processes such as transcription and replication as well as in inhibiting the innate immune response of the cell. The newly identified interaction with RV M might be required for several processes. First of all, the binding could mediate initial association of M with the RNP which is needed for recruitment of genomes to the site of further assembly. The current model is that the bulk of M localizes to membranes in infected cells. A small portion of M already associates with RNPs in the cytoplasm and homotypic M interactions with membrane-associated M then lead to polymerization and subsequently to condensation of the nucleocapsid (Jayakar et al., 2004). The M-P interaction in this model could be required either for primary RNP-binding with M being the nucleating factor for further M recruitment or M-P binding could directly be needed for the RNP condensation process. Further studies on M-RNP association need to be carried out in order to gain a more detailed understanding of the functionality of this newly discovered direct binding.

C-terminal deletion of ten amino acids in the M protein led to a loss of binding to P. Notably, an M mutant (MΔC13) similar to that identified in this work to be defective for P binding (MΔC10) was completely unable to support the release of infectious particles in the NPgrL complementation assay (Finke and Conzelmann, 2003). We suggest that this is due to a loss of P binding and therefore lack of RNP incorporation into budding viruses.

M also acts as a regulator for the switch between transcription and replication but the molecular target remains to be discovered (Finke and Conzelmann, 2003; Finke et al., 2003). It is generally accepted that the condensation of RNPs into the skeleton-like structures shuts down gene expression and replication. It could as well be that M acts more directly on the polymerase complex via interaction with P and thereby modulates its function. However, our data suggest that binding and regulation are carried out by separate domains of M since its regulatory function was dependent on the arginine

residue at position 58 and mutating this amino acid did not affect P binding, assembly and budding.

M-RNP interaction is essential for the formation of infectious particles and has been demonstrated for members of all *Mononegavirales* families. Borna disease virus (BDV) M, as opposed to RV M, was shown to be a stable component of the BDV RNP complex in the nucleus without interfering with the viral polymerase activity (Chase et al., 2007). The Schwemmle laboratory demonstrated in this publication that M directly bound to P and not to N. In respiratory syncytial virus (*Paramyxoviridae*) association of M with the RNP in cytoplasmic inclusions depends on binding to the M2-1 protein present in these complexes (Li et al., 2008). M2-1 functions as a polymerase processivity factor during transcription which in RV is one of the multiple tasks of the P protein (Collins et al., 1996). For EBOV (*Filoviridae*) a direct interaction between VP40 and VP35 (the matrix and phosphoprotein homologs, respectively) was identified in a mammalian two-hybrid screen. This interaction was required for the incorporation of minireplicons into VP40-induced VLPs whereas expression of minigenomes without VP35 but instead together with NP did not lead to uptake by VP40 (Johnson et al., 2006). Also, the VP35 protein was relocated from a cytoplasmic distribution to a more plasma membrane-associated localization in cells which co-expressed VP40. All of these publications are in line with our findings that RV M interacts with the RNP complex via the P protein.

4.3 P significantly contributes to virus release

This work demonstrates for the first time that functional RV P is required for budding of infectious particles. Specifically, SAD P288AAA and SAD P D290A were found to be viable recombinant viruses but almost completely defective in forming cell-free virions even in the presence of wt M. Both P mutants supported viral gene expression as indicated in a minireplicon system and by the detection of RV proteins expressed in infected cells. In addition, the ability to spread infection from cell to cell was retained. However, the supernatants of infected cells contained dramatically reduced amounts of infectious virus particles compared to wt SAD L16 (10,000-100,000fold).

The mutation leading to the specific budding failure in RV resides in the highly conserved C-terminus of P. Crystal structure determination of the C-terminus of RV P revealed two prominent features: (i) a positively charged patch and (ii) a hydrophobic pocket with an exposed tryptophan side chain. Amino acids 288-290 form part of the α6 helix which stretches out adjacent to the hydrophobic pocket (Mavrakis et al., 2004). A comparison between the C-terminal structures of RV and VSV P showed a conservation of the hydrophobic pocket although the two P proteins share no sequence similarities (Ribeiro et al., 2008). The C-terminus of RV P has been shown to be involved in binding to N-RNA complexes as well as STAT binding and PML redistribution (Blondel et al., 2002; Brzózka et al., 2006; Chenik et al., 1994; Schoehn et al., 2001). It seems likely that this preserved surface-exposed C-terminal portion of P represents a platform for protein-protein interactions. Here, it has now been demonstrated that also the formation of progeny virions depends on the integrity of the C-terminus of P.

The RV P-STAT interaction is required for the virus' inhibition of IFN signaling. Specifically, P binds to phosphorylated (p-)STAT1 and (p-)STAT2 and thereby prevents the translocation of STAT homo- and heterodimers to the nucleus (Brzózka et al., 2006; Vidy et al., 2005). P288AAA was unable to bind p-STAT and showed decreased capacity to inhibit IFN signaling compared to wt P (data not shown). The analysis of the phenotype of SAD P288AAA, however, was carried out in BSR T7/5 cells. This cell line is not competent to initiate an IFN response upon infection due to a defect in IRF3 activation (Habjan et al., 2008). The P288AAA's defect in STAT inhibition is therefore negligible with respect to its assembly and budding characteristics in BSR T7/5 cells.

The phenotype of the RV recombinants SAD P 288AAA and SAD P D290A is remarkably similar to that described by Das and Pattnaik for a VSV P mutant (Das and Pattnaik, 2005). Interestingly, in VSV P the hypervariable linker region between structured domains II and III was identified to contribute to the release of infectious particles. An internal deletion within the VSV P protein (Δ140-201) in the virus context led to a defect in passaging the virus after reconstitution from cDNA but complementation with wt P rescued the virus.

In agreement with our data on RV P, the mutation in VSV P did not affect the transcription and replication capacity of the virus and supported gene expression to significant levels. Das and Pattnaik could only speculate that the causal relation between P deletion and

assembly phenotype might be M. In particular, they propose a model in which correct assembly of VSV particles is abolished due to altered M association with nucleocapsids.

We were able to demonstrate a direct interaction between M and P in RV thereby providing experimental evidence for a link of the P protein to viral assembly and budding. However, deletion of an internal stretch presumably preventing M binding (Δ191-219) also affects P´s capacity to act as polymerase cofactor and recombinant viruses lacking the M-P interaction are therefore not available.

Notably, the budding-defective P288AAA still binds to M with comparable affinity as wt P. We therefore hypothesize that P function in RV budding is required to provide appropriate host conditions for correct assembly.

4.4 Cellular requirements for RV release

Published work addressing RV budding and the host factors involved in release focused on the MVB pathway and the viral M protein. Here, a connection of the RV M protein and dynamin2, a large GTPase involved in endocytosis, could be shown for the first time. However, the functional significance in virus release remained uncertain when applying RNAi. Recently, dynamin was also identified as interaction partner of VSV M (Raux et al., 2010). The binding reduced endocytosis in infected cells and thus VSV G accumulated at the plasma membrane. This had a supportive effect on VSV particle release. One reason why we did not observe such effects might be insufficient protein knockdown. Another explanation could be more efficient transport of RV G and/or M to the cell surface. Also, it is possible that VSV and RV make differential use of the cellular systems they interact with.

Data presented in this work strongly suggest that not only RV M interaction partners assist budding of infectious particles but also RV P ligands since P was shown to be required for the release process. Mass spectrometry data obtained after Strep-P pull-down from whole cell lysate carried out in another project in the laboratory were used to identify binding proteins which might play a role in the viral release process. Interestingly, an interaction with a SNARE protein could be confirmed in Co-IP experiments. SNARE proteins are involved in a multitude of membrane trafficking processes including

constitutive and regulated exocytosis. Specifically, VAMP3, the protein interacting with RV P, is the ubiquitously expressed homolog of VAMP2 which is required for neurotransmitter release in the nervous system.

Data presented in this work demonstrated that VAMP3 knockdown cells infected with RV released less infectious virus particles into the supernatant compared to mock siRNA-treated control cells. This indicates a contribution of the SNARE protein to RV budding. The effect was not as dramatic as one would expect from an essential interaction partner. However, VAMP3 null mice were reported to have no defects related to known functions of the protein (Yang et al., 2001). Yang and colleagues speculate that VAMP2 (or other SNARE proteins) could take over VAMP3 tasks. We propose that this applies in our experiments as well since the interaction of RV P with VAMPs seemed to be conserved within the protein family. Binding of the P protein to the neuronal homologs VAMP2 and also to VAMP1, though with weaker affinity, could be demonstrated in this study.

In vivo, RV spread occurs exclusively from post- to presynaptic neurons which is opposite to the conventional neurotransmitter release route. The molecular details of RV transmission are poorly understood. There is, however, frequent exocytic activity at the postsynaptic membrane in the absence of infection. Indeed growth, function, and plasticity of the synapse depend on retrograde signals (reviewed in Kennedy and Ehlers, 2011; Regehr et al., 2009). Also, there is constant membrane trafficking to the plasma membrane in dendrites (Horton et al., 2005). Analyses of the molecular machinery involved in dendritic exocytosis showed that syntaxin4 (Stx4) function is needed for the fusion of recycling endosomes with the plasma membrane (e.g. for reintegration of AMPA receptor into the membrane) at sites close to the postsynaptic density (Kennedy et al., 2010). Also, SNAP-23 and SNAP-25 were shown to be enriched in dendritic spines and involved in retrograde signaling (Lau et al., 2010; Suh et al., 2010). The VAMP involved in the membrane fusion event has yet to be determined. Interestingly, in a more general setting analyzing cell-cell fusion, Hu et al. demonstrated that VAMP3 can form functional SNARE complexes with Stx4/SNAP25 (Hu et al., 2007) and the subcellular localization of VAMP3 has been described to be the recycling endosome (RE) (McMahon et al., 1993).

The cellular machinery involved in retrograde signaling might be hijacked by RV but so far molecular evidence was lacking. Interestingly here, we provide first data that at least one

viral protein (P) can interact with a component of the SNARE complex (VAMP). Yet, the functionality and significance have to be shown in future work.

4.5 Future directions

In this work, an interaction between the RV M and P proteins could be experimentally proven. This is the first time that a direct interaction of M with a protein of the RNP complex of *rhabdoviruses* could be shown. The M-P interaction provides an entirely new basis for future research on basic viral functions. Former work in the laboratory identified a transcription and replication regulatory function of M (Finke et al., 2003). The question whether M acted directly on the viral polymerase complex, indirectly by RNP condensation or even by altering the host cell environment has not yet been answered. Within the order *Mononegavirales*, the functions of the matrix proteins of the family members are considered to be conserved but more detailed comparison reveals intriguing differences amongst them. The BDV M protein for instance is a stable component of the RNP complex which does not seem to regulate the polymerase function (Chase et al., 2007). The data presented here now provide a promising basis for future work in which molecular mechanisms of this phenomenon can be addressed in the RV context.

The identification of RV P as an essential player in the assembly of infectious particles positions the P protein in the center of viral processes: It (i) acts as the polymerase cofactor, (ii) chaperones RV N, (iii) antagonizes IFN induction, (iv) prevents IFN-induced JAK/STAT signaling and (v) is critical during assembly of progeny virions. The C-terminus of P seems to be involved in a variety of different interactions (N-RNA, M, PML, STATs, VAMPs). Site-directed mutagenesis based on the published structure of the P C-terminus (Mavrakis et al., 2004) might allow a more detailed dissection of different P protein functions.

The assembly and budding defect of SAD P288AAA and SAD P D290A identified in this work was characterized biochemically. It would be interesting to analyze these recombinant viruses with optical methods such as transmission EM. In case assembly has already occurred and particles are unable to pinch-off, they would accumulate at the plasma membrane. However, in case the viruses have defects in the overall assembly process (e.g. RNP condensation) it would of course be difficult to detect virus structures

without immunogold labeling. Still, the spread-competence of the budding-defective viruses raises opportunities to study how cell-to-cell spread occurs. These viruses might be used as tool to analyze this phenomenon in the absence of budding and subsequent reinfection.

Already now, RV is used by neuroscientists as monosynaptic tracer due to its retrograde restriction (Wickersham et al., 2007a; Wickersham et al., 2007b). However, the mechanism of action is still unknown. The newly discovered interaction of RV P with VAMPs allows further analyses of this fascinating process. A system in which different SNARE components could be knocked down/out separately or even at the same time would be of significant interest. Treatment of infected cell cultures with neurotoxins such as botulinum toxin B (cleaving VAMPs), botulinum toxin C (cleaving syntaxin), or botulinum toxin A (cleaving SNAP-25) (Schiavo et al., 2000) would allow the analyses of RV release under knock out-like conditions. Comprehension of the molecular basis for RV spread via synaptic connections would allow manipulation of the system and thereby offer a variety of new applications for RV as research tool and for biomedical applications.

5 References

Abraham, G., and Banerjee, A. K. (1976). Sequential transcription of the genes of vesicular stomatitis virus. *Proc Natl Acad Sci U S A* 73(5), 1504-8.

Babst, M. (2011). MVB vesicle formation: ESCRT-dependent, ESCRT-independent and everything in between. *Curr Opin Cell Biol*.

Babst, M., Katzmann, D. J., Estepa-Sabal, E. J., Meerloo, T., and Emr, S. D. (2002). Escrt-III: an endosome-associated heterooligomeric protein complex required for mvb sorting. *Dev Cell* 3(2), 271-82.

Banerjee, A. K. (2008). Response to "Non-segmented negative-strand RNA virus RNA synthesis in vivo". *Virology* 371(2), 231-3.

Barbar, E. (2008). Dynein light chain LC8 is a dimerization hub essential in diverse protein networks. *Biochemistry* 47(2), 503-8.

Besch, R., Berking, C., Kammerbauer, C., and Degitz, K. (2007). Inhibition of urokinase-type plasminogen activator receptor induces apoptosis in melanoma cells by activation of p53. *Cell Death Differ* 14(4), 818-29.

Bieniasz, P. D. (2006). Late budding domains and host proteins in enveloped virus release. *Virology* 344(1), 55-63.

Black, B. L., Rhodes, R. B., McKenzie, M., and Lyles, D. S. (1993). The role of vesicular stomatitis virus matrix protein in inhibition of host-directed gene expression is genetically separable from its function in virus assembly. *J Virol* 67(8), 4814-21.

Blondel, D., Regad, T., Poisson, N., Pavie, B., Harper, F., Pandolfi, P. P., De The, H., and Chelbi-Alix, M. K. (2002). Rabies virus P and small P products interact directly with PML and reorganize PML nuclear bodies. *Oncogene* 21(52), 7957-70.

Bourhy, H., Dautry-Varsat, A., Hotez, P. J., and Salomon, J. (2010). Rabies, still neglected after 125 years of vaccination. *PLoS Negl Trop Dis* 4(11), e839.

Brzózka, K., Finke, S., and Conzelmann, K. K. (2005). Identification of the rabies virus alpha/beta interferon antagonist: phosphoprotein P interferes with phosphorylation of interferon regulatory factor 3. *J Virol* 79(12), 7673-81.

Brzózka, K., Finke, S., and Conzelmann, K. K. (2006). Inhibition of interferon signaling by rabies virus phosphoprotein P: activation-dependent binding of STAT1 and STAT2. *J Virol* 80(6), 2675-83.

Chase, G., Mayer, D., Hildebrand, A., Frank, R., Hayashi, Y., Tomonaga, K., and Schwemmle, M. (2007). Borna disease virus matrix protein is an integral component of the viral ribonucleoprotein complex that does not interfere with polymerase activity. *J Virol* 81(2), 743-9.

Chen, B. J., and Lamb, R. A. (2008). Mechanisms for enveloped virus budding: can some viruses do without an ESCRT? *Virology* 372(2), 221-32.

Chen, B. J., Leser, G. P., Morita, E., and Lamb, R. A. (2007). Influenza virus hemagglutinin and neuraminidase, but not the matrix protein, are required for assembly and budding of plasmid-derived virus-like particles. *J Virol* 81(13), 7111-23.

Chenik, M., Chebli, K., and Blondel, D. (1995). Translation initiation at alternate in-frame AUG codons in the rabies virus phosphoprotein mRNA is mediated by a ribosomal leaky scanning mechanism. *J Virol* 69(2), 707-12.

Chenik, M., Chebli, K., Gaudin, Y., and Blondel, D. (1994). In vivo interaction of rabies virus phosphoprotein (P) and nucleoprotein (N): existence of two N-binding sites on P protein. *J Gen Virol* 75 (Pt 11), 2889-96.

Chenik, M., Schnell, M., Conzelmann, K. K., and Blondel, D. (1998). Mapping the interacting domains between the rabies virus polymerase and phosphoprotein. *J Virol* 72(3), 1925-30.

Chong, L. D., and Rose, J. K. (1993). Membrane association of functional vesicular stomatitis virus matrix protein in vivo. *J Virol* 67(1), 407-14.

Chong, L. D., and Rose, J. K. (1994). Interactions of normal and mutant vesicular stomatitis virus matrix proteins with the plasma membrane and nucleocapsids. *J Virol* 68(1), 441-7.

Collins, P. L., Hill, M. G., Cristina, J., and Grosfeld, H. (1996). Transcription elongation factor of respiratory syncytial virus, a nonsegmented negative-strand RNA virus. *Proc Natl Acad Sci U S A* 93(1), 81-5.

Curran, J., and Kolakofsky, D. (2008). Nonsegmented negative-strand RNA virus RNA synthesis in vivo. *Virology* 371(2), 227-30.

Das, S. C., and Pattnaik, A. K. (2005). Role of the hypervariable hinge region of phosphoprotein P of vesicular stomatitis virus in viral RNA synthesis and assembly of infectious virus particles. *J Virol* 79(13), 8101-12.

Dietzschold, B., Li, J., Faber, M., and Schnell, M. (2008). Concepts in the pathogenesis of rabies. *Future Virol* 3(5), 481-490.

Dietzschold, B., Wang, H. H., Rupprecht, C. E., Celis, E., Tollis, M., Ertl, H., Heber-Katz, E., and Koprowski, H. (1987). Induction of protective immunity against rabies by immunization with rabies virus ribonucleoprotein. *Proc Natl Acad Sci U S A* 84(24), 9165-9.

Doerr, H. W., and Gerlich, W. H. (2009). "Medizinische Virologie: Grundlagen, Diagnostik, Prävention und Therapie viraler Erkrankungen." 2. Auflage Georg Thieme Verlag.

Etessami, R., Conzelmann, K. K., Fadai-Ghotbi, B., Natelson, B., Tsiang, H., and Ceccaldi, P. E. (2000). Spread and pathogenic characteristics of a G-deficient rabies virus recombinant: an in vitro and in vivo study. *J Gen Virol* 81(Pt 9), 2147-53.

Finke, S., and Conzelmann, K. K. (1999). Virus promoters determine interference by defective RNAs: selective amplification of mini-RNA vectors and rescue from cDNA by a 3' copy-back ambisense rabies virus. *J Virol* 73(5), 3818-25.

Finke, S., and Conzelmann, K. K. (2003). Dissociation of rabies virus matrix protein functions in regulation of viral RNA synthesis and virus assembly. *J Virol* 77(22), 12074-82.

Finke, S., Cox, J. H., and Conzelmann, K. K. (2000). Differential transcription attenuation of rabies virus genes by intergenic regions: generation of recombinant viruses overexpressing the polymerase gene. *J Virol* 74(16), 7261-9.

Finke, S., Granzow, H., Hurst, J., Pollin, R., and Mettenleiter, T. C. (2010). Intergenotypic replacement of lyssavirus matrix proteins demonstrates the role of lyssavirus M proteins in intracellular virus accumulation. *J Virol* 84(4), 1816-27.

Finke, S., Mueller-Waldeck, R., and Conzelmann, K. K. (2003). Rabies virus matrix protein regulates the balance of virus transcription and replication. *J Gen Virol* 84(Pt 6), 1613-21.

Gaudin, Y., Tuffereau, C., Benmansour, A., and Flamand, A. (1991). Fatty acylation of rabies virus proteins. *Virology* 184(1), 441-4.

Ge, P., Tsao, J., Schein, S., Green, T. J., Luo, M., and Zhou, Z. H. (2010). Cryo-EM model of the bullet-shaped vesicular stomatitis virus. *Science* 327(5966), 689-93.

Gerard, F. C., Ribeiro Ede, A., Jr., Albertini, A. A., Gutsche, I., Zaccai, G., Ruigrok, R. W., and Jamin, M. (2007). Unphosphorylated rhabdoviridae phosphoproteins form elongated dimers in solution. *Biochemistry* 46(36), 10328-38.

Gerard, F. C., Ribeiro Ede, A., Jr., Leyrat, C., Ivanov, I., Blondel, D., Longhi, S., Ruigrok, R. W., and Jamin, M. (2009). Modular organization of rabies virus phosphoprotein. *J Mol Biol* 388(5), 978-96.

Ghanem, A., Kern, A., and Conzelmann, K. K. (2011). Significantly improved rescue of rabies virus from cDNA plasmids. *Eur J Cell Biol*.

Gottlinger, H. G., Dorfman, T., Sodroski, J. G., and Haseltine, W. A. (1991). Effect of mutations affecting the p6 gag protein on human immunodeficiency virus particle release. *Proc Natl Acad Sci U S A* 88(8), 3195-9.

Graham, S. C., Assenberg, R., Delmas, O., Verma, A., Gholami, A., Talbi, C., Owens, R. J., Stuart, D. I., Grimes, J. M., and Bourhy, H. (2008). Rhabdovirus matrix protein structures reveal a novel mode of self-association. *PLoS Pathog* 4(12), e1000251.

Habjan, M., Penski, N., Spiegel, M., and Weber, F. (2008). T7 RNA polymerase-dependent and -independent systems for cDNA-based rescue of Rift Valley fever virus. *J Gen Virol* 89(Pt 9), 2157-66.

Harrison, M. S., Sakaguchi, T., and Schmitt, A. P. (2010). Paramyxovirus assembly and budding: building particles that transmit infections. *Int J Biochem Cell Biol* 42(9), 1416-29.

Harty, R. N., Brown, M. E., McGettigan, J. P., Wang, G., Jayakar, H. R., Huibregtse, J. M., Whitt, M. A., and Schnell, M. J. (2001). Rhabdoviruses and the cellular ubiquitin-proteasome system: a budding interaction. *J Virol* 75(22), 10623-9.

Heijnen, H. F., Schiel, A. E., Fijnheer, R., Geuze, H. J., and Sixma, J. J. (1999). Activated platelets release two types of membrane vesicles: microvesicles by surface shedding and exosomes derived from exocytosis of multivesicular bodies and alpha-granules. *Blood* 94(11), 3791-9.

Hooper, D. C., Phares, T. W., Fabis, M. J., and Roy, A. (2009). The production of antibody by invading B cells is required for the clearance of rabies virus from the central nervous system. *PLoS Negl Trop Dis* 3(10), e535.

Hornung, V., Ellegast, J., Kim, S., Brzózka, K., Jung, A., Kato, H., Poeck, H., Akira, S., Conzelmann, K. K., Schlee, M., Endres, S., and Hartmann, G. (2006). 5'-Triphosphate RNA is the ligand for RIG-I. *Science* 314(5801), 994-7.

Horton, A. C., Racz, B., Monson, E. E., Lin, A. L., Weinberg, R. J., and Ehlers, M. D. (2005). Polarized secretory trafficking directs cargo for asymmetric dendrite growth and morphogenesis. *Neuron* 48(5), 757-71.

Hu, C., Hardee, D., and Minnear, F. (2007). Membrane fusion by VAMP3 and plasma membrane t-SNAREs. *Exp Cell Res* 313(15), 3198-209.

Huang, M., Orenstein, J. M., Martin, M. A., and Freed, E. O. (1995). p6Gag is required for particle production from full-length human immunodeficiency virus type 1 molecular clones expressing protease. *J Virol* 69(11), 6810-8.

Hung, T., Chou, Z. Y., Zhao, T. X., Xia, S. M., and Hang, C. S. (1985). Morphology and morphogenesis of viruses of hemorrhagic fever with renal syndrome (HFRS). I. Some peculiar aspects of the morphogenesis of various strains of HFRS virus. *Intervirology* 23(2), 97-108.

Hurley, J. H., and Hanson, P. I. (2010). Membrane budding and scission by the ESCRT machinery: it's all in the neck. *Nat Rev Mol Cell Biol* 11(8), 556-66.

Irie, T., Licata, J. M., and Harty, R. N. (2005). Functional characterization of Ebola virus L-domains using VSV recombinants. *Virology* 336(2), 291-8.

Irie, T., Licata, J. M., McGettigan, J. P., Schnell, M. J., and Harty, R. N. (2004). Budding of PPxY-containing rhabdoviruses is not dependent on host proteins TGS101 and VPS4A. *J Virol* 78(6), 2657-65.

Ivanov, I., Crepin, T., Jamin, M., and Ruigrok, R. W. (2010). Structure of the dimerization domain of the rabies virus phosphoprotein. *J Virol* 84(7), 3707-10.

Jacob, Y., Badrane, H., Ceccaldi, P. E., and Tordo, N. (2000). Cytoplasmic dynein LC8 interacts with lyssavirus phosphoprotein. *J Virol* 74(21), 10217-22.

Jayakar, H. R., Jeetendra, E., and Whitt, M. A. (2004). Rhabdovirus assembly and budding. *Virus Res* 106(2), 117-32.

Johnson, R. F., McCarthy, S. E., Godlewski, P. J., and Harty, R. N. (2006). Ebola virus VP35-VP40 interaction is sufficient for packaging 3E-5E minigenome RNA into virus-like particles. *J Virol* 80(11), 5135-44.

Jones, S. M., Howell, K. E., Henley, J. R., Cao, H., and McNiven, M. A. (1998). Role of dynamin in the formation of transport vesicles from the trans-Golgi network. *Science* 279(5350), 573-7.

Justice, P. A., Sun, W., Li, Y., Ye, Z., Grigera, P. R., and Wagner, R. R. (1995). Membrane vesiculation function and exocytosis of wild-type and mutant matrix proteins of vesicular stomatitis virus. *J Virol* 69(5), 3156-60.

Kasai, K., Shin, H. W., Shinotsuka, C., Murakami, K., and Nakayama, K. (1999). Dynamin II is involved in endocytosis but not in the formation of transport vesicles from the trans-Golgi network. *J Biochem* 125(4), 780-9.

Katzmann, D. J., Babst, M., and Emr, S. D. (2001). Ubiquitin-dependent sorting into the multivesicular body pathway requires the function of a conserved endosomal protein sorting complex, ESCRT-I. *Cell* 106(2), 145-55.

Kennedy, M. J., Davison, I. G., Robinson, C. G., and Ehlers, M. D. (2010). Syntaxin-4 defines a domain for activity-dependent exocytosis in dendritic spines. *Cell* 141(3), 524-35.

Kennedy, M. J., and Ehlers, M. D. (2011). Mechanisms and function of dendritic exocytosis. *Neuron* 69(5), 856-75.

Klingen, Y., Conzelmann, K. K., and Finke, S. (2008). Double-labeled rabies virus: live tracking of enveloped virus transport. *J Virol* 82(1), 237-45.

Lafon, M. (2005). Rabies virus receptors. *J Neurovirol* 11(1), 82-7.

Lafon, M., Lafage, M., Martinez-Arends, A., Ramirez, R., Vuillier, F., Charron, D., Lotteau, V., and Scott-Algara, D. (1992). Evidence for a viral superantigen in humans. *Nature* 358(6386), 507-10.

Lahaye, X., Vidy, A., Pomier, C., Obiang, L., Harper, F., Gaudin, Y., and Blondel, D. (2009). Functional characterization of Negri bodies (NBs) in rabies virus-infected cells: Evidence that NBs are sites of viral transcription and replication. *J Virol* 83(16), 7948-58.

Lau, C. G., Takayasu, Y., Rodenas-Ruano, A., Paternain, A. V., Lerma, J., Bennett, M. V., and Zukin, R. S. (2010). SNAP-25 is a target of protein kinase C phosphorylation critical to NMDA receptor trafficking. *J Neurosci* 30(1), 242-54.

Li, D., Jans, D. A., Bardin, P. G., Meanger, J., Mills, J., and Ghildyal, R. (2008). Association of respiratory syncytial virus M protein with viral nucleocapsids is mediated by the M2-1 protein. *J Virol* 82(17), 8863-70.

Li, Y., Luo, L., Schubert, M., Wagner, R. R., and Kang, C. Y. (1993). Viral liposomes released from insect cells infected with recombinant baculovirus expressing the matrix protein of vesicular stomatitis virus. *J Virol* 67(7), 4415-20.

Mavrakis, M., Iseni, F., Mazza, C., Schoehn, G., Ebel, C., Gentzel, M., Franz, T., and Ruigrok, R. W. (2003). Isolation and characterisation of the rabies virus N^0-P complex produced in insect cells. *Virology* 305(2), 406-14.

Mavrakis, M., McCarthy, A. A., Roche, S., Blondel, D., and Ruigrok, R. W. (2004). Structure and function of the C-terminal domain of the polymerase cofactor of rabies virus. *J Mol Biol* 343(4), 819-31.

Mavrakis, M., Mehouas, S., Real, E., Iseni, F., Blondel, D., Tordo, N., and Ruigrok, R. W. (2006). Rabies virus chaperone: identification of the phosphoprotein peptide that keeps nucleoprotein soluble and free from non-specific RNA. *Virology* 349(2), 422-9.

Mazarakis, N. D., Azzouz, M., Rohll, J. B., Ellard, F. M., Wilkes, F. J., Olsen, A. L., Carter, E. E., Barber, R. D., Baban, D. F., Kingsman, S. M., Kingsman, A. J., O'Malley, K., and Mitrophanous, K. A. (2001). Rabies virus glycoprotein pseudotyping of lentiviral vectors enables retrograde axonal transport and access to the nervous system after peripheral delivery. *Hum Mol Genet* 10(19), 2109-21.

McMahon, H. T., Ushkaryov, Y. A., Edelmann, L., Link, E., Binz, T., Niemann, H., Jahn, R., and Sudhof, T. C. (1993). Cellubrevin is a ubiquitous tetanus-toxin substrate homologous to a putative synaptic vesicle fusion protein. *Nature* 364(6435), 346-9.

Mebatsion, T. (2001). Extensive attenuation of rabies virus by simultaneously modifying the dynein light chain binding site in the P protein and replacing Arg333 in the G protein. *J Virol* 75(23), 11496-502.

Mebatsion, T., Konig, M., and Conzelmann, K. K. (1996). Budding of rabies virus particles in the absence of the spike glycoprotein. *Cell* 84(6), 941-51.

Mebatsion, T., Weiland, F., and Conzelmann, K. K. (1999). Matrix protein of rabies virus is responsible for the assembly and budding of bullet-shaped particles and interacts with the transmembrane spike glycoprotein G. *J Virol* 73(1), 242-50.

Naeve, C. W., Kolakofsky, C. M., and Summers, D. F. (1980). Comparison o;f vesicular stomatitis virus intracellular and virion ribonucleoproteins. *J Virol* 33(2), 856-65.

Neumann, G., Ebihara, H., Takada, A., Noda, T., Kobasa, D., Jasenosky, L. D., Watanabe, S., Kim, J. H., Feldmann, H., and Kawaoka, Y. (2005). Ebola virus VP40 late domains are not essential for viral replication in cell culture. *J Virol* 79(16), 10300-7.

Newcomb, W. W., and Brown, J. C. (1981). Role of the vesicular stomatitis virus matrix protein in maintaining the viral nucleocapsid in the condensed form found in native virions. *J Virol* 39(1), 295-9.

Newcomb, W. W., Tobin, G. J., McGowan, J. J., and Brown, J. C. (1982). In vitro reassembly of vesicular stomatitis virus skeletons. *J Virol* 41(3), 1055-62.

Nickerson, D. P., Russell, M. R., and Odorizzi, G. (2007). A concentric circle model of multivesicular body cargo sorting. *EMBO Rep* 8(7), 644-50.

Ogden, J. R., Pal, R., and Wagner, R. R. (1986). Mapping regions of the matrix protein of vesicular stomatitis virus which bind to ribonucleocapsids, liposomes, and monoclonal antibodies. *J Virol* 58(3), 860-8.

Parent, L. J., Bennett, R. P., Craven, R. C., Nelle, T. D., Krishna, N. K., Bowzard, J. B., Wilson, C. B., Puffer, B. A., Montelaro, R. C., and Wills, J. W. (1995). Positionally independent and exchangeable late budding functions of the Rous sarcoma virus and human immunodeficiency virus Gag proteins. *J Virol* 69(9), 5455-60.

Pettersson, R. F. (1991). Protein localization and virus assembly at intracellular membranes. *Curr Top Microbiol Immunol* 170, 67-106.

Pichlmair, A., Schulz, O., Tan, C. P., Naslund, T. I., Liljestrom, P., Weber, F., and Reis e Sousa, C. (2006). RIG-I-mediated antiviral responses to single-stranded RNA bearing 5'-phosphates. *Science* 314(5801), 997-1001.

Pizzato, M., Helander, A., Popova, E., Calistri, A., Zamborlini, A., Palu, G., and Gottlinger, H. G. (2007). Dynamin 2 is required for the enhancement of HIV-1 infectivity by Nef. *Proc Natl Acad Sci U S A* 104(16), 6812-7.

Plutner, H., Cox, A. D., Pind, S., Khosravi-Far, R., Bourne, J. R., Schwaninger, R., Der, C. J., and Balch, W. E. (1991). Rab1b regulates vesicular transport between the endoplasmic reticulum and successive Golgi compartments. *J Cell Biol* 115(1), 31-43.

Puffer, B. A., Parent, L. J., Wills, J. W., and Montelaro, R. C. (1997). Equine infectious anemia virus utilizes a YXXL motif within the late assembly domain of the Gag p9 protein. *J Virol* 71(9), 6541-6.

Raux, H., Flamand, A., and Blondel, D. (2000). Interaction of the rabies virus P protein with the LC8 dynein light chain. *J Virol* 74(21), 10212-6.

Raux, H., Iseni, F., Lafay, F., and Blondel, D. (1997). Mapping of monoclonal antibody epitopes of the rabies virus P protein. *J Gen Virol* 78 (Pt 1), 119-24.

Raux, H., Obiang, L., Richard, N., Harper, F., Blondel, D., and Gaudin, Y. (2010). The matrix protein of vesicular stomatitis virus binds dynamin for efficient viral assembly. *J Virol* 84(24), 12609-18.

Regehr, W. G., Carey, M. R., and Best, A. R. (2009). Activity-dependent regulation of synapses by retrograde messengers. *Neuron* 63(2), 154-70.

Reggiori, F., and Pelham, H. R. (2001). Sorting of proteins into multivesicular bodies: ubiquitin-dependent and -independent targeting. *EMBO J* 20(18), 5176-86.

Ribeiro, E. A., Jr., Favier, A., Gerard, F. C., Leyrat, C., Brutscher, B., Blondel, D., Ruigrok, R. W., Blackledge, M., and Jamin, M. (2008). Solution structure of the C-terminal nucleoprotein-RNA binding domain of the vesicular stomatitis virus phosphoprotein. *J Mol Biol* 382(2), 525-38.

Rieder, M., Brzózka, K., Pfaller, C. K., Cox, J. H., Stitz, L., and Conzelmann, K. K. (2011). Genetic dissection of interferon-antagonistic functions of rabies virus phosphoprotein: inhibition of interferon regulatory factor 3 activation is important for pathogenicity. *J Virol* 85(2), 842-52.

Robison, C. S., and Whitt, M. A. (2000). The membrane-proximal stem region of vesicular stomatitis virus G protein confers efficient virus assembly. *J Virol* 74(5), 2239-46.

Rolls, M. M., Webster, P., Balba, N. H., and Rose, J. K. (1994). Novel infectious particles generated by expression of the vesicular stomatitis virus glycoprotein from a self-replicating RNA. *Cell* 79(3), 497-506.

Schiavo, G., Matteoli, M., and Montecucco, C. (2000). Neurotoxins affecting neuroexocytosis. *Physiol Rev* 80(2), 717-66.

Schnell, M. J., Buonocore, L., Boritz, E., Ghosh, H. P., Chernish, R., and Rose, J. K. (1998). Requirement for a non-specific glycoprotein cytoplasmic domain sequence to drive efficient budding of vesicular stomatitis virus. *EMBO J* 17(5), 1289-96.

Schnell, M. J., and Conzelmann, K. K. (1995). Polymerase activity of in vitro mutated rabies virus L protein. *Virology* 214(2), 522-30.

Schoehn, G., Iseni, F., Mavrakis, M., Blondel, D., and Ruigrok, R. W. (2001). Structure of recombinant rabies virus nucleoprotein-RNA complex and identification of the phosphoprotein binding site. *J Virol* 75(1), 490-8.

Shaw, K. L., Lindemann, D., Mulligan, M. J., and Goepfert, P. A. (2003). Foamy virus envelope glycoprotein is sufficient for particle budding and release. *J Virol* 77(4), 2338-48.

Slavin, I., Garcia, I. A., Monetta, P., Martinez, H., Romero, N., and Alvarez, C. (2011). Role of Rab1b in COPII dynamics and function. *Eur J Cell Biol* 90(4), 301-11.

Solon, J., Gareil, O., Bassereau, P., and Gaudin, Y. (2005). Membrane deformations induced by the matrix protein of vesicular stomatitis virus in a minimal system. *J Gen Virol* 86(Pt 12), 3357-63.

Strecker, T., Eichler, R., Meulen, J., Weissenhorn, W., Dieter Klenk, H., Garten, W., and Lenz, O. (2003). Lassa virus Z protein is a matrix protein and sufficient for the release of virus-like particles [corrected]. *J Virol* 77(19), 10700-5.

Stuffers, S., Brech, A., and Stenmark, H. (2009a). ESCRT proteins in physiology and disease. *Exp Cell Res* 315(9), 1619-26.

Stuffers, S., Sem Wegner, C., Stenmark, H., and Brech, A. (2009b). Multivesicular endosome biogenesis in the absence of ESCRTs. *Traffic* 10(7), 925-37.

Suh, Y. H., Terashima, A., Petralia, R. S., Wenthold, R. J., Isaac, J. T., Roche, K. W., and Roche, P. A. (2010). A neuronal role for SNAP-23 in postsynaptic glutamate receptor trafficking. *Nat Neurosci* 13(3), 338-43.

Superti, F., Derer, M., and Tsiang, H. (1984). Mechanism of rabies virus entry into CER cells. *J Gen Virol* 65 (Pt 4), 781-9.

Superti, F., Hauttecoeur, B., Morelec, M. J., Goldoni, P., Bizzini, B., and Tsiang, H. (1986). Involvement of gangliosides in rabies virus infection. *J Gen Virol* 67 (Pt 1), 47-56.

Sutter, G., Ohlmann, M., and Erfle, V. (1995). Non-replicating vaccinia vector efficiently expresses bacteriophage T7 RNA polymerase. *FEBS Lett* 371(1), 9-12.

Tan, G. S., Preuss, M. A., Williams, J. C., and Schnell, M. J. (2007). The dynein light chain 8 binding motif of rabies virus phosphoprotein promotes efficient viral transcription. *Proc Natl Acad Sci U S A* 104(17), 7229-34.

Taylor, G. M., Hanson, P. I., and Kielian, M. (2007). Ubiquitin depletion and dominant-negative VPS4 inhibit rhabdovirus budding without affecting alphavirus budding. *J Virol* 81(24), 13631-9.

Tooze, J., Tooze, S., and Warren, G. (1984). Replication of coronavirus MHV-A59 in sac- cells: determination of the first site of budding of progeny virions. *Eur J Cell Biol* 33(2), 281-93.

Vidy, A., Chelbi-Alix, M., and Blondel, D. (2005). Rabies virus P protein interacts with STAT1 and inhibits interferon signal transduction pathways. *J Virol* 79(22), 14411-20.

Whelan, S. P. (2008). Response to "Non-segmented negative-strand RNA virus RNA synthesis in vivo". *Virology* 371(2), 234-7.

World Health Organization (2010). Fact Sheet N°99: Rabies. WHO.

Wickersham, I. R., Finke, S., Conzelmann, K. K., and Callaway, E. M. (2007a). Retrograde neuronal tracing with a deletion-mutant rabies virus. *Nat Methods* 4(1), 47-9.

Wickersham, I. R., Lyon, D. C., Barnard, R. J., Mori, T., Finke, S., Conzelmann, K. K., Young, J. A., and Callaway, E. M. (2007b). Monosynaptic restriction of transsynaptic tracing from single, genetically targeted neurons. *Neuron* 53(5), 639-47.

Wilde, H., Hemachudha, T., and Jackson, A. C. (2008). Viewpoint: Management of human rabies. *Trans R Soc Trop Med Hyg* 102(10), 979-82.

Wirblich, C., Tan, G. S., Papaneri, A., Godlewski, P. J., Orenstein, J. M., Harty, R. N., and Schnell, M. J. (2008). PPEY motif within the rabies virus (RV) matrix protein is essential for efficient virion release and RV pathogenicity. *J Virol* 82(19), 9730-8.

Wunner, W. H., Reagan, K. J., and Koprowski, H. (1984). Characterization of saturable binding sites for rabies virus. *J Virol* 50(3), 691-7.

Xiang, Y., Cameron, C. E., Wills, J. W., and Leis, J. (1996). Fine mapping and characterization of the Rous sarcoma virus Pr76gag late assembly domain. *J Virol* 70(8), 5695-700.

Yang, C., Mora, S., Ryder, J. W., Coker, K. J., Hansen, P., Allen, L. A., and Pessin, J. E. (2001). VAMP3 null mice display normal constitutive, insulin- and exercise-regulated vesicle trafficking. *Mol Cell Biol* 21(5), 1573-80.

Ye, Z., Sun, W., Suryanarayana, K., Justice, P., Robinson, D., and Wagner, R. R. (1994). Membrane-binding domains and cytopathogenesis of the matrix protein of vesicular stomatitis virus. *J Virol* 68(11), 7386-96.

Yoneyama, M., Suhara, W., Fukuhara, Y., Sato, M., Ozato, K., and Fujita, T. (1996). Autocrine amplification of type I interferon gene expression mediated by interferon stimulated gene factor 3 (ISGF3). *J Biochem* 120(1), 160-9.

6 Appendix

6.1 List of publications

Publications:

Kern A. and Conzelmann KK.

The rabies virus phosphoprotein is required for the assembly of infectious particles

[in preparation]

Ghanem A., Kern A., Conzelmann KK.

Significantly improved rescue of rabies virus from cDNA plasmids.

Eur J Cell Biol. 2011 Mar 11 [Epub ahead of print]

Voss D., Kern A., Traggiai E., Eickmann M., Stadler K., Lanzavecchia A., Becker S.

Characterization of severe acute respiratory syndrome coronavirus membrane protein.

FEBS Lett. 2006 Feb 6;580(3):968-73.

Oral presentations:

2011 15th International Congress of Virology of the International Union of Microbiological Societies (IUMS) in Sapporo, Japan (accepted for presentation)

2010 14th International Conference on Negative Strand Viruses in Bruges, Belgium

Poster presentations:

2011 21st Annual Meeting of the Society for Virology in Freiburg

2010 4th European Congress of Virology in Cernobbio, Italy

2009 19th Annual Meeting of the Society for Virology in Leipzig

2008 18th Annual Meeting of the Society for Virology in Heidelberg

2007 3rd European Congress of Virology in Nuremberg

2006 17th Annual Meeting of the Society for Virology in Munich

6.2 Danksagung

Ganz herzlich möchte ich mich bei Prof. Dr. Karl-Klaus Conzelmann bedanken, in dessen Labor diese Arbeit mit seiner Unterstützung durchgeführt wurde. Die offene Bürotür hatte nicht nur symbolischen Charakter, sondern wurde auch gelebt.

PD Dr. Stefan Finke, dem ursprünglichen Projektleiter, der mich zu Beginn meiner Doktorarbeit mit der Tollwutvirusarbeit vertraut machte, gilt ebenso mein Dank.

Der gesamten AG Conzelmann gebührt besonderes Lob, da der Zusammenhalt und das Verständnis untereinander wirklich seinesgleichen sucht und das nicht selbstverständlich ist. Zu nennen sind in alphabetischer Reihenfolge Alex (diesmal nicht vergessen, sondern allen voran), Kerstin, Konstantin, Lisa, Martina, Moni, Nadin und Vanessa. Ebenso natürlich die Ehemaligen Adriane, Christian, Christine, Kris, Laetitia, Silva und Yvonne.

Meinen Eltern ein großes Dankeschön für ihre Bereitschaft, mir jederzeit etwas Gutes zu tun und mich zu unterstützen.

Dank der Augsburger konnte ich in meiner Freizeit Abstand zur Arbeit gewinnen. Die Marburger hingegen mussten sich als Leidensgenossen lange Telefonate gefallen lassen. Danke fürs Zuhören.

Mein größter Dank allerdings gilt Jan. Er hat mit viel Verständnis und noch mehr Humor, den gefühlten Wahnsinn der letzten Jahre, mit mir gemeinsam erlebt und durchgestanden.

A.I. sei Dank: Die Hex´ ist tot!

Ehrenwörtliche Versicherung

Hiermit versichere ich ehrenwörtlich, dass die vorgelegte Dissertation von mir selbständig und ohne unerlaubte Hilfe angefertigt wurde.

München, den 08.08.2011

……..

(Anika Kern)

Erklärung

Hiermit erkläre ich, dass ich mich anderweitig einer Doktorprüfung nicht unterzogen habe.

München, den 08.08.2011

……..

(Anika Kern)